Commun Nonlinear Sci Numer Simulat 18 (2013) 2626–2666

Contents lists available at SciVerse ScienceDirect

Commun Nonlinear Sci Numer Simulat

journal homepage: www.elsevier.com/locate/cnsns

Replication of chaos

M.U. Akhmet *, M.O. Fen

Department of Mathematics, Middle East Technical University, 06800 Ankara, Turkey

ARTICLE INFO

Article history:
Received 28 May 2012
Received in revised form 5 December 2012
Accepted 27 January 2013
Available online 9 February 2013

Dedicated to Alan Turing's centennial

Keywords:
Replication of chaos
Hyperbolic set of functions
Chaotic set of functions
Period-doubling cascade
Devaney chaos
Li-Yorke chaos
Intermittency
Chaotic attractor
Chaos control
Shil'nikov orbits
The double-scroll Chua's attractor
Quasiperiodicity
Morphogenesis of chaos

ABSTRACT

We propose a rigorous method for replication of chaos from a prior one to systems with large dimensions. Extension of the formal properties and features of a complex motion can be observed such that ingredients of chaos united as known types of chaos, Devaney's, Li-Yorke and obtained through period-doubling cascade. This is true for other appearances of chaos: intermittency, structure of the chaotic attractor, its fractal dimension, form of the bifurcation diagram, the spectra of Lyapunov exponents, etc. That is why we identify the extension of chaos through the replication as morphogenesis.

To provide rigorous study of the subject, we introduce new definitions such as chaotic sets of functions, the generator and replicator of chaos, and precise description of ingredients for Devaney and Li-Yorke chaos in continuous dynamics. Appropriate simulations which illustrate the chaos replication phenomenon are provided. Moreover, in discussion form we consider inheritance of intermittency, replication of Shil'nikov orbits and quasiperiodical motions as a possible skeleton of a chaotic attractor. Chaos extension in an open chain of Chua circuits is also demonstrated.

1. Introduction

It is known that if one considers the evolution equation $u' = L[u] + I(t)$, where $L[u]$ is a linear operator with spectra placed in the left half of the complex plane, then a function $I(t)$ being considered as an *input* with a certain property (boundedness, periodicity, almost periodicity) produces through the equation the *output*, a solution with a similar property, boundedness/periodicity/almost periodicity [1,2].

A reasonable question appears whether it is possible to use as input a chaotic motion and to obtain output also as a chaos of certain type. Our paper is devoted to answer this question even if the input is inserted non-linearly. One must say that we consider as an input first of all a single function, a member of a chaotic set to obtain a solution, which is a member of another chaotic set. Beside that we consider the chaotic sets as the input and the output. We have been forced to consider sets of functions as inputs and outputs, since Devaney or Li-Yorke chaos are indicated through relation of motions (sensitivity, transitiveness, proximality). Thus, we consider the input and the output not only as single functions, but also as collections of functions. The way of our investigation is arranged in the well accepted traditional mathematical fashion, but with a new and a more complex way of arrangement of the connections between the input and the output.

* Corresponding author. Tel.: +90 312 210 5355; fax: +90 312 210 2972.
E-mail addresses: marat@metu.edu.tr (M.U. Akhmet), ofen@metu.edu.tr (M.O. Fen).

1007-5704/$ - see front matter © 2013 Elsevier B.V. All rights reserved.
http://dx.doi.org/10.1016/j.cnsns.2013.01.021

Since the concept of chaos is much more complex than just single periodic or almost periodic solutions, we have to use a special terminology for the chaos generation through the input-output mechanism, *replication of chaos*.

The technique of replication used in our paper is as follows. We need a source of chaotic inputs, but mostly chaos can be obtained through solving differential or difference equations. For this reason, in our paper we use special generator systems as the source of chaos or chaotic functions. Nevertheless, we emphasize that the generator is not necessarily the element of the replication procedure since it can be replaced by another source of a chaotic input, and in applications present result may be considered with, for example, chaotic inputs obtained from experimental activity. So, initially, we take into account a system of differential equations (the generator) which produces chaos, and we use this system to influence in a unidirectional way, another system (the replicator) in such a manner that the replicator mimics the same ingredients of chaos provided to the generator. In the present paper, we use such ingredients in the form of period-doubling cascade, Devaney and Li-Yorke chaos. For the study of the subject, we introduce new definitions such as chaotic sets of functions, the generator and replicator of chaos, and precise description of ingredients for Devaney and Li-Yorke chaos in continuous dynamics.

Throughout the paper, the generator will be considered as a system of the form

$$x' = F(t,x), \tag{1.1}$$

where $F : \mathbb{R} \times \mathbb{R}^m \to \mathbb{R}^m$ is a continuous function in all its arguments, and the replicator is assumed to have the form

$$y' = Ay + g(x(t),y), \tag{1.2}$$

where $g : \mathbb{R}^m \times \mathbb{R}^n \to \mathbb{R}^n$ is a continuous function in all its arguments, the constant $n \times n$ real valued matrix A has real parts of eigenvalues all negative and the function $x(t)$ is a solution of system (1.1). The generator-replicator couple, (1.1)+(1.2), will be called in the remaining parts of the paper as the *result-system*.

Now, to illustrate the replication mechanism discussed in our paper, let us consider the following example. For our purposes, as the generator we shall take into account the Duffing's oscillator represented by the differential equation

$$x'' + 0.05x' + x^3 = 7.5\cos t. \tag{1.3}$$

It is known that Eq. (1.3) possesses a chaotic attractor [3]. Defining the variables $x_1 = x$ and $x_2 = x'$, Eq. (1.3) can be reduced to the system

$$\begin{aligned} x_1' &= x_2, \\ x_2' &= -0.05x_2 - x_1^3 + 7.5\cos t. \end{aligned} \tag{1.4}$$

Next, let us consider the following system

$$\begin{aligned} x_3' &= x_4 + x_1(t), \\ x_4' &= -3x_3 - 2x_4 - 0.008x_3^3 + x_2(t). \end{aligned} \tag{1.5}$$

In this form system (1.5) is a replicator. One has to emphasize that the linear part of the following non-perturbed system associated with (1.5)

$$\begin{aligned} x_3' &= x_4, \\ x_4' &= -3x_3 - 2x_4 - 0.008x_3^3, \end{aligned} \tag{1.6}$$

has eigenvalues with negative real parts and does not admit chaos.

To visualize the process of replication by the result-system, (1.4)+(1.5), let us consider the Poincaré sections of the both. By marking the trajectory of this system with the initial data $x_1(0) = 2,\ x_2(0) = 3,\ x_3(0) = -1,\ x_4(0) = 1$ stroboscopically at times that are integer multiples of 2π, we obtain the Poincaré section and in Fig. 1, where the chaos replication is apparent, we illustrate its 2-dimensional projections. Fig. 1(a) represents the projection of the Poincaré section on the x_1–x_2 plane, and we note that this projection is in fact the strange attractor of the generator system (1.4). On the other hand, the projection on the x_3–x_4 plane presented in Fig. 1(b) is the attractor corresponding to the replicator system (1.5). One can see that the attractor indicated in Fig. 1(b) repeated the structure of the attractor shown in Fig. 1(a) and this result is a manifestation of the replication of chaos. One has to think about mathematical aspects of this phenomena and in our paper we handle this problem.

In our theoretical results, we use coupled systems in which the generator influences the replicator in a unidirectional way. In other words, the generator affects the behavior of the replicator counterpart in such a way that the solutions of the generator are used as an input for the latter. The possibility of making use of more than one replicator systems with arbitrarily high dimensions in the extension mechanism is an advantage of our procedure. Moreover, we are describing a process involving the replication of chaos which does not occur in the course of time, but instead an **instantaneous** one. In other words, the prior chaos is mimicked in all existing replicators such that the generating mechanism works through arranging connections between systems not with the lapse of time.

Since we do not restrict ourselves in this paper with a simple couple *the generator-the replicator*, but get them in different combinations and numbers, having the geometric features of chaos saved, we shall call the extension of chaos as *morphogenesis*.

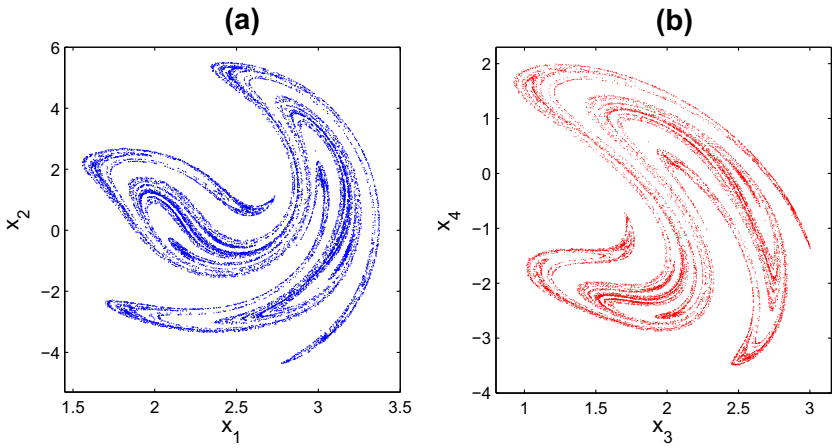

Fig. 1. The picture in (a) not only represents the projection of the whole attractor on the x_1-x_2 plane, but also the strange attractor of the generator. In a similar way, the picture introduced in (b) represents the chaotic attractors of the replicator. The presented chaotic attractors of the generator and the replicator systems reveal that the chaos replication mechanism works consummately.

In our paper, we try to use the term morphogenesis issuing from the sense of the words *morph* meaning "form" and *genesis* meaning "creation" [4]. In other words, similar to the ideas of René Thom [5], we employ the word *morphogenesis* as its etymology indicates, to denote *processes creating forms*. One should understand *morphogenesis of chaos* as a form-generating mechanism emerging from a dynamical process which is based on replication of chaos. Here, we accept the form (morph) not only as a type of chaos, but also accompanying concepts as the structure of the chaotic attractor, its fractal dimension, form of the bifurcation diagram, the spectra of Lyapunov exponents, inheritance of intermittency, etc.

To understand the concept of our paper better, let us consider morphogenesis of fractal structures [6,7]. It is important to say that Mandelbrot fractal structures exhibit the appearance of fractal hierarchy looking **in**, that is, **a part is similar to the whole**. Examples for this are the Julia sets [8,9] and the Sierpinski carpet [10]. In our morphogenesis both directions, **in** and **out**, are present. Indeed, the fractal structure of the prior chaos has hierarchy looking **in**, and the structure for the result-system is obtained considering hierarchy looking **out**, that is, when **the whole is similar to the part**.

One of the fields where coupled systems are used is the study of synchronization of chaotic systems [11,12]. The methods of the continuous control scheme [13,14] and replacement of variables [15,16] can be used to obtain couplings which are proper for synchronization. In our results, we do not consider the chaos synchronization problem, but we say that the type of the chaos is kept *invariant* in the procedure. That is why the classes which can be considered with respect to this *invariance* is expectedly wider then those investigated for synchronization of chaos. Since there is no strong relation and accordance between the solutions of the generator and the replicator in the asymptotic point of view, the terms *master* and *slave* as well as *drive* and *response* are not preferred to be used for the analyzed systems. On the other hand, contrary to the method that we present, in the synchronization of chaotic systems, one does not consider the type of the chaos that the master and slave systems admit. The problem that whether the synchronization of systems implies the same type of chaos for both master and slave has not been taken into account yet.

Symbolic dynamics, whose earliest examples were constructed by Hadamard [17] and Morse [18], is one of the oldest techniques for the study of chaos. Symbolic dynamical systems are systems whose phase space consists of one-sided or two-sided infinite sequences of symbols chosen from a finite alphabet. Such dynamics arises in a variety of situations such as in horseshoe maps and the logistic map. The set of allowed sequences is invariant under the shift map, which is the most important ingredient in symbolic dynamics [19–24]. Moreover, it is known that the symbolic dynamics admits the chaos in the sense of both Devaney and Li-Yorke [21,25–28]. The Smale Horseshoe map is first studied by Smale [29] and it is an example of a diffeomorphism which is structurally stable and possesses a chaotic invariant set [20–22]. The horseshoe arises whenever one has transverse homoclinic orbits, as in the case of the Duffing equation [30]. People used the symbolic dynamics to discover chaos, but we suppose that it can serve as an "embryo" for the morphogenesis of chaos.

The phenomenon of the form recognition for chaotic processes has already begun in pioneering papers. It was Lorenz [31] who discovered that the dynamics of an infinite dimensional system being reduced to three dimensional equation can be next analyzed in its chaotic appearances by application of the simple unimodal one dimensional map. Smale [29] explained that the geometry of the horseshoe map is underneath of the Van der Pol equation's complex dynamics which was investigated by Cartwright and Littlewood [32] and later by Levinson [33]. Nowadays, the Smale horseshoes with its chaotic dynamics, is one of the basic instruments when one tries to recognize a chaos in a process. Guckenheimer and Williams gave a geometric description of the flow of Lorenz attractor to show the structural stability of codimension 2 [34]. In addition to this, it was found out that the topology of the Lorenz attractor is considerably more complicated than the topology of the horseshoe [30]. Moreover, Levi used a geometric approach for a simplified version of the Van der pol equation to show existence of horseshoes embedded within the Van der Pol map and how the horseshoes fit in the phase plane [35]. In other

words, all the mentioned results say about chaos recognition, by reducing complex behavior to the structure with recognizable chaos. In [26,28,36–41], we provide a different and constructive way when a recognized chaos can be extended saving the form of chaos to a multidimensional system. In the present study, we generalize the idea to the morphogenesis of chaos.

Nowadays, one can consider development of a multidimensional chaos from a low-dimensional one in different ways. One of them is the chaotic itinerancy [42–49]. The itinerant motion among varieties of ordered states through high-dimensional chaotic motion can be observed and this behavior is named as chaotic itinerancy. In other words, chaotic itinerancy is a universal dynamics in high-dimensional dynamical systems, showing itinerant motion among varieties of low-dimensional ordered states through high-dimensional chaos. This phenomenon occurs in different real world processes: optical turbulence [44], globally coupled chaotic systems [47,48], non-equilibrium neural networks [45,46], analysis of brain activities [50] and ecological systems [51]. One can see that in its degenerated form chaotic itinerancy relates to intermittency [52,53], since they both represent dynamical interchange of irregularity and regularity.

Likewise the itinerant chaos observed in brain activities, we have low-dimensional chaos in the subsystems considered and high-dimensional chaos is obtained when one considers all subsystems as a whole. The main difference compared to our technique is in the elapsed time for the occurrence of the process. In our discussions, no itinerant motion is observable and all resultant chaotic subsystems process simultaneously, whereas the low-dimensional chaotic motions take place as time elapses in the case of chaotic itinerancy. Knowledge of the type of chaos is another difference between chaotic itinerancy and our procedure. Possibly the present way of replication of chaos will give a light to the solutions of problems about extension of irregular behavior (crises, collapses, etc.) in interrelated or multiple connected systems which can arise in problems of classical mechanics [53], electrical systems [54,55], economic theory [56] and brain activity investigations [50].

In systems whose dimension is at least four, it is possible to observe chaotic attractors with at least two positive Lyapunov exponents and such systems are called hyperchaotic [57]. An example of a four dimensional hyperchaotic system is discovered by Rössler [58]. Combining two or more chaotic, not necessarily identical, systems is a way of achieving hyperchaos [59–61]. However, in the present paper, we take into account exactly one chaotic system with a known type of chaos, and use this system as the generator to reproduce the same type of chaos in other systems. On the other hand, the crucial phenomenon in the hyperchaotic systems is the existence of two or more positive Lyapunov exponents and the type of chaos is not taken into account. In our way of morphogenesis, the critical situation is rather the replication of a known type of chaos.

The paper [62] was one of the first papers that considers mathematically the self-replicating forms using a set of reaction-diffusion equations [63]. Taking inspiration from the ideas of Turing, Smale [64] considers the problem of whether oscillations can be generated through coupling of identical systems which tend to an equilibrium. A similar question is also reasonable for the achievement of chaos in such systems and it is found out that, without using a chaotic input, it is possible to obtain coupled systems which exhibit chaotic behavior. The existence of strange attractors in a family of vector fields consisting of two Brusselators linearly coupled by diffusion is proved analytically in the paper [65] and numerical examples of such a chaotic behavior are provided in [66]. Such couplings display several cases of Hopf-pitchfork singularities of codimensions 2–4. In all these cases, the corresponding bifurcation diagrams provide regions of parameters such that the system exhibits synchronization, regions where synchronization depends on the initial state and regions where orbits show infinitely many transients of synchronization [67]. Another example of a linearly coupled system which exhibit chaotic behavior can be found in [68]. According to the results of paper [68], a sufficiently large coupling coefficient used in a network of linearly coupled identical systems, where each node is located in a non-chaotic region, leads to existence of a positive transversal Lyapunov exponent and makes the system behave chaotically. The Lorenz systems with stable equilibriums can be used in the construction of such a network of linearly coupled systems. Distinctively, in our paper, we make use of coupled systems such that exactly one of them is chaotic with a known type of chaos and prove theoretically that the same type of chaos is extended. Moreover, in the presented mechanism, we are not restricted to use linear couplings as well as identical systems.

In the next section, we will present assumptions for systems (1.1) and (1.2) which are needed for the chaos replication, and introduce the chaotic attractors of these systems in the functional sense.

2. Preliminaries

In the paper $\mathbb{R}$ and $\mathbb{N}$ denote the sets of real numbers and natural numbers, respectively, and the uniform norm $\|\Gamma\| = \sup_{\|v\|=1}\|\Gamma v\|$ for matrices is used in the paper.

Since the matrix A, which is aforementioned in system (1.2), is supposed to admit eigenvalues all with negative real parts, it is easy to verify the existence of positive real numbers N and ω such that $\|e^{At}\| \leqslant Ne^{-\omega t}, t \geqslant 0$. These numbers will be used in the last condition below.

The following assumptions on systems (1.1) and (1.2) are needed throughout the paper:

(A1) There exists a positive real number T such that the function $F(t,x)$ satisfies the periodicity condition $F(t+T,x) = F(t,x)$, for all $t \in \mathbb{R},\ x \in \mathbb{R}^m$;
(A2) There exists a positive real number L_0 such that $\|F(t,x_1) - F(t,x_2)\| \leqslant L_0\|x_1 - x_2\|$, for all $t \in \mathbb{R},\ x_1, x_2 \in \mathbb{R}^m$;
(A3) There exists a positive number $H_0 < \infty$ such that $\sup_{t\in\mathbb{R},\ x\in\mathbb{R}^m}\|F(t,x)\| \leqslant H_0$;
(A4) There exists a positive real number L_1 such that $\|g(x_1,y) - g(x_2,y)\| \geqslant L_1\|x_1 - x_2\|$, for all $x_1, x_2 \in \mathbb{R}^m,\ y \in \mathbb{R}^n$;

(A5) There exist positive real numbers L_2 and L_3 such that $\|g(x_1,y)-g(x_2,y)\| \leqslant L_2\|x_1-x_2\|$, for all $x_1,x_2 \in \mathbb{R}^m,\ y \in \mathbb{R}^n$, and $\|g(x,y_1)-g(x,y_2)\| \leqslant L_3\|y_1-y_2\|$, for all $x \in \mathbb{R}^m,\ y_1,y_2 \in \mathbb{R}^n$;
(A6) There exists a positive number $M_0 < \infty$ such that $\sup_{x\in\mathbb{R}^m,\ y\in\mathbb{R}^n}\|g(x,y)\| \leqslant M_0$;
(A7) $NL_3 - \omega < 0$.

Remark 2.1. The results presented in the remaining parts are also true even if we replace the non-autonomous system (1.1) by the autonomous equation

$$x' = \overline{F}(x), \tag{2.7}$$

where the function $\overline{F}: \mathbb{R}^m \to \mathbb{R}^m$ is continuous with conditions which are counterparts of (A2) and (A3).

At the present time, systems of differential equations which are known to exhibit chaotic behavior are either nonautonomous and periodic in time such as the Duffing and Van der Pol oscillators or autonomous such as the Lorenz, Chua and R"ossler systems. In a similar way, in our investigations of chaos generation, we take advantage of periodic nonautonomous systems as well as autonomous ones as generators.

Using the theory of quasilinear equations [69], one can verify that for a given solution $x(t)$ of system (1.1), there exists a unique bounded on $\mathbb{R}$ solution $y(t)$ of the system $y' = Ay + g(x(t),y)$, denoted by $y(t) = \phi_{x(t)}(t)$ throughout the paper, which satisfies the integral equation

$$y(t) = \int_{-\infty}^{t} e^{A(t-s)}g(x(s),y(s))ds. \tag{2.8}$$

Our main assumption is the existence of a nonempty set $\mathscr{A}_x$ of all solutions of system (1.1), uniformly bounded on $\mathbb{R}$. That is, there exists a positive real number H such that $\sup_{t\in\mathbb{R}}\|x(t)\| \leqslant H$, for all $x(t) \in \mathscr{A}_x$.

Let us introduce the sets of functions

$$\mathscr{A}_y = \left\{\phi_{x(t)}(t) | x(t) \in \mathscr{A}_x\right\} \tag{2.9}$$

and

$$\mathscr{A} = \left\{(x(t), \phi_{x(t)}(t)) | x(t) \in \mathscr{A}_x\right\}. \tag{2.10}$$

We note that for all $y(t) \in \mathscr{A}_y$ one has $\sup_{t\in\mathbb{R}}\|y(t)\| \leqslant M$, where $M = \frac{NM_0}{\omega}$.

Next, we reveal that if the set $\mathscr{A}_x$ is an attractor with basin $\mathscr{U}_x$, that is, for each $x(t) \in \mathscr{U}_x$ there exists $\overline{x}(t) \in \mathscr{A}_x$ such that $\|x(t)-\overline{x}(t)\| \to 0$ as $t \to \infty$, then the set $\mathscr{A}_y$ is also an attractor in the same sense. In the next lemma we specify the basin of attraction of $\mathscr{A}_y$. Define the set

$$\mathscr{U}_y = \{y(t) | y(t) \text{ is a solution of the system } y' = Ay + g(x(t),y) \text{ for some } x(t) \in \mathscr{U}_x\}. \tag{2.11}$$

Lemma 2.1. *$\mathscr{U}_y$ is a basin of $\mathscr{A}_y$.*

Proof. Fix an arbitrary positive real number ϵ and let $y(t) \in \mathscr{U}_y$ be a given solution of the system $y' = Ay + g(x(t),y)$ for some $x(t) \in \mathscr{U}_x$. In this case, there exists $\overline{x}(t) \in \mathscr{A}_x$ such that $\|x(t)-\overline{x}(t)\| \to 0$ as $t \to \infty$. Let $\alpha = \frac{\omega - NL_3}{\omega - NL_3 + NL_2}$ and $\overline{y}(t) = \phi_{\overline{x}(t)}(t)$. Condition (A7) implies that the number α is positive. Under the circumstances, one can find $R_0 = R_0(\epsilon) > 0$ such that if $t \geqslant R_0$ then $\|x(t)-\overline{x}(t)\| < \alpha\epsilon$ and $N\|y(R_0)-\overline{y}(R_0)\|e^{(NL_3-\omega)t} < \alpha\epsilon$. The functions $y(t)$ and $\overline{y}(t)$ satisfy the relations

$$y(t) = e^{A(t-R_0)}y(R_0) + \int_{R_0}^{t} e^{A(t-s)}g(x(s),y(s))ds$$

and

$$\overline{y}(t) = e^{A(t-R_0)}\overline{y}(R_0) + \int_{R_0}^{t} e^{A(t-s)}g(\overline{x}(s),\overline{y}(s))ds,$$

respectively. Making use of these relations one has

$$y(t)-\overline{y}(t) = e^{A(t-R_0)}(y(R_0)-\overline{y}(R_0)) + \int_{R_0}^{t} e^{A(t-s)}[g(x(s),y(s)) - g(x(s),\overline{y}(s))]ds + \int_{R_0}^{t} e^{A(t-s)}[g(x(s),\overline{y}(s)) - g(\overline{x}(s),\overline{y}(s))]ds.$$

Therefore, we have

$$\|y(t)-\overline{y}(t)\| \leqslant Ne^{-\omega(t-R_0)}\|y(R_0)-\overline{y}(R_0)\| + \frac{NL_2\alpha\epsilon}{\omega}e^{-\omega t}\left(e^{\omega t} - e^{\omega R_0}\right) + NL_3\int_{R_0}^{t} e^{-\omega(t-s)}\|y(s)-\overline{y}(s)\|ds.$$

Let $u:[R_0,\infty)\to[0,\infty)$ be a function defined as $u(t)=e^{\omega t}\|y(t)-\overline{y}(t)\|$. Through this definition we reach the inequality

$$u(t)\leqslant Ne^{\omega R_0}\|y(R_0)-\overline{y}(R_0)\|+\frac{NL_2\alpha\epsilon}{\omega}\left(e^{\omega t}-e^{\omega R_0}\right)+NL_3\int_{R_0}^{t}u(s)ds.$$

Now, let $\psi(t)=\frac{NL_2\alpha\epsilon}{\omega}e^{\omega t}$ and $\phi(t)=\psi(t)+c$, where $c=Ne^{\omega R_0}\|y(R_0)-\overline{y}(R_0)\|-\frac{NL_2\alpha\epsilon}{\omega}e^{\omega R_0}$. Using these functions we get

$$u(t)\leqslant\phi(t)+NL_3\int_{R_0}^{t}u(s)ds.$$

Applying Gronwall's Lemma [70] to the last inequality for $t\geqslant R_0$, we attain the inequality

$$u(t)\leqslant c+\psi(t)+NL_3\int_{R_0}^{t}e^{NL_3(t-s)}cds+NL_3\int_{R_0}^{t}e^{NL_3(t-s)}\psi(s)ds$$

and hence,

$$\begin{aligned}u(t)&\leqslant c+\psi(t)+c\left(e^{NL_3(t-R_0)}-1\right)+\frac{N^2L_2L_3\alpha\epsilon}{\omega(\omega-NL_3)}e^{\omega t}\left(1-e^{(NL_3-\omega)(t-R_0)}\right)\\&=\frac{NL_2\alpha\epsilon}{\omega}e^{\omega t}+N\|y(R_0)-\overline{y}(R_0)\|e^{\omega R_0}e^{NL_3(t-R_0)}-\frac{NL_2\alpha\epsilon}{\omega}e^{\omega R_0}e^{NL_3(t-R_0)}+\frac{N^2L_2L_3\alpha\epsilon}{\omega(\omega-NL_3)}e^{\omega t}\left(1-e^{(NL_3-\omega)(t-R_0)}\right).\end{aligned}$$

Thus,

$$\begin{aligned}\|y(t)-\overline{y}(t)\|&\leqslant\frac{NL_2\alpha\epsilon}{\omega}+N\|y(R_0)-\overline{y}(R_0)\|e^{(NL_3-\omega)(t-R_0)}-\frac{NL_2\alpha\epsilon}{\omega}e^{(NL_3-\omega)(t-R_0)}+\frac{N^2L_2L_3\alpha\epsilon}{\omega(\omega-NL_3)}\left(1-e^{(NL_3-\omega)(t-R_0)}\right)\\&<N\|y(R_0)-\overline{y}(R_0)\|e^{(NL_3-\omega)(t-R_0)}+\frac{NL_2\alpha\epsilon}{\omega-NL_3}.\end{aligned}$$

Consequently, for $t\geqslant 2R_0$, we have $\|y(t)-\overline{y}(t)\|<\left(1+\frac{NL_2}{\omega-NL_3}\right)\alpha\epsilon=\epsilon$, and hence $\|y(t)-\overline{y}(t)\|\to 0$ as $t\to\infty$.
The proof of the lemma is completed. □

Now, let us define the set

$$\mathscr{U}=\{(x(t),y(t))|(x(t),y(t))\text{ is a solution of system (1.1) and (1.2) such that }x(t)\in\mathscr{U}_x\}.$$

Next, we state the following corollary of Lemma 2.1.

Corollary 2.1. *$\mathscr{U}$ is a basin of $\mathscr{A}$.*

Proof. Let $(x(t),y(t))\in\mathscr{U}$ be a given solution of the coupled system (1.1)+(1.2). According to Lemma 2.1, one can find $(\overline{x}(t),\overline{y}(t))\in\mathscr{A}$ such that $\|x(t)-\overline{x}(t)\|\to 0$ as $t\to\infty$ and $\|y(t)-\overline{y}(t)\|\to 0$ as $t\to\infty$. Consequently, $\|(x(t),y(t))-(\overline{x}(t),\overline{y}(t))\|\to 0$ as $t\to\infty$. The proof is finalized. □

3. Description of chaotic sets of functions

In this section of the paper, the descriptions for the chaotic sets of continuous functions will be introduced and the definitions of the chaotic features will be presented, both in the Devaney's sense and in the sense of Li-Yorke.

Let us denote by

$$\mathscr{B}=\{\psi(t)|\psi:\mathbb{R}\to K\text{ is continuous}\}\tag{3.12}$$

a collection of functions, where $K\subset\mathbb{R}^q$, $q\in\mathbb{N}$, is a bounded region.

We start with the description of chaotic sets of functions in Devaney's sense and then continue with the Li-Yorke counterpart.

3.1. Chaotic set of functions in Devaney's sense

In this part, we shall elucidate the ingredients of the chaos in Devaney's sense for the set $\mathscr{B}$, which is introduced by (3.12), and the first definition is about the sensitivity of chaotic sets of functions.

Definition 3.1. $\mathscr{B}$ is called sensitive if there exist positive numbers ϵ and Δ such that for every $\psi(t)\in\mathscr{B}$ and for arbitrary $\delta>0$ there exist $\overline{\psi}(t)\in\mathscr{B}$, $t_0\in\mathbb{R}$ and an interval $J\subset[t_0,\infty)$, with length not less than Δ, such that $\|\psi(t_0)-\overline{\psi}(t_0)\|<\delta$ and $\|\psi(t)-\overline{\psi}(t)\|>\epsilon$, for all $t\in J$.

Definition 3.1 considers the inequality ($> \epsilon$) over the interval J. In the Devaney's chaos definition for the map, the inequality is assumed for discrete moments. Let us reveal how one can extend the inequality from a discrete point to an interval by considering continuous flows.

In [21], it is indicated that a continuous map $\varphi : \Lambda \to \Lambda$, with an invariant domain $\Lambda \subset \mathbb{R}^k,\ k \in \mathbb{N}$, has sensitive dependence on initial conditions if there exists $\overline{\epsilon} > 0$ such that for any $x \in \Lambda$ and any neighborhood $\mathscr{U}$ of x, there exist $y \in \mathscr{U}$ and a natural number n such that $\|\varphi^n(x) - \varphi^n(y)\| > \overline{\epsilon}$.

Suppose that the set $\mathscr{A}_x$ satisfies the definition of sensitivity in the following sense. There exists $\overline{\epsilon} > 0$ such that for every $x(t) \in \mathscr{A}_x$ and arbitrary $\delta > 0$, there exist $\overline{x}(t) \in \mathscr{A}_x,\ t_0 \in \mathbb{R}$ and a real number $\zeta \geqslant t_0$ such that $\|x(t_0) - \overline{x}(t_0)\| < \delta$ and $\|x(\zeta) - \overline{x}(\zeta)\| > \overline{\epsilon}$.

In this case, for given $x(t) \in \mathscr{A}_x$ and $\delta > 0$, one can find $\overline{x}(t) \in \mathscr{A}_x$ and $\zeta \geqslant t_0$ such that $\|x(t_0) - \overline{x}(t_0)\| < \delta$ and $\|x(\zeta) - \overline{x}(\zeta)\| > \overline{\epsilon}$. Let $\Delta = \frac{\overline{\epsilon}}{8HL_0}$ and take a number Δ_1 such that $\Delta \leqslant \Delta_1 \leqslant \frac{\overline{\epsilon}}{4HL_0}$. Using appropriate integral equations for $t \in [\zeta, \zeta + \Delta_1]$, it can be verified that

$$\|x(t) - \overline{x}(t)\| \geqslant \|x(\zeta) - \overline{x}(\zeta)\| - \left\| \int_\zeta^t [F(s, x(s)) - F(s, \overline{x}(s))] ds \right\| > \overline{\epsilon} - 2HL_0\Delta_1 \geqslant \frac{\overline{\epsilon}}{2}.$$

The last inequality confirms that $\mathscr{A}_x$ satisfies Definition 3.1 with $\epsilon = \overline{\epsilon}/2$ and $J = [\zeta, \zeta + \Delta_1]$. So the definition is a natural one. It provides more information then discrete moments and for us it is important that the extension on the interval is useful to prove the property for chaos extension.

In the next two definitions, we continue with the existence of a dense function in the set of chaotic functions followed by the transitivity property.

Definition 3.2. $\mathscr{B}$ possesses a dense function $\psi^*(t) \in \mathscr{B}$ if for every function $\psi(t) \in \mathscr{B}$, arbitrary small $\epsilon > 0$ and arbitrary large $E > 0$, there exist a number $\xi > 0$ and an interval $J \subset \mathbb{R}$, with length E, such that $\|\psi(t) - \psi^*(t + \xi)\| < \epsilon$, for all $t \in J$.

Definition 3.3. $\mathscr{B}$ is called transitive if it possesses a dense function.

Now, let us recall the definition of transitivity for maps [21]. A continuous map φ with an invariant domain $\Lambda \subset \mathbb{R}^k,\ k \in \mathbb{N}$, possesses a dense orbit if there exists $c^* \in \Lambda$ such that for each $c \in \Lambda$ and arbitrary real number $\epsilon > 0$, there exist natural numbers k_0 and l_0 such that $\|\varphi^{l_0}(c) - \varphi^{l_0+k_0}(c^*)\| < \epsilon$, and maps which have dense orbits are called transitive.

Suppose that $\mathscr{A}_x$ satisfies the transitivity property in the following sense. There exists a function $x^*(t) \in \mathscr{A}_x$ such that for each $x(t) \in \mathscr{A}_x$ and arbitrary positive real number ϵ, there exist a real number ζ_0 and a natural number m_0 such that $\|x(\zeta_0) - x^*(\zeta_0 + m_0T)\| < \epsilon$.

Fix an arbitrary function $x(t) \in \mathscr{A}_x$, arbitrary small $\epsilon > 0$ and arbitrary large $E > 0$. Under the circumstances, one can find $\zeta_0 \in \mathbb{R}$ and $m_0 \in \mathbb{N}$ such that $\|x(\zeta_0) - x^*(\zeta_0 + m_0T)\| < \epsilon e^{-L_0E}$.

Using the condition (A2) together with the convenient integral equations that $x(t)$ and $x^*(t)$ satisfy, it is easy to obtain for $t \in [\zeta_0, \zeta_0 + E]$ that

$$\|x(t) - x^*(t + m_0T)\| \leqslant \|x(\zeta_0) - x^*(\zeta_0 + m_0T)\| + \int_{\zeta_0}^t L_0\|x(s) - x^*(s + m_0T)\| ds$$

and by the help of the Gronwall–Bellman inequality [71], we get

$$\|x(t) - x^*(t + m_0T)\| \leqslant \|x(\zeta_0) - x^*(\zeta_0 + m_0T)\| e^{L_0(t-\zeta_0)} < \epsilon.$$

The last inequality shows that the set $\mathscr{A}_x$ satisfies Definition 3.2 with $\xi = k_0T$ and is transitive in accordance with Definition 3.3.

The following definition describes the density of periodic functions inside $\mathscr{B}$.

Definition 3.4. $\mathscr{B}$ admits a dense collection $\mathscr{G} \subset \mathscr{B}$ of periodic functions if for every function $\psi(t) \in \mathscr{B}$, arbitrary small $\epsilon > 0$ and arbitrary large $E > 0$, there exist $\widetilde{\psi}(t) \in \mathscr{G}$ and an interval $J \subset \mathbb{R}$, with length E, such that $\left\|\psi(t) - \widetilde{\psi}(t)\right\| < \epsilon$, for all $t \in J$.

Let us remind the definition of density of periodic orbits for maps [21]. The set of periodic orbits of a continuous map φ with an invariant domain $\Lambda \subset \mathbb{R}^k,\ k \in \mathbb{N}$, is called dense in Λ if for each $c \in \Lambda$, arbitrary positive real number ϵ, there exist a natural number l_0 and a point $\widetilde{c} \in \Lambda$ such that the sequence $\{\varphi^i(\widetilde{c})\}$ is periodic and $\left\|\varphi^{l_0}(c) - \varphi^{l_0}(\widetilde{c})\right\| < \epsilon$.

Let us denote by $\mathscr{G}_x$ the set of all periodic functions inside $\mathscr{A}_x$. Suppose that $\mathscr{A}_x$ satisfies density of periodic solutions as follows. For an arbitrary function $x(t) \in \mathscr{A}_x$ and arbitrary small $\epsilon > 0$ there exist a periodic function $\widetilde{x}(t) \in \mathscr{G}_x$ and a number $\zeta_0 \in \mathbb{R}$ such that $\|x(\zeta_0) - \widetilde{x}(\zeta_0)\| < \epsilon$.

Let us fix an arbitrary function $x(t) \in \mathscr{A}_x$, arbitrary small $\epsilon > 0$ and arbitrary large $E > 0$. In that case, there exist a periodic function $\widetilde{x}(t) \in \mathscr{G}_x$ and $\zeta_0 \in \mathbb{R}$ such that $\|x(\zeta_0) - \widetilde{x}(\zeta_0)\| < \epsilon e^{-L_0E}$.

It can be easily verified for $t \in [\zeta_0, \zeta_0 + E]$ that the inequality

$$\left\|x(t) - \widetilde{x}(t)\right\| \leqslant \left\|x(\zeta_0) - \widetilde{x}(\zeta_0)\right\| + \int_{\zeta_0}^t L_0\left\|x(s) - \widetilde{x}(s)\right\| ds,$$

holds, and therefore for each t from the same interval of time we have

$$\|x(t) - \widetilde{x}(t)\| \leqslant \|x(\zeta_0) - \widetilde{x}(\zeta_0)\| e^{L_0(t-\zeta_0)} < \epsilon.$$

Consequently, the set $\mathscr{A}_x$ satisfies Definition 3.4 with $J = [\zeta_0, \zeta_0 + E]$.

Finally, we introduce in the next definition the chaotic set of functions in Devaney's sense.

Definition 3.5. The collection $\mathscr{B}$ of functions is called a Devaney's chaotic set if

(D1) $\mathscr{B}$ is sensitive;
(D2) $\mathscr{B}$ is transitive;
(D3) $\mathscr{B}$ admits a dense collection of periodic functions.

In the next subsection, the chaotic properties of the set $\mathscr{B}$ will be imposed in the sense of Li-Yorke.

3.2. Chaotic set of functions in Li-Yorke sense

The ingredients of Li-Yorke chaos for the collection of functions $\mathscr{B}$, which is defined by (3.12), will be described in this part of the paper. Making use of discussions similar to the ones made in the previous subsection, we extend, below, the definitions for the ingredients of Li-Yorke chaos from maps [72–75] to continuous flows and we just omit these indications here.

Definition 3.6. A couple of functions $(\psi(t), \overline{\psi}(t)) \in \mathscr{B} \times \mathscr{B}$ is called proximal if for arbitrary small $\epsilon > 0$ and arbitrary large $E > 0$, there exist infinitely many disjoint intervals of length not less than E such that $\|\psi(t) - \overline{\psi}(t)\| < \epsilon$, for each t from these intervals.

Definition 3.7. A couple of functions $(\psi(t), \overline{\psi}(t)) \in \mathscr{B} \times \mathscr{B}$ is frequently (ϵ_0, Δ) – separated if there exist positive real numbers ϵ_0, Δ and infinitely many disjoint intervals of length not less than Δ, such that $\|\psi(t) - \overline{\psi}(t)\| > \epsilon_0$, for each t from these intervals.

Remark 3.1. The numbers ϵ_0 and Δ taken into account in Definition 3.7 depend on the functions $\psi(t)$ and $\overline{\psi}(t)$.

Definition 3.8. A couple of functions $(\psi(t), \overline{\psi}(t)) \in \mathscr{B} \times \mathscr{B}$ is a Li-Yorke pair if they are proximal and frequently (ϵ_0, Δ) – separated for some positive numbers ϵ_0 and Δ.

Definition 3.9. An uncountable set $\mathscr{C} \subset \mathscr{B}$ is called a scrambled set if $\mathscr{C}$ does not contain any periodic functions and each couple of different functions inside $\mathscr{C} \times \mathscr{C}$ is a Li-Yorke pair.

Definition 3.10. $\mathscr{B}$ is called a Li-Yorke chaotic set if

(LY1) There exists a positive real number T_0 such that $\mathscr{B}$ admits a periodic function of period kT_0, for any $k \in \mathbb{N}$;
(LY2) $\mathscr{B}$ possesses a scrambled set $\mathscr{C}$;
(LY3) For any function $\psi(t) \in \mathscr{C}$ and any periodic function $\overline{\psi}(t) \in \mathscr{B}$, the couple $(\psi(t), \overline{\psi}(t))$ is frequently (ϵ_0, Δ) – separated for some positive real numbers ϵ_0 and Δ.

4. Hyperbolic set of functions

The definitions of stable and unstable sets of hyperbolic periodic orbits of autonomous systems are given in [76], and information about such sets of solutions of perturbed non-autonomous systems can be found in [77]. Moreover, homoclinic structures in almost periodic systems were studied in [78–80]. In this section, we give a definition for hyperbolic collection of uniformly bounded functions and before this, we start with the descriptions of stable and unstable sets of a function.

We define the stable set of a function $\psi(t) \in \mathscr{B}$, where the collection $\mathscr{B}$ is defined by (3.12), as the set of functions

$$W^s(\psi(t)) = \{u(t) \in \mathscr{B} | \|u(t) - \psi(t)\| \to 0 \text{ as } t \to \infty\}, \tag{4.13}$$

and, similarly, we define the unstable set of a function $\psi(t) \in \mathscr{B}$ as the set of functions

$$W^u(\psi(t)) = \{v(t) \in \mathscr{B} | \|v(t) - \psi(t)\| \to 0 \text{ as } t \to -\infty\}. \tag{4.14}$$

Definition 4.1. The set of functions $\mathscr{B}$ is called hyperbolic if each function inside this set has nonempty stable and unstable sets.

Theorem 4.1. *If $\mathscr{A}_x$ is hyperbolic, then the same is true for $\mathscr{A}_y$.*

Proof. Fix arbitrary $\epsilon > 0, y(t) = \phi_{x(t)}(t) \in \mathscr{A}_y$, and let $\alpha = \frac{\omega - NL_3}{\omega - NL_3 + NL_2}, \beta = \frac{\omega - NL_3}{1 + NL_2}$. By condition (A7), one can verify that the numbers α and β are both positive.

Due to hyperbolicity of $\mathscr{A}_x$, the function $x(t)$ has a nonempty stable set $W^s(x(t))$ and a nonempty unstable set $W^u(x(t))$.

Let us take an arbitrary function $u(t) \in W^s(x(t))$. Since $\|x(t) - u(t)\| \to 0$ as $t \to \infty$ and $NL_3 - \omega < 0$, there exists a positive number R_1, which depends on ϵ, such that $\|x(t) - u(t)\| < \alpha\epsilon$ and $e^{(NL_3 - \omega)t} < \frac{\omega\alpha\epsilon}{2M_0N}$, for $t \geqslant R_1$. Let $\overline{y}(t) = \phi_{u(t)}(t)$. We shall prove that the function $\overline{y}(t)$ belongs to the stable set of $y(t)$.

The bounded on $\mathbb{R}$ functions $y(t)$ and $\overline{y}(t)$ satisfy the relations

$$y(t) = \int_{-\infty}^{t} e^{A(t-s)} g(x(s), y(s)) ds$$

and

$$\overline{y}(t) = \int_{-\infty}^{t} e^{A(t-s)} g(u(s), \overline{y}(s)) ds,$$

respectively, for $t \geqslant R_1$.

Therefore one can easily reach up the equation

$$\begin{aligned} y(t) - \overline{y}(t) = &\int_{-\infty}^{R_1} e^{A(t-s)} [g(x(s), y(s)) - g(u(s), \overline{y}(s))] ds \\ &+ \int_{R_1}^{t} e^{A(t-s)} \{[g(x(s), y(s)) - g(x(s), \overline{y}(s))] + [g(x(s), \overline{y}(s)) - g(u(s), \overline{y}(s))]\} ds, \end{aligned}$$

which implies that

$$\begin{aligned} \|y(t) - \overline{y}(t)\| &\leqslant \int_{-\infty}^{R_1} 2M_0 N e^{-\omega(t-s)} ds + \int_{R_1}^{t} e^{-\omega(t-s)} (NL_3 \|y(s) - \overline{y}(s)\| + NL_2 \|x(s) - u(s)\|) ds \\ &\leqslant \frac{2M_0 N}{\omega} e^{-\omega(t-R_1)} + \int_{R_1}^{t} e^{-\omega(t-s)} (NL_3 \|y(s) - \overline{y}(s)\| + NL_2 \alpha\epsilon) ds. \end{aligned}$$

Using the Gronwall type inequality indicated in [81], we achieve that

$$\|y(t) - \overline{y}(t)\| \leqslant \frac{2M_0 N}{\omega} e^{(NL_3 - \omega)(t-R_1)} + \frac{NL_2 \alpha\epsilon}{\omega - NL_3} [1 - e^{(NL_3 - \omega)(t-R_1)}], \ t \geqslant R_1.$$

For this reason, for all $t \geqslant 2R_1$, one has

$$\|y(t) - \overline{y}(t)\| \leqslant \frac{2M_0 N}{\omega} e^{(NL_3 - \omega)R_1} + \frac{NL_2 \alpha\epsilon}{\omega - NL_3} < \left(1 + \frac{NL_2}{\omega - NL_3}\right) \alpha\epsilon = \epsilon.$$

The last inequality reveals that $\|y(t) - \overline{y}(t)\| \to 0$ as $t \to \infty$, and hence $\overline{y}(t)$ belongs to the stable set $W^s(y(t))$ of $y(t)$.

On the other hand, let $v(t)$ be a function inside the unstable set $W^u(x(t))$.

Since $\|x(t) - v(t)\| \to 0$ as $t \to -\infty$, there exists a negative real number $R_2(\epsilon)$ such that $\|x(t) - v(t)\| < \beta\epsilon$, for $t \leqslant R_2$. Let $\widetilde{y}(t) = \phi_{v(t)}(t)$. Now, our purpose is to show that $\widetilde{y}(t)$ belongs to the unstable set of $y(t)$.

By the help of the integral equations

$$y(t) = \int_{-\infty}^{t} e^{A(t-s)} g(x(s), y(s)) ds$$

and

$$\widetilde{y}(t) = \int_{-\infty}^{t} e^{A(t-s)} g(v(s), \widetilde{y}(s)) ds,$$

we obtain that

$$y(t) - \widetilde{y}(t) = \int_{-\infty}^{t} e^{A(t-s)} [g(x(s), y(s)) - g(v(s), y(s))] ds + \int_{-\infty}^{t} e^{A(t-s)} [g(v(s), y(s)) - g(v(s), \widetilde{y}(s))] ds.$$

Therefore, for $t \leqslant R_2$, one has

$$\|y(t)-\widetilde{y}(t)\| \leqslant \int_{-\infty}^{t} NL_2 e^{-\omega(t-s)}\|x(t)-v(t)\|ds + \int_{-\infty}^{t} e^{-\omega(t-s)}NL_3\|y(s)-\widetilde{y}(s)\|ds \leqslant \frac{NL_2\beta\epsilon}{\omega} + \frac{NL_3}{\omega}\sup_{t\leqslant R_2}\|y(t)-\widetilde{y}(t)\|.$$

Hence,

$$\sup_{t\leqslant R_2}\|y(t)-\widetilde{y}(t)\| \leqslant \frac{NL_2\beta\epsilon}{\omega} + \frac{NL_3}{\omega}\sup_{t\leqslant R_2}\|y(t)-\widetilde{y}(t)\|$$

and

$$\sup_{t\leqslant R_2}\|y(t)-\widetilde{y}(t)\| \leqslant \frac{NL_2\beta\epsilon}{\omega - NL_3} < \epsilon.$$

The last inequality confirms that $\|y(t)-\widetilde{y}(t)\| \to 0$ as $t \to -\infty$. Therefore $\widetilde{y}(t) \in W^u(y(t))$.

Consequently, $\mathscr{A}_y$ is hyperbolic since $y(t)$ possesses both nonempty stable and unstable sets, denoted by $W^s(y(t))$ and $W^u(y(t))$, respectively.

The theorem is proved. □

Theorem 4.1 implies the following corollary.

Corollary 4.1. *If $\mathscr{A}_x$ is hyperbolic, then the same is true for $\mathscr{A}$.*

Next, we continue with another corollary of Theorem 4.1, following the definitions of homoclinic and heteroclinic functions.

A function $\psi_1(t) \in \mathscr{B}$ is said to be homoclinic to the function $\psi_0(t) \in \mathscr{B},\ \psi_0(t) \neq \psi_1(t)$, if $\psi_1(t) \in W^s(\psi_0(t)) \cap W^u(\psi_0(t))$.

On the other hand, a function $\psi_2(t) \in \mathscr{B}$ is called heteroclinic to the functions $\psi_0(t), \psi_1(t) \in \mathscr{B},\ \psi_0(t) \neq \psi_2(t),\ \psi_1(t) \neq \psi_2(t)$, if $\psi_2(t) \in W^s(\psi_0(t)) \cap W^u(\psi_1(t))$.

Corollary 4.2. *If $x_1(t) \in \mathscr{A}_x$ is homoclinic to the function $x_0(t) \in \mathscr{A}_x, x_0(t) \neq x(t)$, then $\phi_{x_1(t)}(t) \in \mathscr{A}_y$ is homoclinic to the function $\phi_{x_0(t)}(t) \in \mathscr{A}_y$. Similarly, if $x_2(t) \in \mathscr{A}_x$ is heteroclinic to the functions $x_0(t), x_1(t) \in \mathscr{A}_x,\ x_0(t) \neq x_2(t),\ x_1(t) \neq x_2(t)$, then $\phi_{x_2(t)}(t)$ is heteroclinic to the functions $\phi_{x_0(t)}(t), \phi_{x_1(t)}(t) \in \mathscr{A}_y$.*

In the next section, we theoretically prove that the set $\mathscr{A}_y$ replicates the ingredients of Devaney's chaos provided to the set $\mathscr{A}_x$ and as a consequence the same is valid also for the set $\mathscr{A}$. The same problem for the chaos in the sense of Li-Yorke will be handled in Section 6.

5. Replication of Devaney's chaos

In this part of our paper, we will prove theoretically that the ingredients of Devaney's chaos furnished to the set $\mathscr{A}_x$ are all replicated by the set $\mathscr{A}_y$. We start with the replication of sensitivity.

Lemma 5.1. *Sensitivity of the set $\mathscr{A}_x$ implies the same feature for the set $\mathscr{A}_y$.*

Proof. Fix an arbitrary $\delta > 0$ and let $y(t) \in \mathscr{A}_y$ be a given solution of system (1.2). In this case, there exists $x(t) \in \mathscr{A}_x$ such that $y(t) = \phi_{x(t)}(t)$.

Let us choose a number $\overline{\epsilon} = \overline{\epsilon}(\delta) > 0$ small enough which satisfies the inequality $\left(1 + \frac{NL_2}{\omega - NL_3}\right)\overline{\epsilon} < \delta$. Then take $R = R(\overline{\epsilon}) < 0$ sufficiently large in absolute value such that $\frac{2M_0N}{\omega}e^{(\omega - NL_3)R} < \overline{\epsilon}$, and let $\delta_1 = \delta_1(\overline{\epsilon}, R) = \overline{\epsilon}e^{L_0R}$. Since the set of functions $\mathscr{A}_x$ is sensitive, there exist positive real numbers ϵ_0 and Δ such that the inequalities $\|x(t_0) - \overline{x}(t_0)\| < \delta_1$ and $\|x(t) - \overline{x}(t)\| > \epsilon_0, t \in J$, hold for some $\overline{x}(t) \in \mathscr{A}_x, t_0 \in \mathbb{R}$ and for some interval $J \subset [t_0, \infty)$ whose length is not less than Δ.

Using the couple of integral equations

$$x(t) = x(t_0) + \int_{t_0}^{t} F(s, x(s))ds,$$

$$\overline{x}(t) = \overline{x}(t_0) + \int_{t_0}^{t} F(s, \overline{x}(s))ds$$

together with condition (A2), one see that the inequality

$$\|x(t) - \overline{x}(t)\| \leqslant \|x(t_0) - \overline{x}(t_0)\| + \left|\int_{t_0}^{t} L_0\|x(s) - \overline{x}(s)\|ds\right|$$

holds for $t \in [t_0 + R, t_0]$. Applying Gronwall–Bellman inequality [71], we obtain

$$\|x(t) - \overline{x}(t)\| \leqslant \|x(t_0) - \overline{x}(t_0)\|e^{L_0|t - t_0|}$$

and therefore $\|x(t) - \overline{x}(t)\| < \overline{\epsilon}$, for $t \in [t_0 + R, t_0]$.

Suppose that $\overline{y}(t) = \phi_{\overline{x}(t)}(t) \in \mathscr{A}_y$. First, we will show that $\|y(t_0) - \overline{y}(t_0)\| < \delta$.

The functions $y(t)$ and $\overline{y}(t)$ satisfy the integral equations

$$y(t) = \int_{-\infty}^{t} e^{A(t-s)} g(x(s), y(s)) ds$$

and

$$\overline{y}(t) = \int_{-\infty}^{t} e^{A(t-s)} g(\overline{x}(s), \overline{y}(s)) ds,$$

respectively. Therefore,

$$y(t) - \overline{y}(t) = \int_{-\infty}^{t} e^{A(t-s)} [g(x(s), y(s)) - g(\overline{x}(s), \overline{y}(s))] ds$$

and hence we obtain

$$\begin{aligned} \|y(t) - \overline{y}(t)\| \leqslant & \int_{t_0+R}^{t} N e^{-\omega(t-s)} \|g(x(s), y(s)) - g(x(s), \overline{y}(s))\| ds + \int_{t_0+R}^{t} N e^{-\omega(t-s)} \|g(x(s), \overline{y}(s)) - g(\overline{x}(s), \overline{y}(s))\| ds \\ & + \int_{-\infty}^{t_0+R} N e^{-\omega(t-s)} \|g(x(s), y(s)) - g(\overline{x}(s), \overline{y}(s))\| ds. \end{aligned}$$

Since $\|x(t) - \overline{x}(t)\| < \overline{\epsilon}$ for $t \in [t_0 + R, t_0]$, one has

$$\|y(t) - \overline{y}(t)\| \leqslant NL_3 \int_{t_0+R}^{t} e^{-\omega(t-s)} \|y(s) - \overline{y}(s)\| ds + \frac{NL_2\overline{\epsilon}}{\omega} e^{-\omega t}(e^{\omega t} - e^{\omega(t_0+R)}) + \frac{2M_0N}{\omega} e^{-\omega(t-t_0-R)}.$$

Now, let us introduce the functions $u(t) = e^{\omega t}\|y(t) - \overline{y}(t)\|$, $k(t) = \frac{NL_2\overline{\epsilon}}{\omega} e^{\omega t}$ and $h(t) = c + k(t)$, where $c = \left(\frac{2M_0N}{\omega} - \frac{NL_2\overline{\epsilon}}{\omega}\right) e^{\omega(t_0+R)}$.

These definitions give us the inequality

$$u(t) \leqslant h(t) + \int_{t_0+R}^{t} NL_3 u(s) ds.$$

Applying Lemma 2.2 [82] to the last inequality, we achieve that $u(t) \leqslant h(t) + NL_3 \int_{t_0+R}^{t} e^{NL_3(t-s)} h(s) ds$.

Therefore, on the time interval $[t_0 + R, t_0]$, the inequality

$$\begin{aligned} u(t) &\leqslant c + k(t) + c\left(e^{NL_3(t-t_0-R)} - 1\right) + \frac{N^2L_2L_3\overline{\epsilon}}{\omega} e^{NL_3 t} \int_{t_0+R}^{t} e^{(\omega - NL_3)s} ds \\ &= \frac{NL_2\overline{\epsilon}}{\omega} e^{\omega t} + \left(\frac{2M_0N}{\omega} - \frac{NL_2\overline{\epsilon}}{\omega}\right) e^{\omega R} e^{NL_3(t-t_0-R)} + \frac{N^2L_2L_3\overline{\epsilon}}{\omega(\omega - NL_3)} e^{\omega t}\left[1 - e^{(NL_3-\omega)(t-t_0-R)}\right] \end{aligned}$$

holds.

The last inequality leads to

$$\|y(t) - \overline{y}(t)\| \leqslant \frac{NL_2\overline{\epsilon}}{\omega - NL_3} + \frac{2M_0N}{\omega} e^{(NL_3-\omega)(t-t_0-R)}$$

and consequently we obtain that

$$\|y(t_0) - \overline{y}(t_0)\| \leqslant \frac{NL_2\overline{\epsilon}}{\omega - NL_3} + \frac{2M_0N}{\omega} e^{(\omega - NL_3)R} < \left(1 + \frac{NL_2}{\omega - NL_3}\right)\overline{\epsilon} < \delta.$$

In the remaining part of the proof, we will show the existence of a positive number ϵ_1 and an interval $J^1 \subset J$, with a fixed length which is independent of $y(t), \overline{y}(t) \in \mathscr{A}_y$, such that the inequality $\|y(t) - \overline{y}(t)\| > \epsilon_1$ holds for all $t \in J^1$.

Suppose that $g(x, y) = \begin{pmatrix} g_1(x, y) \\ g_2(x, y) \\ \vdots \\ g_n(x, y) \end{pmatrix}$, where each g_j, $1 \leqslant j \leqslant n$, is a real valued function.

Since for each $x(t) \in \mathscr{A}_x$ the functions $x'(t)$ and $\phi'_{x(t)}(t)$ lie inside the tubes with radii H_0 and $\|A\|M + M_0$, respectively, one can conclude that the set of functions $\mathscr{A}_x$ and $\mathscr{A}_y$ are both equicontinuous on $\mathbb{R}$. Making use of the uniform continuity of the function $\overline{g} : \mathbb{R}^m \times \mathbb{R}^m \times \mathbb{R}^n \to \mathbb{R}^n$ defined as $\overline{g}(x_1, x_2, x_3) = g(x_1, x_3) - g(x_2, x_3)$ on the compact region

$$\mathscr{D} = \{(x_1, x_2, x_3) \in \mathbb{R}^m \times \mathbb{R}^m \times \mathbb{R}^n | \|x_1\| \leqslant H, \|x_2\| \leqslant H, \|x_3\| \leqslant M\},$$

together with the equicontinuity of the sets $\mathscr{A}_x$ and $\mathscr{A}_y$, one can easily verify that the set

$$\mathscr{F} = \left\{ g_j(x(t), \phi_{x(t)}(t)) - g_j(\bar{x}(t), \phi_{x(t)}(t)) | 1 \leqslant j \leqslant n, x(t) \in \mathscr{A}_x, \bar{x}(t) \in \mathscr{A}_x \right\} \tag{5.15}$$

is an equicontinuous family on $\mathbb{R}$.

Therefore, there exists a positive real number $\tau < \Delta$, independent of the functions $x(t), \bar{x}(t) \in \mathscr{A}_x,\ y(t), \bar{y}(t) \in \mathscr{A}_y$, such that for any $t_1, t_2 \in \mathbb{R}$ with $|t_1 - t_2| < \tau$ the inequality

$$\left| \left(g_j(x(t_1), y(t_1)) - g_j(\bar{x}(t_1), y(t_1)) \right) - \left(g_j(x(t_2), y(t_2)) - g_j(\bar{x}(t_2), y(t_2)) \right) \right| < \frac{L_1 \epsilon_0}{2n} \tag{5.16}$$

holds, for all $1 \leqslant j \leqslant n$.

Condition (A4) implies that, for all $t \in J$, the inequality $\|g(x(t), y(t)) - g(\bar{x}(t), y(t))\| \geqslant L_1 \|x(t) - \bar{x}(t)\|$ is satisfied. Therefore, for each $t \in J$, there exists an integer $j_0 = j_0(t),\ 1 \leqslant j_0 \leqslant n$, such that

$$\left| g_{j_0}(x(t), y(t)) - g_{j_0}(\bar{x}(t), y(t)) \right| \geqslant \frac{L_1}{n} \|x(t) - \bar{x}(t)\|$$

Otherwise, if there exists $s \in J$ such that for all $1 \leqslant j \leqslant n$, the inequality

$$\left| g_j(x(s), y(s)) - g_j(\bar{x}(s), y(s)) \right| < \frac{L_1}{n} \|x(s) - \bar{x}(s)\|$$

holds, then one encounters with a contradiction since

$$\|g(x(s), y(s)) - g(\bar{x}(s), y(s))\| \leqslant \sum_{j=1}^{n} \left| g_j(x(s), y(s)) - g_j(\bar{x}(s), y(s)) \right| < L_1 \|x(s) - \bar{x}(s)\|.$$

Now, let s_0 be the midpoint of the interval J and $\theta = s_0 - \tau/2$. One can find an integer $j_0 = j_0(s_0),\ 1 \leqslant j_0 \leqslant n$, such that

$$\left| g_{j_0}(x(s_0), y(s_0)) - g_{j_0}(\bar{x}(s_0), y(s_0)) \right| \geqslant \frac{L_1}{n} \|x(s_0) - \bar{x}(s_0)\| > \frac{L_1 \epsilon_0}{n}. \tag{5.17}$$

On the other hand, making use of inequality (5.16), for all $t \in [\theta, \theta + \tau]$ we have

$$\begin{aligned} &\left| g_{j_0}(x(s_0), y(s_0)) - g_{j_0}(\bar{x}(s_0), y(s_0)) \right| - \left| g_{j_0}(x(t), y(t)) - g_{j_0}(\bar{x}(t), y(t)) \right| \\ &\quad \leqslant \left| \left(g_{j_0}(x(t), y(t)) - g_{j_0}(\bar{x}(t), y(t)) \right) - \left(g_{j_0}(x(s_0), y(s_0)) - g_{j_0}(\bar{x}(s_0), y(s_0)) \right) \right| < \frac{L_1 \epsilon_0}{2n} \end{aligned}$$

and therefore by means of (5.17), we obtain that the inequality

$$\left| g_{j_0}(x(t), y(t)) - g_{j_0}(\bar{x}(t), y(t)) \right| > \left| g_{j_0}(x(s_0), y(s_0)) - g_{j_0}(\bar{x}(s_0), y(s_0)) \right| - \frac{L_1 \epsilon_0}{2n} > \frac{L_1 \epsilon_0}{2n} \tag{5.18}$$

holds for all $t \in [\theta, \theta + \tau]$.

By applying the mean value theorem for integrals, one can find $s_1, s_2, \ldots, s_n \in [\theta, \theta + \tau]$ such that

$$\int_{\theta}^{\theta+\tau} [g(x(s), y(s)) - g(\bar{x}(s), y(s))] ds = \begin{pmatrix} \tau [g_1(x(s_1), y(s_1)) - g_1(\bar{x}(s_1), y(s_1))] \\ \tau [g_2(x(s_2), y(s_2)) - g_2(\bar{x}(s_2), y(s_2))] \\ \vdots \\ \tau [g_n(x(s_n), y(s_n)) - g_n(\bar{x}(s_n), y(s_n))] \end{pmatrix}.$$

Thus, using (5.18), one can obtain that

$$\left\| \int_{\theta}^{\theta+\tau} [g(x(s), y(s)) - g(\bar{x}(s), y(s))] ds \right\| \geqslant \tau \left| g_{j_0}(x(s_{j_0}), y(s_{j_0})) - g_{j_0}(\bar{x}(s_{j_0}), y(s_{j_0})) \right| > \frac{\tau L_1 \epsilon_0}{2n}. \tag{5.19}$$

It is clear that, for $t \in [\theta, \theta + \tau], y(t)$ and $\bar{y}(t)$ satisfy the integral equations

$$y(t) = y(\theta) + \int_{\theta}^{t} A y(s) ds + \int_{\theta}^{t} g(x(s), y(s)) ds$$

and

$$\bar{y}(t) = \bar{y}(\theta) + \int_{\theta}^{t} A \bar{y}(s) ds + \int_{\theta}^{t} g(\bar{x}(s), \bar{y}(s)) ds,$$

respectively, and herewith the equation

$$y(t) - \bar{y}(t) = (y(\theta) - \bar{y}(\theta)) + \int_{\theta}^{t} A(y(s) - \bar{y}(s)) ds + \int_{\theta}^{t} [g(x(s), y(s)) - g(\bar{x}(s), y(s))] ds + \int_{\theta}^{t} [g(\bar{x}(s), y(s)) - g(\bar{x}(s), \bar{y}(s))] ds$$

is achieved. Hence, we have the inequality

$$\|y(\theta+\tau)-\overline{y}(\theta+\tau)\| \geqslant \left\|\int_{\theta}^{\theta+\tau}[g(x(s),y(s))-g(\overline{x}(s),y(s))]ds\right\| - \|y(\theta)-\overline{y}(\theta)\| - \int_{\theta}^{\theta+\tau}\|A\|\|y(s)-\overline{y}(s)\|ds - \int_{\theta}^{\theta+\tau}L_3\|y(s)-\overline{y}(s)\|ds. \tag{5.20}$$

Now, assume that $\max_{t\in[\theta,\theta+\tau]}\|y(t)-\overline{y}(t)\| \leqslant \frac{\tau L_1\epsilon_0}{2n[2+\tau(L_3+\|A\|)]}$. In the present case, one encounters with a contradiction since, by means of the inequalities (5.19) and (5.20), we have

$$\max_{t\in[\theta,\theta+\tau]}\|y(t)-\overline{y}(t)\| \geqslant \|y(\theta+\tau)-\overline{y}(\theta+\tau)\| > \frac{\tau L_1\epsilon_0}{2n} - [1+\tau(L_3+\|A\|)]\max_{t\in[\theta,\theta+\tau]}\|y(t)-\overline{y}(t)\| \geqslant \frac{\tau L_1\epsilon_0}{2n[2+\tau(L_3+\|A\|)]}.$$

Therefore, one can see that the inequality $\max_{t\in[\theta,\theta+\tau]}\|y(t)-\overline{y}(t)\| > \frac{\tau L_1\epsilon_0}{2n[2+\tau(L_3+\|A\|)]}$ is valid.

Suppose that at the point η, the real valued function $\|y(t)-\overline{y}(t)\|$ takes its maximum on the interval $[\theta,\theta+\tau]$, that is,

$$\max_{t\in[\theta,\theta+\tau]}\|y(t)-\overline{y}(t)\| = \|y(\eta)-\overline{y}(\eta)\|$$

for some $\theta \leqslant \eta \leqslant \theta+\tau$.

For $t\in[\theta,\theta+\tau]$, by virtue of the integral equations

$$y(t) = y(\eta) + \int_{\eta}^{t}Ay(s)ds + \int_{\eta}^{t}g(x(s),y(s))ds$$

and

$$\overline{y}(t) = \overline{y}(\eta) + \int_{\eta}^{t}A\overline{y}(s)ds + \int_{\eta}^{t}g(\overline{x}(s),\overline{y}(s))ds,$$

we obtain

$$y(t)-\overline{y}(t) = (y(\eta)-\overline{y}(\eta)) + \int_{\eta}^{t}A(y(s)-\overline{y}(s))ds + \int_{\eta}^{t}[g(x(s),y(s))-g(\overline{x}(s),\overline{y}(s))]ds.$$

Define

$$\tau^1 = \min\left\{\frac{\tau}{2}, \frac{\tau L_1\epsilon_0}{8n(M\|A\|+M_0)[2+\tau(L_3+\|A\|)]}\right\}$$

and let

$$\theta^1 = \begin{cases}\eta, & \text{if } \eta \leqslant \theta+\tau/2\\ \eta-\tau^1, & \text{if } \eta > \theta+\tau/2\end{cases}.$$

We note that the interval $J^1=[\theta^1,\theta^1+\tau^1]$ is a subset of $[\theta,\theta+\tau]$ and hence of J.

For $t\in J^1$, we have

$$\|y(t)-\overline{y}(t)\| \geqslant \|y(\eta)-\overline{y}(\eta)\| - \left|\int_{\eta}^{t}\|A\|\|y(s)-\overline{y}(s)\|ds\right| - \left|\int_{\eta}^{t}\|g(x(s),y(s))-g(\overline{x}(s),\overline{y}(s))\|ds\right| > \frac{\tau L_1\epsilon_0}{2n[2+\tau(L_3+\|A\|)]} - 2\tau^1(M\|A\|+M_0) \geqslant \frac{\tau L_1\epsilon_0}{4n[2+\tau(L_3+\|A\|)]}.$$

Consequently, we get $\|y(t)-\overline{y}(t)\| > \epsilon_1, t\in J^1$, where $\epsilon_1 = \frac{\tau L_1\epsilon_0}{4n[2+\tau(L_3+\|A\|)]}$ and the length of the interval J^1 does not depend on the functions $x(t),\overline{x}(t)\in\mathscr{A}_x$.

The proof of the lemma is finalized. □

Through Lemma 5.1, we mention the replication of sensitivity feature from the set of functions $\mathscr{A}_x$ to $\mathscr{A}_y$, that is, from the generator system to the replicator counterpart. In a similar way, it is reasonable to analyze the sensitivity of the set of functions $\mathscr{A}$, which is defined through Eq. (2.10). In the present case, we shall say that the set $\mathscr{A}$ is sensitive provided that $\mathscr{A}_y$ is sensitive. This description is a natural one since, otherwise, the inequality $\|x(t)-\overline{x}(t)\|>\epsilon_0$ implies that $\left\|\left(x(t),\phi_{x(t)}(t)\right)-\left(\overline{x}(t),\phi_{\overline{x}(t)}(t)\right)\right\| > \epsilon_0$ in the same interval of time, which already signifies sensitivity of $\mathscr{A}$. But in replication of chaos, the crucial idea is the extension of sensitivity not only by the result-system, but also by the replicator, and one should understand sensitivity of the result-system as a property which is equivalent to the sensitivity of the replicator. According to this explanation, we note that if $\mathscr{A}_x$ is sensitive, then Lemma 5.1 implies the same feature for the set $\mathscr{A}_y$, and hence for the set $\mathscr{A}$.

Now, let us illustrate the replication of sensitivity through an example. It is known that the Lorenz system

$$\begin{aligned} x_1' &= \sigma(-x_1 + x_2) \\ x_2' &= -x_2 + rx_1 - x_1x_3 \\ x_3' &= -bx_3 + x_1x_2, \end{aligned} \tag{5.21}$$

with the coefficients $\sigma = 10,\ b = 8/3,\ r = 28$ admits sensitivity [31]. We use system (5.21) with the specified coefficients as the generator and constitute the 6-dimensional result-system

$$\begin{aligned} x_1' &= 10(-x_1 + x_2) \\ x_2' &= -x_2 + 28x_1 - x_1x_3 \\ x_3' &= -\frac{8}{3}x_3 + x_1x_2 \\ x_4' &= -5x_4 + x_3 \\ x_5' &= -2x_5 + 0.0002(x_2 - x_5)^3 + 4x_2 \\ x_6' &= -3x_6 - 3x_1. \end{aligned} \tag{5.22}$$

When system (5.22) is considered in the form of system (1.1)+(1.2), one can see that the diagonal matrix A whose entries on the diagonal are $-5,\ -2,\ -3$ satisfies the inequality $\|e^{At}\| \leqslant Ne^{-\omega t}$ with the coefficients $N = 1$ and $\omega = 2$. We note that the function $g : \mathbb{R}^3 \times \mathbb{R}^3 \to \mathbb{R}^3$ defined as

$$g(x_1, x_2, x_3, x_4, x_5, x_6) = \left(x_3, 0.0002(x_2 - x_5)^3 + 4x_2, -3x_1\right)$$

provides the conditions (A4) and (A5) with constants $L_1 = 1/\sqrt{3},\ L_2 = 11\sqrt{3}/2$ and $L_3 = 3/2$ since the chaotic attractor of system (5.22) is inside a compact region such that $|x_2| \leqslant 30$ and $|x_5| \leqslant 50$. Consequently, system (5.22) satisfies the condition (A7).

In Fig. 2, one can see the 3-dimensional projections in the x_1–x_2–x_3 and x_4–x_5–x_6 spaces of two different trajectories of the result-system (5.22) with adjacent initial conditions, such that one of them is in blue color and the other in red color. For the trajectory with blue color, we make use of the initial data $x_1(0) = -8.57,\ x_2(0) = -2.39,\ x_3(0) = 33.08,\ x_4(0) = 5.32,\ x_5(0) = 10.87,\ x_6(0) = -6.37$ and for the one with red color, we use the initial data $x_1(0) = -8.53,\ x_2(0) = -2.47,\ x_3(0) = 33.05,\ x_4(0) = 5.33,\ x_5(0) = 10.86,\ x_6(0) = -6.36$. In the simulation, the trajectories move on the time interval $[0, 3]$. The results seen in Fig. 2 supports our theoretical results indicated in Lemma 5.1 such that the replicator system, likewise the generator counterpart, admits the sensitivity feature. That is, the solutions of both the generator and the replicator given by blue and red colors diverge, even though they start and move close to each other in the first stage.

Through the next lemma we continue with the replication of transitivity.

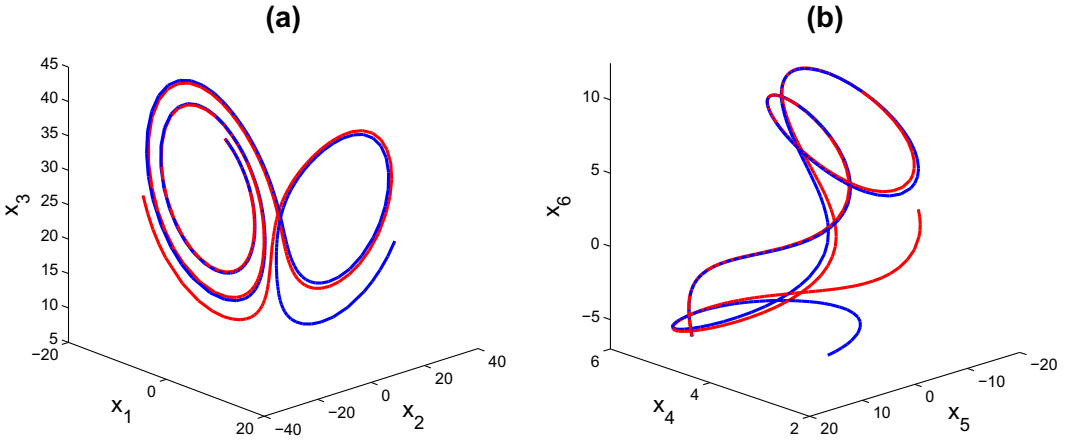

Fig. 2. Replication of sensitivity in the result-system (5.22). (a) 3-dimensional projection in the x_1–x_2–x_3 space. (b) 3-dimensional projection in the x_4–x_5–x_6 space. The sensitivity property is observable both in (a) and (b) such that the trajectories presented by blue and red colors move together in the first stage and then diverge. In other words, the sensitivity property of the generator system is mimicked by the replicator counterpart. (For interpretation of the references to color in this figure legend, the reader is referred to the web version of this article.)

Lemma 5.2. *Transitivity of $\mathscr{A}_x$ implies the same feature for $\mathscr{A}_y$.*

Proof. Fix arbitrary small $\epsilon > 0$, arbitrary large $E > 0$ and let $y(t) \in \mathscr{A}_y$ be a given function. Arising from the definition, introduced by (2.9), of the set $\mathscr{A}_y$, there exists a function $x(t) \in \mathscr{A}_x$ such that $y(t) = \phi_{x(t)}(t)$. Let $\gamma = \frac{\omega(\omega - NL_3)}{2M_0N(\omega - NL_3) + NL_2\omega}$. Condition (A7) guarantees that γ is positive. Since there exists a solution $x^*(t) \in \mathscr{A}_x$, which is dense in $\mathscr{A}_x$, one can find $\xi > 0$ and an interval $J \subset \mathbb{R}$ with length E such that $\|x(t) - x^*(t+\xi)\| < \gamma\epsilon$, for all $t \in J$. Without loss of generality, assume that J is a closed interval, that is, $J = [a, a+E]$ for some real number a.

Let $y^*(t) = \phi_{x^*(t)}(t)$. For $t \in J$, the bounded on $\mathbb{R}$ functions $y(t)$ and $y^*(t)$ must satisfy the relations

$$y(t) = \int_{-\infty}^{t} e^{A(t-s)} g(x(s), y(s)) ds$$

and

$$y^*(t) = \int_{-\infty}^{t} e^{A(t-s)} g(x^*(s), y^*(s)) ds,$$

respectively. The second equation above implies that

$$y^*(t+\xi) = \int_{-\infty}^{t+\xi} e^{A(t+\xi-s)} g(x^*(s), y^*(s)) ds.$$

Using the transformation $\bar{s} = s - \xi$, and replacing $\bar{s}$ by s again, we get

$$y^*(t+\xi) = \int_{-\infty}^{t} e^{A(t-s)} g(x^*(s+\xi), y^*(s+\xi)) ds.$$

Therefore, for $t \in J$, we have

$$\begin{aligned} y(t) - y^*(t+\xi) = &\int_{-\infty}^{a} e^{A(t-s)} [g(x(s), y(s)) - g(x^*(s+\xi), y^*(s+\xi))] ds + \int_{a}^{t} e^{A(t-s)} [g(x(s), y(s)) - g(x(s), y^*(s+\xi))] ds \\ &+ \int_{a}^{t} e^{A(t-s)} [g(x(s), y^*(s)) - g(x^*(s+\xi), y^*(s+\xi))] ds, \end{aligned}$$

which implies the inequality

$$e^{\omega t} \|y(t) - y^*(t+\xi)\| \leqslant \frac{2M_0N}{\omega} e^{\omega a} + \frac{NL_2\gamma\epsilon}{\omega} \left(e^{\omega t} - e^{\omega a}\right) + \int_{a}^{t} NL_3 e^{\omega s} \|y(s) - y^*(s+\xi)\| ds.$$

Through the implementation of Lemma 2.2 [82] to the last inequality, we attain

$$\begin{aligned} e^{\omega t} \|y(t) - y^*(t+\xi)\| &\leqslant \frac{2M_0N}{\omega} e^{\omega a} + \frac{NL_2\gamma\epsilon}{\omega} \left(e^{\omega t} - e^{\omega a}\right) + \int_{a}^{t} NL_3 \left[\frac{2M_0N}{\omega} e^{\omega a} + \frac{NL_2\gamma\epsilon}{\omega} \left(e^{\omega s} - e^{\omega a}\right)\right] e^{NL_3(t-s)} ds \\ &= \frac{NL_2\gamma\epsilon}{\omega} e^{\omega t} + \left(\frac{2M_0N}{\omega} - \frac{NL_2\gamma\epsilon}{\omega}\right) e^{\omega a} e^{NL_3(t-a)} + \frac{N^2L_2L_3\gamma\epsilon}{\omega(\omega - NL_3)} e^{NL_3 t} \left(e^{(\omega - NL_3)t} - e^{(\omega - NL_3)a}\right). \end{aligned}$$

Multiplying both sides by $e^{-\omega t}$, we achieve that

$$\|y(t) - y^*(t+\xi)\| \leqslant \frac{2M_0N}{\omega} e^{(NL_3 - \omega)(t-a)} + \frac{NL_2\gamma\epsilon}{\omega - NL_3} \left(1 - e^{(NL_3 - \omega)(t-a)}\right).$$

Now, suppose that $E > \frac{2}{\omega - NL_3} \ln\left(\frac{1}{\gamma\epsilon}\right)$. If $t \in \left[a + \frac{E}{2}, a + E\right]$, then it is true that $e^{(NL_3 - \omega)(t-a)} \leqslant e^{(NL_3 - \omega)E/2} < \gamma\epsilon$. As a result, we have

$$\|y(t) - y^*(t+\xi)\| < \left[\frac{2M_0N}{\omega} + \frac{NL_2}{\omega - NL_3}\right] \gamma\epsilon = \epsilon,$$

for $t \in J_1 = [a_1, a_1 + E_1]$, where $a_1 = a + E/2$ and $E_1 = E/2$. Consequently, the set $\mathscr{A}_y$ is transitive in compliance with Definition 3.3.

The lemma is proved. □

The extension of the last ingredient of chaos in the sense of Devaney is presented in the following lemma.

Lemma 5.3. *If $\mathscr{A}_x$ admits a dense collection of periodic functions, then the same is true for $\mathscr{A}_y$.*

Proof. Fix $y(t) = \phi_{x(t)}(t) \in \mathscr{A}_y$, arbitrary small $\epsilon > 0$ and arbitrary large $E > 0$. Assume that $\mathscr{A}_x$ admits a dense collection $\mathscr{G}_x \subset \mathscr{A}_x$ of periodic functions. Let $\gamma = \frac{\omega(\omega - NL_3)}{2M_0N(\omega - NL_3) + NL_2\omega}$, which is a positive real number by condition (A7). In this case, there exist $\widetilde{x}(t) \in \mathscr{G}_x$ and an interval $J \subset \mathbb{R}$ with length E such that $\|x(t) - \widetilde{x}(t)\| < \gamma\epsilon$, for all $t \in J$. Without loss of generality, assume that J is a closed interval, that is, $J = [a, a+E]$ for some $a \in \mathbb{R}$.

We note that by condition (A4) there is a one-to-one correspondence between the sets $\mathscr{G}_x$ and

$$\mathscr{G}_y = \left\{\phi_{x(t)}(t) | x(t) \in \mathscr{G}_x\right\} \tag{5.23}$$

such that if $x(t) \in \mathscr{G}_x$ is periodic then $\phi_{x(t)}(t) \in \mathscr{G}_y$ is also periodic with the same period, and vice versa. Therefore $\mathscr{G}_y \subset \mathscr{A}_y$ is a collection of periodic functions and in the proof our aim is to verify that the set $\mathscr{G}_y$ is dense in $\mathscr{A}_y$ in accordance with Definition 3.4.

Let $\widetilde{y}(t) = \phi_{\widetilde{x}(t)}(t)$, which clearly belongs to the set $\mathscr{G}_y$. Making use of the relations

$$y(t) = \int_{-\infty}^{t} e^{A(t-s)} g(x(s), y(s)) ds$$

and

$$\widetilde{y}(t) = \int_{-\infty}^{t} e^{A(t-s)} g(\widetilde{x}(s), \widetilde{y}(s)) ds$$

for $t \in J$, we attain

$$y(t) - \widetilde{y}(t) = \int_{-\infty}^{a} e^{A(t-s)}[g(x(s), y(s)) - g(\widetilde{x}(s), \widetilde{y}(s))]ds + \int_{a}^{t} e^{A(t-s)}[g(x(s), y(s)) - g(x(s), \widetilde{y}(s))]ds + \int_{a}^{t} e^{A(t-s)}[g(x(s), \widetilde{y}(s)) - g(\widetilde{x}(s), \widetilde{y}(s))]ds.$$

The last equation implies that

$$\left\|y(t) - \widetilde{y}(t)\right\| \leqslant \frac{2M_0N}{\omega} e^{-\omega(t-a)} + \frac{NL_2\gamma\epsilon}{\omega} e^{-\omega t}\left(e^{\omega t} - e^{\omega a}\right) + \int_{a}^{t} NL_3 e^{-\omega(t-s)} \left\|y(s) - \widetilde{y}(s)\right\| ds.$$

Using a procedure which is similar to the one presented in the proof of Lemma 5.2, it is possible to show that

$$\left\|y(t) - \widetilde{y}(t)\right\| \leqslant \frac{2M_0N}{\omega} e^{(NL_3-\omega)(t-a)} + \frac{NL_2\gamma\epsilon}{\omega - NL_3}$$

for all $t \in J$.

Now, suppose that $E > \frac{2}{\omega - NL_3} \ln\left(\frac{1}{\gamma\epsilon}\right)$. In the case that $a + \frac{E}{2} \leqslant t \leqslant a + E$, we have $e^{(NL_3-\omega)(t-a)} \leqslant e^{(NL_3-\omega)E/2} < \gamma\epsilon$. Consequently, the inequality

$$\left\|y(t) - \widetilde{y}(t)\right\| < \left[\frac{2M_0N}{\omega} + \frac{NL_2}{\omega - NL_3}\right]\gamma\epsilon = \epsilon$$

holds for $t \in J_1 = [a_1, a_1 + E_1]$, where $a_1 = a + E/2$ and $E_1 = E/2$.

The proof of the lemma is accomplished. □

We end up the present section by stating the following theorem and its immediate corollary, which can be verified as consequences of Lemmas 5.1–5.3.

Theorem 5.1. *If the set $\mathscr{A}_x$ is Devaney's chaotic, then the same is true for the set $\mathscr{A}_y$.*

Corollary 5.1. *If the set $\mathscr{A}_x$ is Devaney's chaotic, then $\mathscr{A}$ is chaotic in the same way.*

In the next part, the replication of chaos in the Li-Yorke sense is taken into account.

6. Replication of Li-Yorke chaos

Our aim in this section is to prove that if $\mathscr{A}_x$ is chaotic in the sense of Li-Yorke, then the same is valid for the set $\mathscr{A}_y$, and consequently for the set $\mathscr{A}$.

We start by indicating the following lemma, which presents the replication of proximality property in accordance with Definition 3.6.

Lemma 6.1. *If a couple of functions $(x(t), \overline{x}(t)) \in \mathscr{A}_x \times \mathscr{A}_x$ is proximal, then the same is true for the couple $\left(\phi_{x(t)}(t), \phi_{\overline{x}(t)}(t)\right) \in \mathscr{A}_y \times \mathscr{A}_y$.*

Proof. Let us fix arbitrary small positive real number ϵ and arbitrary large positive real number E. Define $\gamma = \frac{\omega(\omega - NL_3)}{2M_0N(\omega - NL_3) + NL_2\omega}$. Condition (A7) implies that γ is positive. Suppose that a given couple of functions $(x(t), \overline{x}(t)) \in \mathscr{A}_x \times \mathscr{A}_x$ is proximal. In such a case, one can find a sequence of real numbers $\{E_i\}$ satisfying $E_i \geqslant E$ for each $i \in \mathbb{N}$, and a sequence $\{a_i\}, a_i \to \infty$ as $i \to \infty$, such that we have $\|x(t) - \overline{x}(t)\| < \gamma\epsilon$, for each t from the intervals $J_i = [a_i, a_i + E_i],\ i \in \mathbb{N}$, and $J_i \cap J_j = \emptyset$ whenever $i \neq j$.

Now, we continue our proof by fixing an arbitrary natural number i. Taking advantage of the technique specified in the proof of Lemma 5.3, one can verify that

$$\left\|\phi_{x(t)}(t)-\phi_{\overline{x}(t)}(t)\right\|\leqslant\frac{2M_0N}{\omega}e^{(NL_3-\omega)(t-a_i)}+\frac{NL_2\gamma\epsilon}{\omega-NL_3}$$

for all $t\in J_i$.

If $E>\frac{2}{\omega-NL_3}\ln\left(\frac{1}{\gamma\epsilon}\right)$ and t belongs to the interval $\left[a_i+\frac{E_i}{2},a_i+E_i\right]$, then one has

$$e^{(NL_3-\omega)(t-a_i)}<e^{(NL_3-\omega)E_i/2}\leqslant e^{(NL_3-\omega)E/2}<\gamma\epsilon.$$

Since the natural number i was chosen arbitrarily, for each $i\in\mathbb{N}$, one can conclude that the inequality

$$\left\|\phi_{x(t)}(t)-\phi_{\overline{x}(t)}(t)\right\|<\left[\frac{2M_0N}{\omega}+\frac{NL_2}{\omega-NL_3}\right]\gamma\epsilon=\epsilon$$

holds, for each $t\in\widetilde{J}_i=\left[\widetilde{a}_i,\widetilde{a}_i+\widetilde{E}_i\right]$, where $\widetilde{a}_i=a_i+E_i/2$ and $\widetilde{E}_i=E_i/2$. Note that $\widetilde{J}_i\subset\mathbb{R}$ is an interval with length not less than $\widetilde{E}=E/2$. As a consequence, the couple of functions $\left(\phi_{x(t)}(t),\phi_{\overline{x}(t)}(t)\right)\in\mathscr{A}_y\times\mathscr{A}_y$ is proximal according to the Definition 3.6.

The proof of the lemma is completed. □

The following lemma indicates the replication of the next characteristic feature of Li-Yorke chaos.

Lemma 6.2. *If a couple of functions $(x(t),\overline{x}(t))\in\mathscr{A}_x\times\mathscr{A}_x$ is frequently (ϵ_0,Δ) – separated for some positive real numbers ϵ_0 and Δ, then the couple of functions $\left(\phi_{x(t)}(t),\phi_{\overline{x}(t)}(t)\right)\in\mathscr{A}_y\times\mathscr{A}_y$ is frequently $(\epsilon_1,\overline{\Delta})$ – separated for some positive real numbers ϵ_1 and $\overline{\Delta}$.*

Proof. Suppose that a given couple of functions $(x(t),\overline{x}(t))\in\mathscr{A}_x\times\mathscr{A}_x$ is frequently (ϵ_0,Δ) separated, for some $\epsilon_0>0$ and $\Delta>0$. In this case, there exist infinitely many disjoint intervals, each with length not less than Δ, such that $\|x(t)-\overline{x}(t)\|>\epsilon_0$, for each t from these intervals. Without loss of generality, assume that these intervals are all closed subsets of $\mathbb{R}$. In that case, one can find a sequence $\{\Delta_i\}$ satisfying $\Delta_i\geqslant\Delta,\ i\in\mathbb{N}$, and a sequence $\{d_i\},d_i\to\infty$ as $i\to\infty$, such that for each $i\in\mathbb{N}$ the inequality $\|x(t)-\overline{x}(t)\|>\epsilon_0$ holds for $t\in J_i=[d_i,d_i+\Delta_i]$, and $J_i\cap J_j=\emptyset$ whenever $i\neq j$.

Throughout the proof, let us denote $y(t)=\phi_{x(t)}(t)\in\mathscr{A}_y$ and $\overline{y}(t)=\phi_{\overline{x}(t)}(t)\in\mathscr{A}_y$.

Our aim is to show the existence of positive real numbers $\epsilon_1,\ \overline{\Delta}$ and infinitely many disjoint intervals $\overline{J}_i\subset J_i,\ i\in\mathbb{N}$, each with length $\overline{\Delta}$, such that the inequality $\|y(t)-\overline{y}(t)\|>\epsilon_1$ holds for each t from the intervals $\overline{J}_i,\ i\in\mathbb{N}$.

As in the proof of Lemma 5.1, we again suppose that $g(x,y)=\begin{pmatrix}g_1(x,y)\\g_2(x,y)\\\vdots\\g_n(x,y)\end{pmatrix}$, where each $g_j,\ 1\leqslant j\leqslant n$, is a real valued function. Using the equicontinuity on $\mathbb{R}$ of the family $\mathscr{F}$, defined by Eq. (5.15), one can find a positive real number $\tau<\Delta$,

independent of the functions $x(t),\overline{x}(t)\in\mathscr{A}_x,y(t),\overline{y}(t)\in\mathscr{A}_y$, such that for any $t_1,t_2\in\mathbb{R}$ with $|t_1-t_2|<\tau$ the inequality

$$\left|\left(g_j(x(t_1),y(t_1))-g_j(\overline{x}(t_1),y(t_1))\right)-\left(g_j(x(t_2),y(t_2))-g_j(\overline{x}(t_2),y(t_2))\right)\right|<\frac{L_1\epsilon_0}{2n}\tag{6.24}$$

holds, for all $1\leqslant j\leqslant n$.

Suppose that the sequence $\{s_i\}$ denotes the midpoints of the intervals J_i, that is, $s_i=d_i+\Delta_i/2$, for each $i\in\mathbb{N}$. Let us define a sequence $\{\theta_i\}$ through the equation $\theta_i=s_i-\tau/2$.

Now, let us fix an arbitrary natural number i. In a similar way to the method specified in the proof of Lemma 5.1, one can verify that

$$\max_{t\in[\theta_i,\theta_i+\tau]}\|y(t)-\overline{y}(t)\|>\frac{\tau L_1\epsilon_0}{2n[2+\tau(L_3+\|A\|)]}.$$

Suppose that the real valued function $\|y(t)-\overline{y}(t)\|$ assumes its maximum on the interval $[\theta_i,\theta_i+\tau]$, at a point η_i. In other words, for some $\eta_i\in[\theta_i,\theta_i+\tau]$, we have

$$\max_{t\in[\theta_i,\theta_i+\tau]}\|y(t)-\overline{y}(t)\|=\|y(\eta_i)-\overline{y}(\eta_i)\|.$$

Define $\overline{\Delta}=\min\left\{\frac{\tau}{2},\frac{\tau L_1\epsilon_0}{8n(M\|A\|+M_0)[2+\tau(L_3+\|A\|)]}\right\}$ and let $\theta_i^1=\begin{cases}\eta_i, & \text{if } \eta_i\leqslant\theta_i+\tau/2\\ \eta_i-\tau^1, & \text{if } \eta_i>\theta_i+\tau/2\end{cases}$.

Making use of the integral equations

$$y(t)=y(\eta_i)+\int_{\eta_i}^{t}Ay(s)ds+\int_{\eta_i}^{t}g(x(s),y(s))ds$$

and

$$\overline{y}(t) = \overline{y}(\eta_i) + \int_{\eta_i}^{t} A\overline{y}(s)ds + \int_{\eta_i}^{t} g(\overline{x}(s), \overline{y}(s))ds,$$

one can confirm that

$$\|y(t) - \overline{y}(t)\| > \frac{\tau L_1 \epsilon_0}{4n[2 + \tau(L_3 + \|A\|)]},$$

for each $t \in [\theta_i^1, \theta_i^1 + \overline{\Delta}]$.

The information mentioned above is true for an arbitrarily chosen natural number i. Therefore, for each $i \in \mathbb{N}$, the interval $\overline{J}_i = [\theta_i^1, \theta_i^1 + \overline{\Delta}]$ is a subset of $[\theta_i, \theta_i + \tau]$, and hence of J_i. Moreover, for any $i \in \mathbb{N}$, we have $\|y(t) - \overline{y}(t)\| > \epsilon_1, t \in \overline{J}_i$, where $\epsilon_1 = \frac{\tau L_1 \epsilon_0}{4n[2+\tau(L_3+\|A\|)]}$.

Consequently, according to Definition 3.7, the couple of functions $\left(\phi_{x(t)}(t), \phi_{\overline{x}(t)}(t)\right) \in \mathscr{A}_y \times \mathscr{A}_y$ is frequently $(\epsilon_1, \overline{\Delta})$ – separated.

The proof of the lemma is finalized. □

Now, we state and prove the main theorem of the present section. In the proof, we suppose that $\mathscr{G}_x \subset \mathscr{A}_x$ denotes the set of periodic functions inside $\mathscr{A}_x$ and the set $\mathscr{G}_y \subset \mathscr{A}_y$, defined through Eq. (5.23), denotes the set of periodic functions inside $\mathscr{A}_y$.

Theorem 6.1. *If the set $\mathscr{A}_x$ is Li-Yorke chaotic, then the same is true for the set $\mathscr{A}_y$.*

Proof. Assume that the set $\mathscr{A}_x$ is Li-Yorke chaotic. It can be easily verified that for any natural number $k, x(t) \in \mathscr{G}_x$ is a kT-periodic function if and only if $\phi_{x(t)}(t) \in \mathscr{G}_y$ is kT-periodic, where $\mathscr{G}_x$ and $\mathscr{G}_y$ denote the sets of all periodic functions inside $\mathscr{A}_x$ and $\mathscr{A}_y$, respectively. Therefore, the set $\mathscr{A}_y$ admits a kT-periodic function for any $k \in \mathbb{N}$.

Next, suppose that the set $\mathscr{C}_x$ is a scrambled set inside $\mathscr{A}_x$ and define the set

$$\mathscr{C}_y = \left\{\phi_{x(t)}(t) | x(t) \in \mathscr{C}_x\right\}. \tag{6.25}$$

Condition (A4) implies that there is a one-to-one correspondence between the sets $\mathscr{C}_x$ and $\mathscr{C}_y$. Since the scrambled set $\mathscr{C}_x$ is uncountable, it is clear that the set $\mathscr{C}_y$ is also uncountable. Moreover, using the same condition one can show that no periodic functions exist inside $\mathscr{C}_y$, since no such functions take place inside the set $\mathscr{C}_x$. That is, $\mathscr{C}_y \cap \mathscr{G}_y = \emptyset$.

Since each couple of functions inside $\mathscr{C}_x \times \mathscr{C}_x$ is proximal, Lemma 6.1 implies the same feature for each couple of functions inside $\mathscr{C}_y \times \mathscr{C}_y$.

Similarly, Lemma 6.2 implies that if each couple of functions $(x(t), \overline{x}(t)) \in \mathscr{C}_x \times \mathscr{C}_x (\mathscr{C}_x \times \mathscr{G}_x)$ is frequently (ϵ_0, Δ) – separated for some positive real numbers ϵ_0 and Δ, then each couple of functions $(y(t), \overline{y}(t)) \in \mathscr{C}_y \times \mathscr{C}_y (\mathscr{C}_y \times \mathscr{G}_y)$ is frequently $(\epsilon_1, \overline{\Delta})$ – separated for some positive real numbers ϵ_1 and $\overline{\Delta}$. Consequently, the set $\mathscr{C}_y$ is a scrambled set inside $\mathscr{A}_x$, and according to Definition 3.10, $\mathscr{A}_y$ is Li-Yorke chaotic.

The proof of the theorem is accomplished. □

An immediate corollary of Theorem 6.1 is the following.

Corollary 6.1. *If the set $\mathscr{A}_x$ is Li-Yorke chaotic, then the set $\mathscr{A}$ is chaotic in the same way.*

7. Morphogenesis of chaos

Two different mechanisms of chaos extension (morphogenesis) through applying replication are considered in our paper. The first one is illustrated schematically in Fig. 3. The figure represents consecutively connected systems as boxes and the blue arrows symbolize unidirectional couplings between two systems. In the first coupling, we take into account a generator

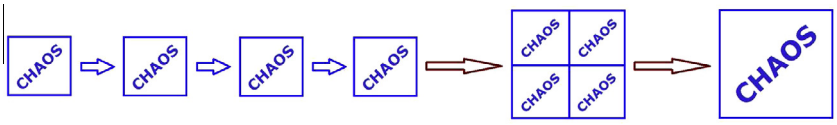

Fig. 3. Morphogenesis of chaos through consecutive replications.

system, the leftmost box in the figure, which is connected with a second system considered as a replicator in the couple. In the next coupling, the second system is considered as a generator with respect to the third one. That is, it changes its role in the extension process. In the third coupling, the third system is considered as a generator and the forth one as a replicator. In summary, the mechanism proceeds as follows. We take into account consecutive unidirectionally coupled systems such that the initial one is a generator and at each next coupling the role of the previously chaotified replicator changes and we start to use it as a generator. As a result of the mechanism all individual subsystems are chaotic as well as the system which consists of all subsystems. Moreover, the type of the chaos is saved under this procedure.

In Fig. 4 we show another mechanism of chaos extension. Here, the generator is surrounded by three replicators and the blue arrows symbolize, again, unidirectional couplings between two systems. Distinctively from the former mechanism, the replicators do not change their role with respect to each other according to the special topology of connection. The generator is coupled with all other replicators such that it is rather a core than a beginning element. The result of the mechanism is similar to the former such that all replicators as well as the system consisting of all subsystems become chaotic, saving the chaos type of the generator.

We call the two ways as *the chain* and *the core* mechanisms, respectively, and the system which unites the generator and several replicators, of type (1.2), in either extension mechanism as *the result-system*. Theoretically, we do not discuss constraints on the dimension of the result-system, but under certain conditions it seems that the dimension is not restricted for both mechanisms. However, this is definitely true for the core mechanism even with infinite dimensions. We will discuss and simulate the chain mechanism in our paper, mainly, since the core mechanism can be discussed very similarly. One can invent other mechanisms, for example, by considering "composition" of the two mechanisms proposed presently.

Next, to exemplify the chaos extension procedure of our paper, according to the chain mechanism shown in Fig. 3 we set up the following 8-dimensional result-system

$$\begin{aligned}
x_1' &= x_2\\
x_2' &= -0.05x_2 - x_1^3 + 7.5\cos t\\
x_3' &= x_4 + x_1\\
x_4' &= -3x_3 - 2x_4 - 0.008x_3^3 + x_2\\
x_5' &= x_6 + x_3\\
x_6' &= -3x_5 - 2.1x_6 - 0.007x_5^3 + x_4\\
x_7' &= x_8 + x_5\\
x_8' &= -3.1x_7 - 2.2x_8 - 0.006x_7^3 + x_6.
\end{aligned} \tag{7.26}$$

We note that system (7.26) consists of four subsystems with coordinates (x_1, x_2), (x_3, x_4), (x_5, x_6) and (x_7, x_8) such that the subsystem (x_1, x_2) is exactly the generator used in system (1.4)+(1.5), while the subsystem (x_3, x_4) is the replicator of (1.4) and (1.5).

According to the theoretical results of the present paper, system (7.26) possesses a chaotic attractor in the 8-dimensional phase space. By marking the trajectory of this system with the initial data $x_1(0) = 2,\ x_2(0) = 3,\ x_3(0) = x_5(0) = x_7(0) = -1,$ $x_4(0) = x_6(0) = x_8(0) = 1$ stroboscopically at times that are integer multiples of 2π, we obtain the Poincaré section inside the 8-dimensional space. In Fig. 5, which informs us about morphogenesis, the 3-dimensional projections of the whole Poincaré section on the x_2–x_4–x_6 and x_3–x_5–x_7 spaces are shown. One can see in Fig. 5(a) and in Fig. 5(b) the additional *foldings* which are not possible to observe in the classical strange attractor shown in Fig. 1(a).

Despite we are restricted to make illustrations at most in 3-dimensional spaces, taking inspiration from Figs. 1 and 5, one can imagine that the structure of the original Poincaré section in the 8-dimensional space will be similar through its fractal structure, but more beautiful and impressive than its projections. From this point of view, we are not surprised since these facts have been proved theoretically in the paper.

Next, we shall handle the problem that whether the chaos extension procedure works for all existing systems in the mechanisms presented above, from the theoretical point of view. Since the core mechanism does not need any additional theoretical discussions, we will consider the chain mechanism.

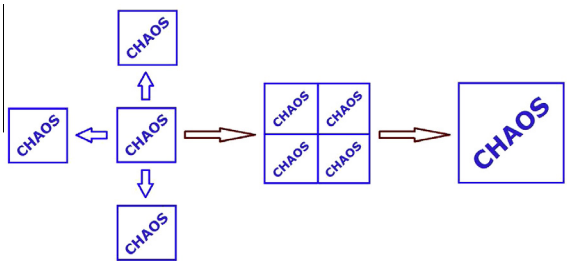

Fig. 4. Morphogenesis of chaos from a prior chaos as a core.

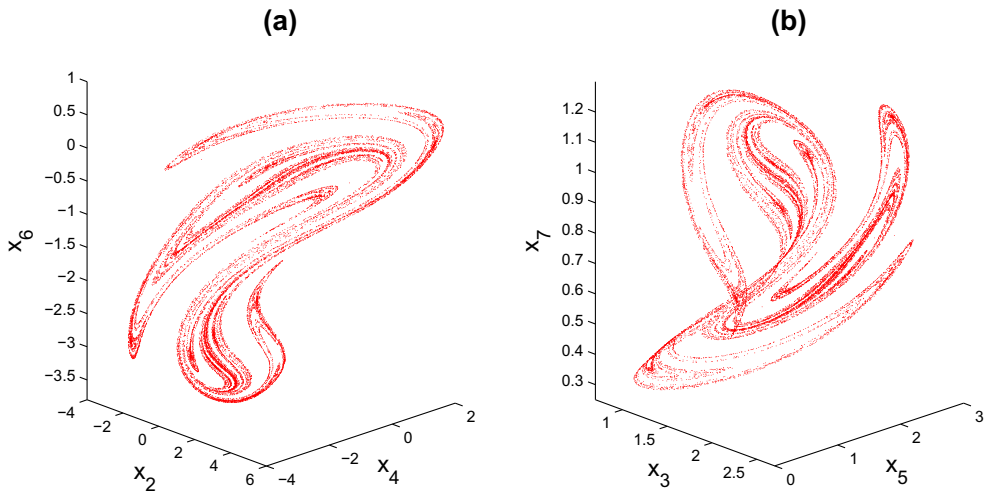

Fig. 5. In (a) and (b) projections of the result chaotic attractor on the x_2–x_4–x_6 and x_3–x_5–x_7 spaces are respectively presented. One can see in (a) and (b) the additional *foldings* which are not possible to observe in the 2-dimensional picture of the prior classical chaos shown in Fig. 1(a). In the same time, the shape of the original attractor is seen in the resulting chaos. The illustrations in (a) and (b) repeat the structure of the attractor of the generator and the similarity between these pictures is a manifestation of the morphogenesis of chaos.

In addition to the system (1.1)+(1.2), we take into account the system

$$z' = Bz + h(y(t), z), \tag{7.27}$$

where $h : \mathbb{R}^n \times \mathbb{R}^l \to \mathbb{R}^l$ is a continuous function in all of its arguments, the constant $l \times l$ real valued matrix B has real parts of eigenvalues all negative and $y(t)$ is a solution system (1.2).

It is easy to verify the existence of positive real numbers $\widetilde{N}$ and $\widetilde{\omega}$ such that $\|e^{Bt}\| \leqslant \widetilde{N}e^{-\widetilde{\omega}t}$, for all $t \geqslant 0$.

In our next theoretical discussions, the system (7.27) will serve as the third system in the chain mechanism presented by Fig. 3, and we need the following assumptions which are counterparts of the conditions (A4)–(A7) presented in Section 2.

(A8) There exists a positive real number $\widetilde{L}_1$ such that $\|h(y_1, z) - h(y_2, z)\| \geqslant \widetilde{L}_1\|y_1 - y_2\|$, for all $y_1, y_2 \in \mathbb{R}^n,\ z \in \mathbb{R}^l$;
(A9) There exist positive real numbers $\widetilde{L}_2$ and $\widetilde{L}_3$ such that $\|h(y_1, z) - h(y_2, z)\| \leqslant \widetilde{L}_2\|y_1 - y_2\|$, for all $y_1, y_2 \in \mathbb{R}^n,\ z \in \mathbb{R}^l$, and $\|h(y, z_1) - h(y, z_2)\| \leqslant \widetilde{L}_3\|z_1 - z_2\|$, for all $y \in \mathbb{R}^n,\ z_1, z_2 \in \mathbb{R}^l$;
(A10) There exists a positive number $K_0 < \infty$ such that $\sup_{y\in\mathbb{R}^n,\ z\in\mathbb{R}^l}\|h(y, z)\| = K_0$;
(A11) $\widetilde{N}\widetilde{L}_3 - \widetilde{\omega} < 0$.

Likewise the definition for the set of functions $\mathscr{A}_y$, given by (2.9), let us denote by $\mathscr{A}_z$ the set of all bounded on $\mathbb{R}$ solutions of system $z' = Bz + h(y(t), z)$, for any $y(t) \in \mathscr{A}_y$.

In a similar way to the Lemma 2.1, one can show that the set

$$\mathscr{U}_z = \{z(t) | z(t) \text{ is a solution of the system } z' = Az + g(y(t), z) \text{ for some } y(t) \in \mathscr{U}_y\} \tag{7.28}$$

is a basin of $\mathscr{A}_z$. Furthermore, a similar result of Theorem 4.1 introduced in Section 4, hold also for the set $\mathscr{A}_z$.

We state in the next theorem that similar results of the Theorems 5.1 and 6.1 presented in Sections 5 and 6, respectively, hold also for the set $\mathscr{A}_z$.

We note that, in the case of the presence of arbitrary finite number of systems, which obey conditions that are counterparts of (A4)–(A7), one can prove that a similar result of the next theorem holds for the chain mechanism.

Theorem 7.1. *If the set $\mathscr{A}_x$ is Devaney chaotic or Li-Yorke chaotic, then the set $\mathscr{A}_z$ is chaotic in the same way as both $\mathscr{A}_x$ and $\mathscr{A}_y$.*

Proof. In the proof, we will show that for each $z(t) \in \mathscr{A}_z$ and arbitrary $\delta > 0$, there exist $\bar{z}(t) \in \mathscr{A}_z$ and $t_0 \in \mathbb{R}$ such that $\|z(t_0) - \bar{z}(t_0)\| < \delta$, which is needed to show sensitivity of $\mathscr{A}_z$. The remaining parts of the proof can be performed in a similar way to the proofs presented in Sections 5 and 6, and therefore are omitted.

Suppose that the set $\mathscr{A}_x$ is sensitive. Fix an arbitrary $\delta > 0$ and let $z(t) \in \mathscr{A}_z$ be a given solution of system (7.27). In this case, there exists $y(t) = \phi_{x(t)}(t) \in \mathscr{A}_y$, where $x(t) \in \mathscr{A}_x$, such that $z(t)$ is the unique bounded on $\mathbb{R}$ solution of the system $z' = Bz + h(y(t), z)$.

Let us choose a real number $\overline{\epsilon} = \overline{\epsilon}(\delta) > 0$ small enough which satisfies the inequality

$$\left(1 + \frac{\widetilde{N}\widetilde{L}_2}{\widetilde{\omega} - \widetilde{N}\widetilde{L}_3}\right)\left(1 + \frac{NL_2}{\omega - NL_3}\right)\overline{\epsilon} < \delta$$

and denote $\epsilon_1 = \left(1 + \frac{NL_2}{\omega - NL_3}\right)\overline{\epsilon}$. Now, take $R = R(\overline{\epsilon}) < 0$ sufficiently large in absolute value such that both of the inequalities $\frac{2M_0N}{\omega}e^{-(NL_3-\omega)R/2} \leqslant \overline{\epsilon}$ and $\frac{2\widetilde{M}_0\widetilde{N}}{\widetilde{\omega}}e^{-(\widetilde{NL}_3-\widetilde{\omega})R/2} \leqslant \epsilon_1$ are valid, and let $\delta_1 = \delta_1(\overline{\epsilon}, R) = \overline{\epsilon}e^{L_0R}$. Since the set $\mathscr{A}_x$ is sensitive, one can find $\overline{x}(t) \in \mathscr{A}_x$ and $t_0 \in \mathbb{R}$ such that the inequality $\|x(t_0) - \overline{x}(t_0)\| < \delta_1$ holds.

As in the case of the proof of Lemma 5.1, for $t \in [t_0 + R, t_0]$, one can verify that $\|x(t) - \overline{x}(t)\| < \overline{\epsilon}$, and

$$\|y(t) - \overline{y}(t)\| \leqslant \frac{NL_2\overline{\epsilon}}{\omega - NL_3} + \frac{2M_0N}{\omega}e^{(NL_3-\omega)(t-t_0-R)}.$$

According to the last inequality, we have $\|y(t) - \overline{y}(t)\| \leqslant \epsilon_1$, for $t \in [t_0 + R/2, t_0]$.

Suppose that $\overline{z}(t)$ is the unique bounded on $\mathbb{R}$ solution of the system $z' = Bz + h(\overline{y}(t), z)$. One can see that the relations

$$z(t) = \int_{-\infty}^{t} e^{B(t-s)}h(y(s), z(s))ds$$

and

$$\overline{z}(t) = \int_{-\infty}^{t} e^{B(t-s)}h(\overline{y}(s), \overline{z}(s))ds,$$

are valid. Using these equations, it can be verified that

$$\begin{aligned}\|z(t) - \overline{z}(t)\| \leqslant{}& \int_{t_0+\frac{R}{2}}^{t} \widetilde{N}e^{-\widetilde{\omega}(t-s)}\|h(y(s), z(s)) - h(y(s), \overline{z}(s))\|ds + \int_{t_0+\frac{R}{2}}^{t} \widetilde{N}e^{-\widetilde{\omega}(t-s)}\|h(y(s), \overline{z}(s)) - h(\overline{y}(s), \overline{z}(s))\|ds \\ &+ \int_{-\infty}^{t_0+\frac{R}{2}} \widetilde{N}e^{-\widetilde{\omega}(t-s)}\|h(y(s), z(s)) - h(\overline{y}(s), \overline{z}(s))\|ds.\end{aligned}$$

Since $\|y(t) - \overline{y}(t)\| < \epsilon_1$ for $t \in [t_0 + R/2, t_0]$, one has

$$\begin{aligned}\|z(t) - \overline{z}(t)\| &\leqslant \widetilde{N}\widetilde{L}_3 \int_{t_0+\frac{R}{2}}^{t} e^{-\widetilde{\omega}(t-s)}\|z(s) - \overline{z}(s)\|ds + \widetilde{N}\widetilde{L}_2\epsilon_1 \int_{t_0+\frac{R}{2}}^{t} e^{-\widetilde{\omega}(t-s)}ds + 2\widetilde{M}_0\widetilde{N}\int_{-\infty}^{t_0+\frac{R}{2}} e^{-\widetilde{\omega}(t-s)}ds \\ &\leqslant \widetilde{N}\widetilde{L}_3 \int_{t_0+\frac{R}{2}}^{t} e^{-\widetilde{\omega}(t-s)}\|z(s) - \overline{z}(s)\|ds + \frac{\widetilde{N}\widetilde{L}_2\epsilon_1}{\widetilde{\omega}}e^{-\widetilde{\omega}t}(e^{\widetilde{\omega}t} - e^{\widetilde{\omega}(t_0+R/2)}) + \frac{2\widetilde{M}_0\widetilde{N}}{\widetilde{\omega}}e^{-\widetilde{\omega}(t-t_0-R/2)}.\end{aligned}$$

Now, let us introduce the functions $u(t) = e^{\widetilde{\omega}t}\|z(t) - \overline{z}(t)\|$, $k(t) = \frac{\widetilde{NL}_2\epsilon_1}{\widetilde{\omega}}e^{\widetilde{\omega}t}$, and $v(t) = c + k(t)$ where $c = \left(\frac{2\widetilde{M}_0\widetilde{N}}{\widetilde{\omega}} - \frac{\widetilde{NL}_2\epsilon_1}{\widetilde{\omega}}\right)e^{\widetilde{\omega}(t_0+R/2)}$.

These definitions imply that $u(t) \leqslant v(t) + \int_{t_0+\frac{R}{2}}^{t} \widetilde{N}\widetilde{L}_3u(s)ds$ and applying Lemma 2.2 [82] leads to

$$u(t) \leqslant v(t) + \widetilde{N}\widetilde{L}_3 \int_{t_0+\frac{R}{2}}^{t} e^{\widetilde{NL}_3(t-s)}h(s)ds.$$

Therefore, for $t \in [t_0 + R/2, t_0]$ we have

$$\begin{aligned}u(t) &\leqslant c + k(t) + c\left(e^{\widetilde{NL}_3(t-t_0-R/2)} - 1\right) + \frac{N^2\widetilde{L}_2\widetilde{L}_3\epsilon_1}{\widetilde{\omega}}e^{\widetilde{NL}_3t}\int_{t_0+\frac{R}{2}}^{t} e^{(\widetilde{\omega}-\widetilde{NL}_3)s}ds \\ &= \frac{\widetilde{N}\widetilde{L}_2\epsilon_1}{\widetilde{\omega}}e^{\widetilde{\omega}t} + \left(\frac{2\widetilde{M}_0N}{\widetilde{\omega}} - \frac{\widetilde{N}\widetilde{L}_2\epsilon_1}{\widetilde{\omega}}\right)e^{\widetilde{\omega}T}e^{\widetilde{NL}_3(t-t_0-R/2)} + \frac{\widetilde{N}^2\widetilde{L}_2\widetilde{L}_3\epsilon_1}{\widetilde{\omega}(\widetilde{\omega} - \widetilde{N}\widetilde{L}_3)}e^{\widetilde{\omega}t}\left[1 - e^{(\widetilde{NL}_3-\widetilde{\omega})(t-t_0-R/2)}\right]\end{aligned}$$

and hence

$$\|z(t) - \overline{z}(t)\| \leqslant \frac{\widetilde{N}\widetilde{L}_2\epsilon_1}{\widetilde{\omega} - \widetilde{N}\widetilde{L}_3}\left[1 - e^{(\widetilde{NL}_3-\widetilde{\omega})(t-t_0-R/2)}\right] + \frac{2\widetilde{M}_0N}{\widetilde{\omega}}e^{(\widetilde{NL}_3-\widetilde{\omega})(t-t_0-R/2)}.$$

Consequently, the inequality

$$\|z(t_0)-\bar{z}(t_0)\| \leqslant \frac{\widetilde{N}\widetilde{L}_2\epsilon_1}{\widetilde{\omega}-\widetilde{N}\widetilde{L}_3}+\frac{2\widetilde{M}_0\widetilde{N}}{\widetilde{\omega}}e^{(\widetilde{\omega}-\widetilde{N}\widetilde{L}_3)R/2} < \left(1+\frac{\widetilde{N}\widetilde{L}_2}{\widetilde{\omega}-\widetilde{N}\widetilde{L}_3}\right)\epsilon_1 < \delta$$

is valid.

The theorem is proved. □

8. Replication of period-doubling cascade

We start this section by describing the chaos through period-doubling cascade [24,83,84] for the set of functions $\mathscr{A}_x$, and deal with its replication by the set of functions $\mathscr{A}_y$, which is defined by Eq. (2.9).

Suppose that there exists a function $G:\mathbb{R}\times\mathbb{R}^m\times\mathbb{R}\to\mathbb{R}^m$ which is continuous in all of its arguments such that $F(t,x)=G(t,x,\mu_\infty)$ for some finite number μ_∞, which will be explained below.

To discuss chaos through period-doubling cascade, let us consider the system

$$x'=G(t,x,\mu), \tag{8.29}$$

where μ is a parameter.

We say that the set $\mathscr{A}_x$ is chaotic through period-doubling cascade if there exist a natural number k and a sequence of period-doubling bifurcation values $\{\mu_m\}$, $\mu_m\to\mu_\infty$ as $m\to\infty$, such that for each $m\in\mathbb{N}$ as the parameter μ increases (or decreases) through μ_m, system (8.29) undergoes a period-doubling bifurcation and a periodic solution with period $k2^mT$ appears. As a consequence, at $\mu=\mu_\infty$, there exist infinitely many unstable periodic solutions of system (8.29), and hence of system (1.1), all lying in a bounded region. In this case, the set $\mathscr{A}_x$ admits periodic functions of periods $kT, 2kT, 4kT, 8kT, \ldots$.

Now, making use of Eq. (2.8), one can show that for any natural number p, if $x(t)\in\mathscr{A}_x$ is a pT-periodic function then $\phi_{x(t)}(t)\in\mathscr{A}_y$ is also pT-periodic. Moreover, condition (A4) implies that the converse is also true. Consequently, if the set $\mathscr{A}_x$ admits periodic functions of periods $kT, 2kT, 4kT, 8kT, \ldots$, then the same is valid for $\mathscr{A}_y$, with no additional periodic functions of any other period. Furthermore, the technique indicated in the proof of Lemma 5.1 can be used to show that these periodic solutions are all unstable and this provides us an opportunity to state the following theorem.

Theorem 8.1. *If the set $\mathscr{A}_x$ is chaotic through period-doubling cascade, then the same is true for $\mathscr{A}_y$.*

The following corollary of Theorem 8.1 states that the result-system (1.1)+(1.2) is chaotic through the period-doubling cascade, provided the system (1.1) is.

Corollary 8.1. *If the set $\mathscr{A}_x$ is chaotic through period-doubling cascade, then the same is true for $\mathscr{A}$.*

Our theoretical results show that the replicator system (1.2), likewise the generator counterpart, undergoes period-doubling bifurcations as the parameter μ increases or decreases through the values μ_m, $m\in\mathbb{N}$. That is, the sequence $\{\mu_m\}$ of bifurcation parameters is exactly the same for both generator and replicator systems. In this case, if the generator system obeys the Feigenbaum universality [3,85–87] then one can conclude that the same is true also for the replicator. In other words, when $\lim_{m\to\infty}\frac{\mu_m-\mu_{m+1}}{\mu_{m+1}-\mu_{m+2}}$ is evaluated, the universal constant known as the Feigenbaum number 4.6692016… is achieved and this universal number is the same for both generator and replicator.

It is worth saying that the results about replication of period-doubling cascade as well as the Feigenbaum's universal behavior, which can be perceived as another aspect of morphogenesis of chaos, are true also for chaos extension mechanisms shown in Figs. 3 and 4. In our next example, using the chain mechanism, we will illustrate through simulations the morphogenesis of period-doubling cascade.

In paper [88], it is indicated that the Duffing's equation

$$x''+0.3x'+x^3=\mu\cos t \tag{8.30}$$

admits the chaos through period-doubling cascade at the parameter value $\mu=\mu_\infty\equiv 40$. Defining the new variables $x_1=x$ and $x_2=x'$, Eq. (8.30) can be rewritten as a system in the following form

$$\begin{aligned} x_1' &= x_2\\ x_2' &= -0.3x_2-x_1^3+\mu\cos t. \end{aligned} \tag{8.31}$$

Making use of system (8.31) as the generator, let us constitute the following 8-dimensional result-system

$$
\begin{aligned}
x_1' &= x_2\\
x_2' &= -0.3x_2 - x_1^3 + \mu\cos t\\
x_3' &= 2x_3 - x_4 + 0.4\tan\left((x_1+x_3)/10\right)\\
x_4' &= 17x_3 - 6x_4 + x_2\\
x_5' &= -2x_5 + 0.5\sin x_6 - 4x_4\\
x_6' &= -x_5 - 4x_6 - \tan\left(x_3/2\right)\\
x_7' &= 2x_7 + 5x_8 - 0.0003(x_7 - x_8)^3 - 1.5x_6\\
x_8' &= -5x_7 - 8x_8 + 4x_5.
\end{aligned}
\tag{8.32}
$$

System (8.32) is designed according to the chain mechanism indicated in Fig. 3. In the coupling between the subsystems with coordinates (x_1, x_2) and (x_3, x_4) the former is the generator and the latter is the replicator. In the second coupling between the subsystems with coordinates (x_3, x_4) and (x_5, x_6), this time the former is used as the generator although it was the replicator in the previous coupling. The final coupling between the subsystems with coordinates (x_5, x_6) and (x_7, x_8) is constructed in a similar way. In this exemplification we will refer to subsystems with coordinates (x_1, x_2), (x_3, x_4), (x_5, x_6) and (x_7, x_8) as the first, second, third and the fourth subsystems, respectively.

According to our theoretical discussions, the result-system (8.32) with the parameter value $\mu = \mu_\infty \equiv 40$ admits a chaotic attractor in the 8-dimensional phase space, which is obtained through period-doubling cascade. For the parameter value μ between 30 and 40, the bifurcation diagrams corresponding to the x_2, x_4, x_6 and x_8 coordinates of system (8.32) are illustrated in Fig. 6. The picture shown in Fig. 6(a) is the bifurcation diagram of the system (8.31), while the pictures presented in Fig. 6(b)–(d) correspond to the second, third and the fourth subsystems, respectively. For the parameter values where stable periodic solutions exist, the one-to-one correspondence between the periodic solutions of the subsystems is observable in the figure. Moreover, it is seen in Fig. 6(b)–(d) that, likewise the first subsystem, all other subsystems undergo period-doubling bifurcations at the same parameter values such that for $\mu = \mu_\infty$ all of them are chaotic. One should recognize that the similarities between the presented bifurcation diagrams indicate morphogenesis of period-doubling cascade.

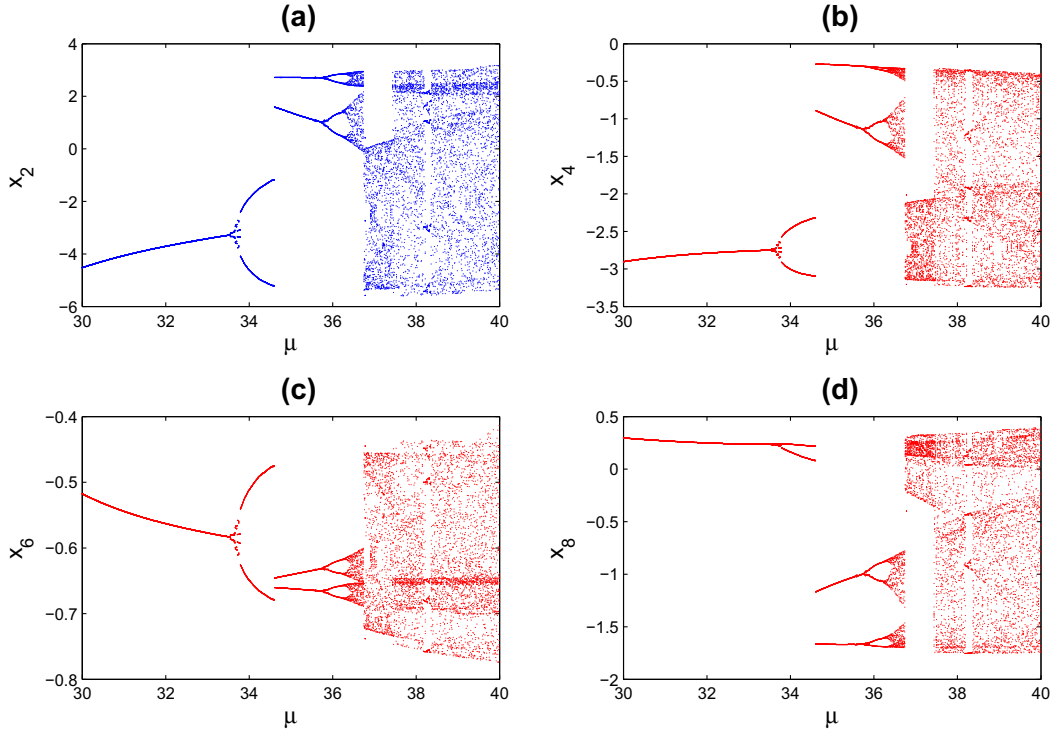

Fig. 6. The bifurcation diagrams of system (8.32) according to coordinates. (a) The bifurcation diagram corresponding to x_2-coordinate, (b) The bifurcation diagram corresponding to x_4-coordinate, (c) The bifurcation diagram corresponding to x_6-coordinate, (d) The bifurcation diagram corresponding to x_8-coordinate. The picture in (a) is the bifurcation diagram of the generator system (8.31) and the pictures shown in (b)–(d) correspond to the second, third and fourth replicator systems, respectively. It is observable that all replicators, likewise the generator, undergo period-doubling bifurcations at the same values of the parameter and all of them are chaotic for $\mu = \mu_\infty \equiv 40$. The one-to-one correspondence between the stable periodic solutions of the generator and replicators are also seen in the figure. The resemblances between the bifurcation diagrams corresponding to the coordinates x_2, x_4, x_6, and x_8 reveal morphogenesis of chaos.

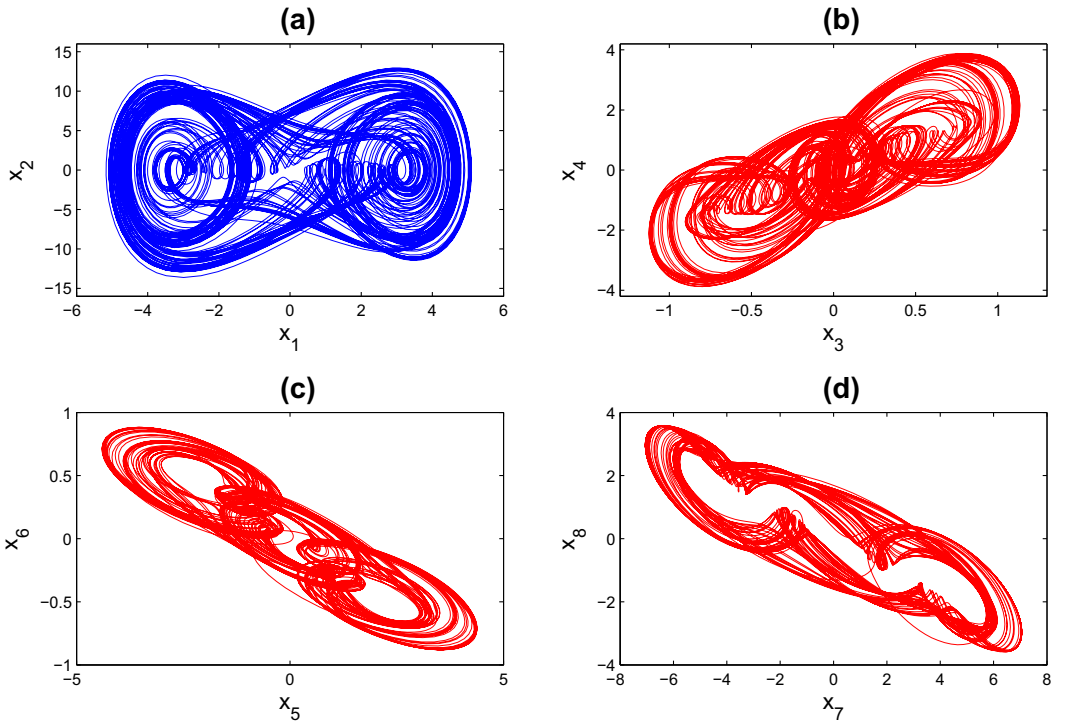

Fig. 7. 2-dimensional projections of the chaotic attractor of the result-system (8.32). (a) Projection on the x_1–x_2 plane, (b) Projection on the x_3–x_4 plane, (c) Projection on the x_5–x_6 plane, (d) Projection on the x_7–x_8 plane. The picture in (a) shows the attractor of the prior chaos produced by the generator system (8.31) and in (b)–(d) the chaotic attractors of the remaining subsystems are observable. The illustrations in (b)–(d) repeated the structure of the attractor shown in (a), and these pictures are indicators of the chaos extension.

In Fig. 7(a)–(d), we illustrate the 2-dimensional projections of the trajectory of system (8.32), with the initial data $x_1(0) = 2.16,\ x_2(0) = -9.28,\ x_3(0) = -0.21,\ x_4(0) = -2.03,\ x_5(0) = 3.36,\ x_6(0) = -0.52,\ x_7(0) = 3.07,\ x_8(0) = -0.32,$ on the planes x_1–$x_2,\ x_3$–$x_4,\ x_5$–x_6, and x_7–x_8, respectively. The picture in Fig. 7(a) shows in fact the attractor of the prior chaos produced by the generator system (8.31) and similarly the illustrations in Fig. 7(b)–(d) correspond to the chaotic attractors of the second, third and the fourth subsystems, respectively. The resemblance between the shapes of the attractors of the subsystems reflect the morphogenesis of chaos in the result-system (8.32).

To obtain a better impression about the chaotic attractor of system (8.32), in Fig. 8 we demonstrate the 3-dimensional projections of the trajectory with the same initial data as above, on the x_3–x_5–x_7 and x_4–x_6–x_8 spaces. Although we are restricted to make illustrations at most in 3-dimensional spaces and not able to provide a picture of the whole chaotic attractor, the results shown both in Figs. 7 and 8 give us an idea about the spectacular chaotic attractor of system (8.32).

We note that system (8.32) exhibits a symmetry under the transformation

$$\mathscr{K} : (x_1, x_2, x_3, x_4, x_5, x_6, x_7, x_8, t) \to (-x_1, -x_2, -x_3, -x_4, -x_5, -x_6, -x_7, -x_8, t + \pi)$$

and the presented attractors are symmetric around the origin due to the symmetry of the result-system (8.32) under this transformation.

Now, let us show that the first replicator system which is included inside (8.32) satisfies the condition (A7).

In the calculations below, we will denote by $\|.\|$ the matrix norm which is induced by the usual Euclidean norm in $\mathbb{R}^l$. That is,

$$\|\Gamma\| = \max\left\{\sqrt{\varsigma} : \varsigma \textit{ is an eigenvalue of } \Gamma^T\Gamma\right\} \tag{8.33}$$

for any $l \times l$ matrix Γ with real entries, and Γ^T denotes the transpose of the matrix Γ [89].

When the system

$$\begin{aligned} x_3' &= 2x_3 - x_4 + 0.4\tan((x_1 + x_3)/10) \\ x_4' &= 17x_3 - 6x_4 + x_2 \end{aligned} \tag{8.34}$$

is considered in the form of system (1.2), one can see that the matrix A can be written as $A = \begin{bmatrix} 2 & -1 \\ 17 & -6 \end{bmatrix}$, which admits the complex conjugate eigenvalues $-2 \mp i$.

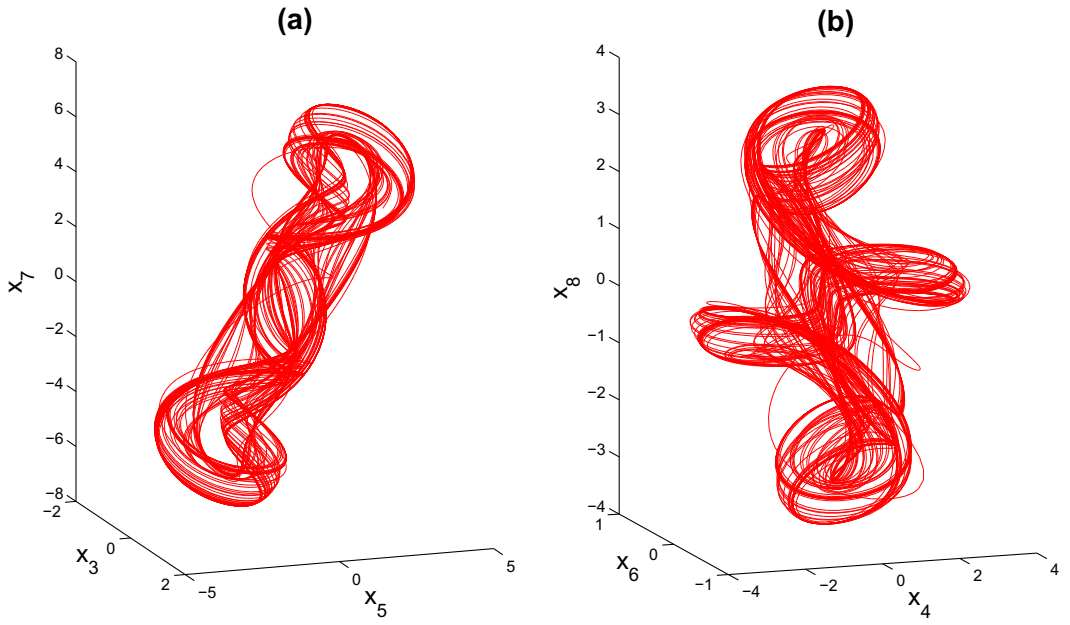

Fig. 8. 3-dimensional projections of the chaotic attractor of the result-system (8.32). (a) Projection on the x_3–x_5–x_7 space, (b) Projection on the x_4–x_6–x_8 space. The illustrations presented in (a) and (b) give information about the impressive chaotic attractor in the 8-dimensional space.

The real Jordan form of the matrix A is given by $J = \begin{bmatrix} -2 & -1 \\ 1 & -2 \end{bmatrix}$ and the identity $P^{-1}AP = J$ is satisfied where $P = \begin{bmatrix} 0 & 1 \\ -1 & 4 \end{bmatrix}$. Evaluating the exponential matrix e^{At} we obtain that

$$e^{At} = e^{-2t} P \begin{bmatrix} \cos t & -\sin t \\ \sin t & \cos t \end{bmatrix} P^{-1}. \tag{8.35}$$

Taking $N = \|P\|\left\|P^{-1}\right\| < 18$ and $\omega = 2$, one can see that the inequality $\left\|e^{At}\right\| \leqslant Ne^{-\omega t}$ holds for all $t \geqslant 0$. The function $g : \mathbb{R}^2 \times \mathbb{R}^2 \to \mathbb{R}^2$ defined as

$$g(x_1, x_2, x_3, x_4) = \left(0.4 \tan\left(\frac{x_1 + x_3}{10}\right), x_2\right)$$

satisfies the conditions (A4) and (A5) with constants $L_1 = \sqrt{2}/50,\ L_2 = \sqrt{2}$ and $L_3 = 0.08$ since the chaotic attractor of system (8.32) satisfies the inequalities $|x_1| \leqslant 6,\ |x_3| \leqslant 3/2$, and consequently $\left|\frac{x_1 + x_3}{10}\right| \leqslant 3/4$. Therefore, the condition (A7) is satisfied.

In a similar way, for the second replicator system, making use of $|x_3| \leqslant 3/2$ once again, one can show that the function $h : \mathbb{R}^2 \times \mathbb{R}^2 \to \mathbb{R}^2$ defined as

$$h(x_3, x_4, x_5, x_6) = \left(0.5 \sin x_6 - 4x_4, -\tan\left(\frac{x_3}{2}\right)\right)$$

satisfies the counterparts of the conditions (A4) and (A5) with constants $L_1 = \sqrt{2}/4,\ L_2 = 4\sqrt{2}$ and $L_3 = 1/2$.

On the other hand, when one considers the third replicator, it is easy to show that the function $k : \mathbb{R}^2 \times \mathbb{R}^2 \to \mathbb{R}^2$ defined as

$$k(x_5, x_6, x_7, x_8) = \left(0.0003(x_7 - x_8)^3 - 1.5x_6, 4x_5\right)$$

satisfies the counterparts of the conditions (A4) and (A5) with constants $L_1 = 3\sqrt{2}/4,\ L_2 = 4\sqrt{2}$ and $L_3 = 0.19$ since the chaotic attractor of system (8.32) satisfies the inequalities $|x_7| \leqslant 8,\ |x_8| \leqslant 4$.

9. Controlling replication of chaos

In the previous section we have theoretically proved replication of chaos for specific types and controlling the extended chaos is another interesting problem. The next theorem and its corollary indicate a method to control the chaos of the replicator system (1.2) and the result-system (1.1)+(1.2), respectively, and reveal that controlling the chaos of system (1.1) is sufficient for this.

Theorem 9.1. *Assume that for arbitrary $\epsilon > 0$, a periodic solution $x_p(t) \in \mathscr{A}_x$ is stabilized such that for any solution $x(t)$ of system (1.1) there exist real numbers a and $E > 0$ such that the inequality $\|x(t) - x_p(t)\| < \epsilon$ holds for $t \in [a, a+E]$. Then, the periodic solution $\phi_{x_p(t)}(t) \in \mathscr{A}_y$ is stabilized such that for any solution $y(t)$ of system (1.2) there exists a number $b \geqslant a$ such that the inequality $\left\|y(t) - \phi_{x_p(t)}(t)\right\| < \left(1 + \frac{NL_2}{\omega - NL_3}\right)\epsilon$ holds for $t \in [b, a+E]$, provided that the number E is sufficiently large.*

Proof. Fix an arbitrary solution $y(t)$ of system $y' = Ay + g(x(t), y)$ for some solution $x(t)$ of system (1.1). According to our assumption, there exist numbers a and $E > 0$ such that the inequality $\|x(t) - x_p(t)\| < \epsilon$ holds for $t \in [a, a+E]$. Let us denote $y_p(t) = \phi_{x_p(t)}(t) \in \mathscr{A}_y$. It is clear that the function $y_p(t)$ is periodic with the same period as $x_p(t)$. Since $y(t)$ and $y_p(t)$ satisfy the integral equations

$$y(t) = e^{A(t-a)}y(a) + \int_a^t e^{A(t-s)}g(x(s), y(s))ds$$

and

$$y_p(t) = e^{A(t-a)}y_p(a) + \int_a^t e^{A(t-s)}g(x_p(s), y_p(s))ds,$$

respectively, one has

$$\begin{aligned} y(t) - y_p(t) = e^{A(t-a)}(y(a) - y_p(a)) &+ \int_a^t e^{A(t-s)}\left[g(x(s), y(s)) - g(x(s), y_p(s))\right]ds \\ &+ \int_a^t e^{A(t-s)}\left[g(x(s), y_p(s)) - g(x_p(s), y_p(s))\right]ds. \end{aligned}$$

By the help of the last equation, we have

$$\|y(t) - y_p(t)\| \leqslant Ne^{-\omega(t-a)}\|y(a) - y_p(a)\| + \frac{NL_2\epsilon}{\omega}e^{-\omega t}\left(e^{\omega t} - e^{\omega a}\right) + NL_3\int_a^t e^{-\omega(t-s)}\|y(s) - y_p(s)\|ds.$$

Let $u : [a, a+E] \to [0, \infty)$ be a function defined as $u(t) = e^{\omega t}\|y(t) - y_p(t)\|$. In this case, we reach the inequality

$$u(t) \leqslant Ne^{\omega a}\|y(a) - y_p(a)\| + \frac{NL_2\epsilon}{\omega}\left(e^{\omega t} - e^{\omega a}\right) + NL_3\int_a^t u(s)ds.$$

Implementation of Lemma 2.2 [82] to the last inequality, where $t \in [a, a+E]$, provides us

$$u(t) \leqslant \frac{NL_2\epsilon}{\omega}e^{\omega t} + N\|y(a) - y_p(a)\|e^{\omega a}e^{NL_3(t-a)} - \frac{NL_2\epsilon}{\omega}e^{\omega a}e^{NL_3(t-a)} + \frac{N^2L_2L_3\epsilon}{\omega(\omega - NL_3)}e^{\omega t}\left(1 - e^{(NL_3-\omega)(t-a)}\right).$$

and consequently,

$$\begin{aligned} \|y(t) - y_p(t)\| &\leqslant \frac{NL_2\epsilon}{\omega} + N\|y(a) - y_p(a)\|e^{(NL_3-\omega)(t-a)} - \frac{NL_2\epsilon}{\omega}e^{(NL_3-\omega)(t-a)} + \frac{N^2L_2L_3\epsilon}{\omega(\omega - NL_3)}\left(1 - e^{(NL_3-\omega)(t-a)}\right) \\ &< N\|y(a) - y_p(a)\|e^{(NL_3-\omega)(t-a)} + \frac{NL_2\epsilon}{\omega - NL_3}. \end{aligned}$$

If $y(a) = y_p(a)$, then clearly $\|y_p(t) - y(t)\| < \left(1 + \frac{NL_2}{\omega - NL_3}\right)\epsilon,\ t \in [a, a+E]$. Suppose that $y(a) \neq y_p(a)$. For $t \geqslant a + \frac{1}{NL_3 - \omega}\ln\left(\frac{\epsilon}{N\|y(a) - y_p(a)\|}\right)$, the inequality $e^{(NL_3-\omega)(t-a)} \leqslant \frac{\epsilon}{N\|y(a) - y_p(a)\|}$ is satisfied. Assume that the number E is sufficiently large so that $E > \frac{1}{NL_3 - \omega}\ln\left(\frac{\epsilon}{N\|y(a) - y_p(a)\|}\right)$. Thus, taking

$$b = \max\left\{a, a + \frac{1}{NL_3 - \omega}\ln\left(\frac{\epsilon}{N\|y(a) - y_p(a)\|}\right)\right\}$$

and

$$\widetilde{E} = \min\left\{E, E - \frac{1}{NL_3 - \omega}\ln\left(\frac{\epsilon}{N\|y(a) - y_p(a)\|}\right)\right\}$$

one attains $\|y(t) - y_p(t)\| < \left(\frac{\omega - NL_3 + NL_2}{\omega - NL_3}\right)\epsilon$, for $t \in [b, b + \widetilde{E}]$. Here the number $\widetilde{E}$ stands for the duration of control for system (1.2). We note that $b \geqslant a,\ 0 < \widetilde{E} \leqslant E$ and $b + \widetilde{E} = a + E$.

Hence $\|y(t)-y_p(t)\| < \left(1+\frac{NL_2}{\omega-NL_3}\right)\epsilon$, for $t \in [b, a+E]$.
The proof of the theorem is finalized. □
An immediate corollary of Theorem 9.1 is the following.

Corollary 9.1. *Assume that the conditions of Theorem 9.1 hold. In this case, the periodic solution* $z_p(t) = \left(x_p(t), \phi_{x_p(t)}(t)\right) \in \mathscr{A}$ *is stabilized such that for any solution* $z(t)$ *of system (1.1)+(1.2) there exists a number* $b \geqslant a$ *such that the inequality* $\|z_p(t)-z(t)\| < \left(2+\frac{NL_2}{\omega-NL_3}\right)\epsilon$ *holds for* $t \in [b, a+E]$, *provided that the number* E *is sufficiently large.*

Proof. On account of the inequality $\|z(t)-z_p(t)\| \leqslant \|x(t)-x_p(t)\| + \left\|y(t)-\phi_{x_p(t)}(t)\right\|$, and using the conclusion of Theorem 9.1 one can show that $\|z_p(t)-z(t)\| < \left(2+\frac{NL_2}{\omega-NL_3}\right)\epsilon$ holds for $t \in [b, a+E]$ and for some $b \geqslant a$. The proof is completed. □

Remark 9.1. As a conclusion of Theorem 9.1, the transient time for control to take effect may increase and the duration of control may decrease as the number of consecutive replicator systems increase.

In the remaining part of this section, our aim is to present an illustration which confirms the results of Theorem 9.1, and for our purposes, we will make use of the Pyragas control method [90]. Therefore, primarily, we continue with a brief explanation of this method.

A delayed feedback control method for the stabilization of unstable periodic orbits of a chaotic system was proposed by Pyragas [90]. In this method, one considers a system of the form

$$x' = H(x,q), \tag{9.36}$$

where $q = q(t)$ is an externally controllable parameter and for $q = 0$ it is assumed that the system (9.36) is in the chaotic state of interest, whose periodic orbits are to be stabilized [11,87,90,91]. According to Pyragas method, an unstable ξ-periodic solution of the system (9.36) with $q = 0$, can be stabilized by the control law $q(t) = C[s(t-\xi) - s(t)]$, where the parameter C represents the strength of the perturbation and $s(t) = \sigma[x(t)]$ is a scalar signal given by some function of the state of the system.

It is indicated in [11] that in order to apply the Pyragas control method to the chaotic Duffing oscillator given by the system

$$\begin{aligned} x_1' &= x_2 \\ x_2' &= -0.10x_2 + 0.5x_1(1-x_1^2) + 0.24\sin t, \end{aligned} \tag{9.37}$$

one can construct the corresponding control system

$$\begin{aligned} v_1' &= v_2 \\ v_2' &= -0.10v_2 + 0.5v_1(1-v_1^2) + 0.24\sin(v_3) + C[v_2(t-2\pi) - v_2(t)] \\ v_3' &= 1, \end{aligned} \tag{9.38}$$

where $q(t) = C[v_2(t-2\pi) - v_2(t)]$ is the control law and an unstable 2π-periodic solution can be stabilized by choosing an appropriate value for the parameter C.

Now, let us combine system (9.37) with two consecutive replicator systems and set up the following 6-dimensional result-system

$$\begin{aligned} x_1' &= x_2 \\ x_2' &= -0.10x_2 + 0.5x_1(1-x_1^2) + 0.24\sin t \\ x_3' &= x_4 - 0.1x_1 \\ x_4' &= -3x_3 - 2x_4 - 0.008x_3^3 + 1.6x_2 \\ x_5' &= x_6 + 0.6x_3 \\ x_6' &= -3.1x_5 - 2.1x_6 - 0.007x_5^3 + 2.5x_4. \end{aligned} \tag{9.39}$$

In system (9.39) the subsystems with coordinates (x_3, x_4) and (x_5, x_6) correspond to the first and the second replicator systems, respectively. Since our procedure of morphogenesis is valid for specific types of chaos such as in Devaney's and Li-Yorke sense and through period-doubling cascade, we expect that our procedure is also applicable to any other chaotic system with an unspecified type of chaos. Accordingly, system (9.39) is chaotic since the generator system (9.37) is chaotic.

Theorem 9.1 specifies that in order to control the chaos of system (9.39) one should control the chaos of the generator system, which is the subsystem of (9.39) with coordinates (x_1, x_2). In accordance with this purpose, we will use the Pyragas control method by means of the system

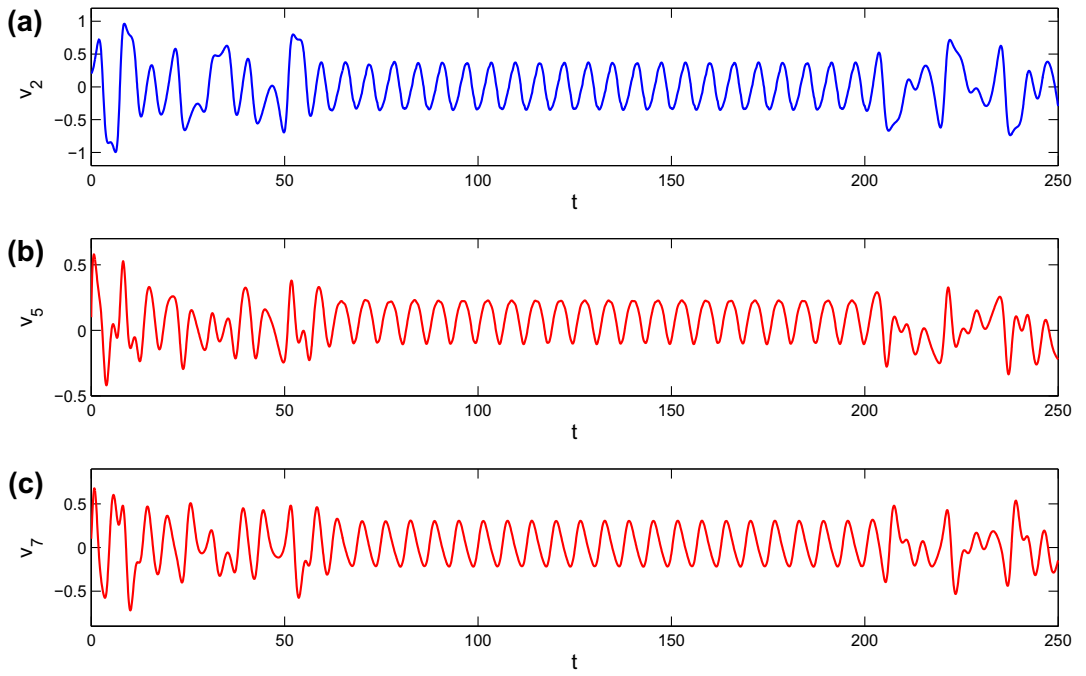

Fig. 9. Pyragas control method applied to the result-system (9.39) with the aid of the corresponding control system (9.40). (a) The graph of v_2-coordinate, (b) The graph of v_5-coordinate, (c) The graph of v_7-coordinate. The result of Pyragas control method applied to the generator system (9.37) is seen in (a). Through this method, the 2π-periodic solution of the generator and accordingly the 2π-periodic solutions of the first and the second replicator systems are stabilized. In other words, the chaos of the result-system (9.39) is controlled. For the coordinates v_1, v_4 and v_6 we have similar results which are not just pictured here. The control starts at $t = 60$ and ends at $t = 200$, after which emergence of the chaos is observable again.

$$
\begin{aligned}
v_1' &= v_2\\
v_2' &= -0.10v_2 + 0.5v_1(1 - v_1^2) + 0.24\sin(v_3) + C[v_2(t - 2\pi) - v_2(t)]\\
v_3' &= 1\\
v_4' &= v_5 - 0.1v_1\\
v_5' &= -3v_4 - 2v_5 - 0.008v_4^3 + 1.6v_2\\
v_6' &= v_7 + 0.6v_4\\
v_7' &= -3.1v_6 - 2.1v_7 - 0.007v_6^3 + 2.5v_5,
\end{aligned}
\tag{9.40}
$$

which is the control system corresponding to (9.39).

Let us consider a solution of system (9.40) with the initial data $v_1(0) = 0.2$, $v_2(0) = 0.2$, $v_3(0) = 0$, $v_4(0) = -0.5$, $v_5(0) = 0.1$, $v_6 = -0.2$ and $v_7(0) = 0.1$. We let the system evolve freely taking $C = 0$ until $t = 60$, and at that moment we switch on the control by taking $C = 0.84$. At $t = 200$, we switch off the control and start to use the value of the parameter $C = 0$ again. In Fig. 9 one can see the graphs of the v_2, v_5, v_7 coordinates of the solution. Supporting the result of Theorem 9.1, it is observable in Fig. 9 that stabilizing a 2π-periodic solution of the generator system provides the stabilization of the corresponding 2π-periodic solutions of the replicator systems. After switching off the control, the 2π-periodic solutions of the generator and replicators lose their stability and chaos emerges again.

10. Discussion

In this part of the paper, we intend to consider not rigorously proved, but interesting phenomena which can be considered in the framework of our results. So, we shall give some additional light on the results obtained above and say about the possibility for the replication of intermittency, Shil'nikov orbits and relay systems. We also demonstrate the possibility of quasiperiodic motions as an infinite basis of chaos.

We start our discussions with replication of intermittency.

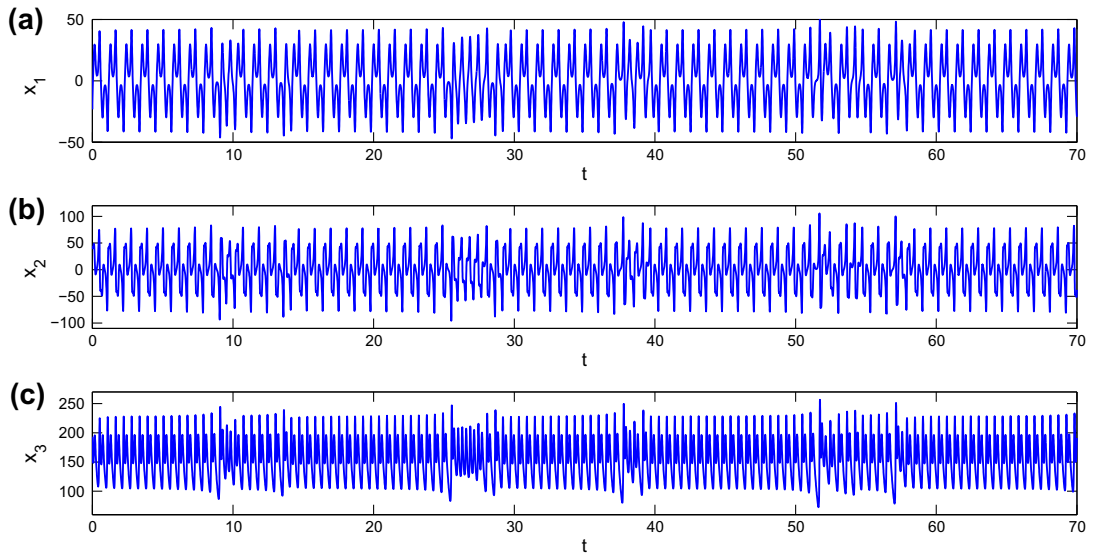

Fig. 10. Intermittency in the Lorenz system (5.21), where $\sigma = 10,\ b = 8/3$ and $r = 166.25$. (a) The graph of the x_1-coordinate, (b) The graph of the x_2-coordinate, (c) The graph of the x_3-coordinate.

10.1. Replication of intermittency

In previous sections of the paper, we have rigorously proved replication of specific types of chaos such as period-doubling cascade, Devaney's and Li-Yorke chaos. Consequently, one can expect that the same procedure also works for the intermittency route.

Pomeau and Manneville [52] observed chaos through intermittency in the Lorenz system (5.21), with the coefficients $\sigma = 10,\ b = 8/3$ and values of r slightly larger than the critical value $r_c \approx 166.06$. To observe intermittent behavior in the Lorenz system, let us consider a solution of system (5.21) together with the coefficients $\sigma = 10,\ b = 8/3,\ r = 166.25$ using the initial data $x_1(0) = -23.3,\ x_2(0) = 38.3$ and $x_3(0) = 193.4$. The time-series for the $x_1,\ x_2$ and x_3 coordinates of the solution are indicated in Fig. 10, where one can see that regular oscillations are interrupted by irregular ones.

To perform replication of intermittency, let us consider the Lorenz system (5.21) as a generator and set up the 6-dimensional result-system

$$\begin{aligned} x_1' &= \sigma(-x_1 + x_2)\\ x_2' &= -x_2 + rx_1 - x_1x_3\\ x_3' &= -bx_3 + x_1x_2\\ x_4' &= -x_4 + 4x_1\\ x_5' &= x_6 + 2x_2\\ x_6' &= -3x_5 - 2x_6 - 0.00005x_5^3 + 0.5x_4, \end{aligned} \tag{10.41}$$

again with the coefficients $\sigma = 10,\ b = 8/3$ and $r = 166.25$. It can be easily verified that condition (A7) is valid for system (10.41). We consider the trajectory of system (10.41) corresponding to the initial data $x_1(0) = -23.3,\ x_2(0) = 38.3,\ x_3(0) = 193.4,\ x_4(0) = -17.7,\ x_5(0) = 11.4$, and $x_6(0) = 2.5$, and represent the graphs for the $x_4,\ x_5$ and x_6 coordinates in Fig. 11 such that the intermittent behavior in the replicator system is observable. The similarity between the graphs of the coordinates corresponding to the generator and the replicator counterpart reveals the replication of intermittency.

10.2. Replication of Shil'nikov orbits

To illustrate that by our method it may also be possible to replicate strange attractors [19,30,65], let us provide simulations of homoclinic and complicated Shil'nikov orbits (Fig. 12 and Fig. 13 correspondingly).

As a model for Shilnikov's orbits, the paper [92] considers the system

$$\begin{aligned} x_1' &= x_2\\ x_2' &= x_3\\ x_3' &= -x_2 - \beta x_3 + f_\mu(x_1), \end{aligned} \tag{10.42}$$

where

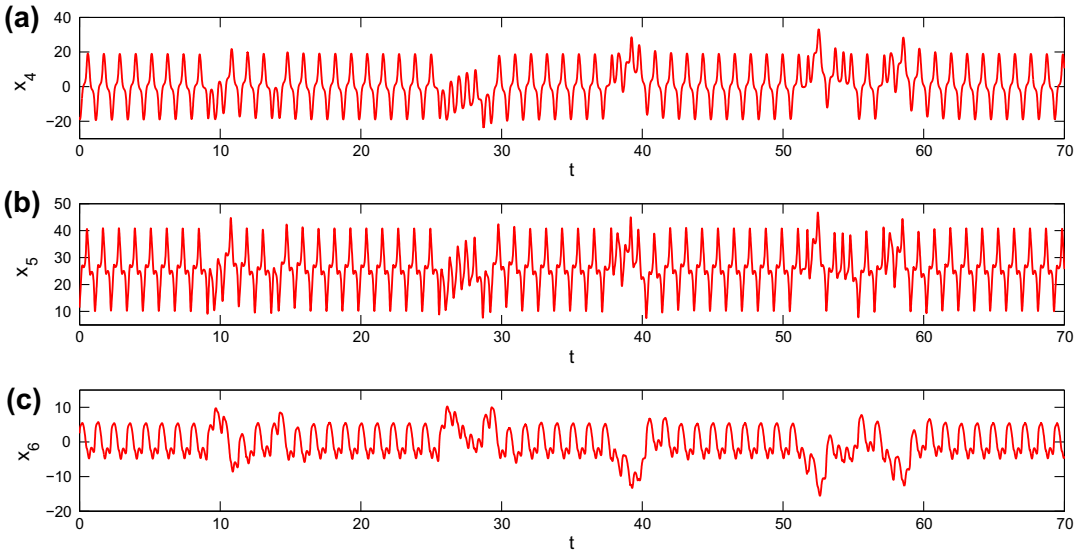

Fig. 11. Intermittency in the replicator system. (a) The graph of the x_4-coordinate, (b) The graph of the x_5-coordinate, (c) The graph of the x_6-coordinate. The analogy between the time-series of the generator and the replicator systems indicates the replication of intermittency.

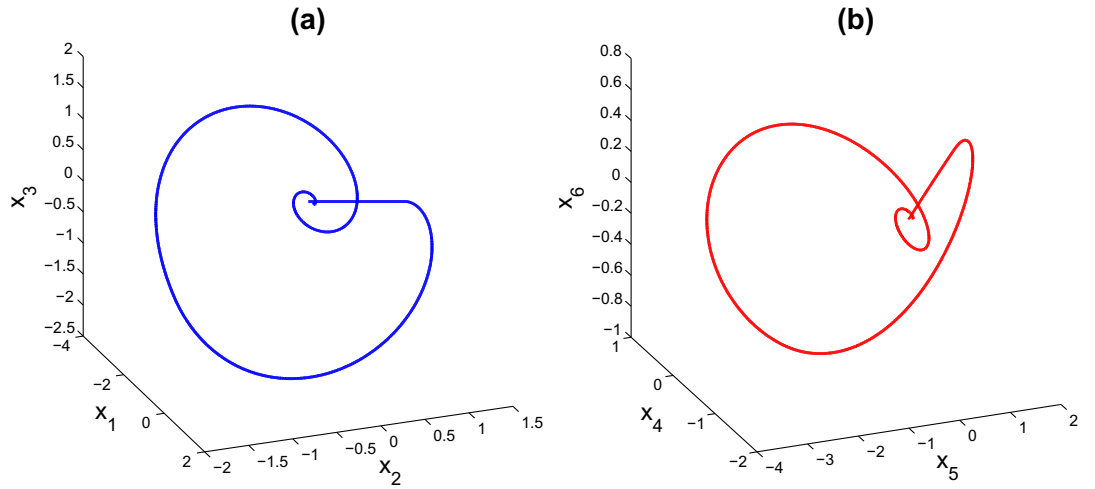

Fig. 12. Replication of a Shil'nikov type homoclinic orbit. In picture (a), one can see the projection on the $x_1{-}x_2{-}x_3$ space of the trajectory of system (10.44) corresponding to the initial data $x_1(0) - 1.57590,\ x_2(0) = 0,\ x_3(0) = 0,\ x_4(0) = -0.78795,\ x_5(0) = 0$ and $x_6(0) = 0$. The picture in (b) shows the projection on the $x_4{-}x_5{-}x_6$ space of the same trajectory. The parameter values $\alpha = 0.633625,\ \beta = 0.3375$ and $\mu = 2.16$ are used in the simulation. The picture in (a) represents a Shil'nikov type homoclinic orbit corresponding to the generator system (10.42), while the picture in (b) shows its replication through the system (10.44).

$$f_\mu(x) = \begin{cases} 1 - \mu x, & \text{if } x > 0 \\ 1 + \alpha x, & \text{if } x \leqslant 0. \end{cases} \tag{10.43}$$

The values $\alpha = 0.633625,\ \beta = 0.3375$ and the parameter μ used in system (10.42) are taken from [24]. There exists an equilibrium point $e_0 = (-1/\alpha, 0, 0)$ of system (10.42) and the eigenvalues of the matrix of linearization at e_0 are $0.4625, -0.4 \pm 1.1i$ such that the condition of the Shil'nikov's theorem about eigenvalues [93] is satisfied. For values of the parameter μ near 2.16 system (10.42) possesses a special type homoclinic orbit – *Shil'nikov orbit*, and its presence implies chaotic dynamics [24]. In this case, Shil'nikov's theorem asserts that every neighborhood of the homoclinic orbit contains a countably infinite number of unstable periodic orbits [92,93].

To demonstrate numerically the replication of a Shil'nikov orbit, let us consider the following system

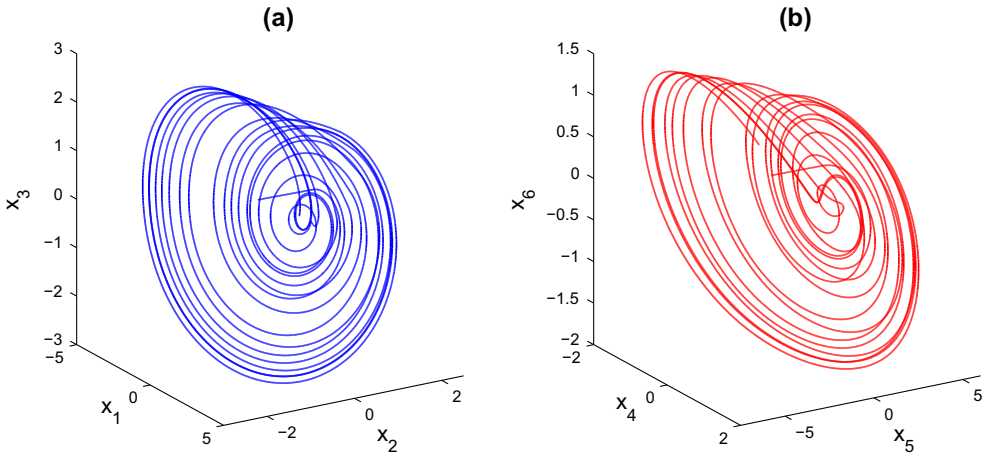

Fig. 13. Projections of a complicated orbit of system (10.44) with $\alpha = 0.633625,\ \beta = 0.3375$ and $\mu = 0.83$. (a) Projection on the x_1—x_2—x_3 space, (b) Projection on the x_4—x_5—x_6 space. The initial data $x_1(0) - 1.57590,\ x_2(0) = 0,\ x_3(0) = 0,\ x_4(0) = -0.78795,\ x_5(0) = 0,\ x_6(0) = 0$ is used for the illustration. The picture in (a) represents the behavior of the trajectory corresponding to the generator (10.42), while the picture in (b) illustrates its replication.

$$\begin{aligned} x_1' &= x_2 \\ x_2' &= x_3 \\ x_3' &= -x_2 - \beta x_3 + f_\mu(x_1) \\ x_4' &= -2x_4 + x_1 \\ x_5' &= -0.6x_5 + 2x_2 + 0.1x_2^3 \\ x_6' &= -1.2x_6 + 0.001\sin(x_6) + x_3, \end{aligned} \tag{10.44}$$

where, again, the function $f_\mu(x)$ is given by formula (10.43).

System (10.42) is used as a generator in system (10.43), where the last three coordinates are of a replicator. Let us consider system (10.44) with the values $\alpha = 0.633625,\ \beta = 0.3375$ and $\mu = 2.16$ once again. In Fig. 12 we show the trajectory of this system with initial data $x_1(0) - 1.5759,\ x_2(0) = 0,\ x_3(0) = 0,\ x_4(0) = -0.78795,\ x_5(0) = 0$ and $x_6(0) = 0$. The picture in Fig. 12(a), where we illustrate the projection of the trajectory on the x_1—x_2—x_3 space represents, in fact, the Shil'nikov orbit corresponding to the generator system (10.42). On the other hand, the picture in Fig. 12(b), shows the projection of the trajectory on the x_4—x_5—x_6 space and in this picture the replication of the Shil'nikov orbit is observable.

Next, we consider system (10.44) with the values $\alpha = 0.633625,\ \beta = 0.3375,\ \mu = 0.83$ and take the trajectory of this system with the same initial data as above. In Fig. 13(a) and (b), we represent the projections of this trajectory on the x_1—x_2—x_3 and x_4—x_5—x_6 spaces, respectively. The picture in (a) represents the complicated behavior of the generator system (10.42) and one can see in picture (b) the replication of this behavior.

We suppose that theoretical affirmation of our simulation results can be done if one considers interpretation of Shil'nikov's theorem [93] for the multidimensional replicator. That is, we are still questioning whether our approach can be somehow combined with methods indicating chaos through Shil'nikov type strange attractors [19,65]. At least, it is easy to see that a homoclinic trajectory exists for a replicator as well as a denumerable set of unstable periodic solutions.

In next our discussion, we will emphasize by means of simulations the morphogenesis of the double-scroll Chua's attractor in a unidirectionally coupled open chain of Chua circuits. Approaches for the generation of hyperchaotic systems have already been discussed making use of Chua circuits which are all chaotic [61,94]. It deserves to remark that to create hyperchaotic attractors in previous papers, others consider both involved interacting systems chaotic, but in our case only the first link of the chain is chaotic and other consecutive Chua systems are all non-chaotic.

10.3. Morphogenesis of the double-scroll Chua's attractor

The type of chaos for the double-scroll Chua circuit is proposed in paper [95]. It is an interesting problem to prove that this type of chaos can be replicated through the method discussed in our paper. Nevertheless, we will show by simulations that the regular behavior in Chua circuits placed in the extension mechanism can also be seen. This means that next special investigation has to be done. Moreover, this will show how one can use morphogenesis not only for chaos, but also for Chua circuits by uniting them in complexes in electrical (physical) sense, and observing the same properties as a unique separated Chua circuit admits. This is an interesting problem which can give a light for the complex behavior of huge electrical circuits.

There is a well known result of the chaoticity based on the double-scroll Chua's attractor [96]. It was proven first in the paper [95] rigorously and the proof is based on the Shil'nikov's theorem [93]. Since the Chua circuit and its chaotic behavior is of extreme importance from the theoretical point of view and its usage area in electrical circuits by radio physicists and nonlinear scientists from other disciplines, one can suppose that morphogenesis of the chaos will also be of a practical and a theoretical interest.

We just take into account a simulation result which supports that morphogenesis idea can be developed also from this point of view.

Let us consider the dimensionless form of the Chua's oscillator given by the system

$$\begin{aligned} x_1' &= k\alpha[x_2 - x_1 - f(x_1)] \\ x_2' &= k(x_1 - x_2 + x_3) \\ x_3' &= k(-\beta x_2 - \gamma x_3) \\ f(x) &= bx + 0.5(a-b)(|x+1| + |x-1|), \end{aligned} \tag{10.45}$$

where $\alpha,\ \beta,\ \gamma,\ a,\ b$ and k are constants.

In paper [97], it is indicated that system (10.45) with the coefficients $\alpha = 21.32/5.75,\ \beta = 7.8351,\ \gamma = 1.38166392/12,\ a = -1.8459,\ b = -0.86604$ and $k = 1$ admits a stable equilibrium.

In what follows, as the generator, we make use of system (10.45) together with the coefficients $\alpha = 15.6,\ \beta = 25.58,\ \gamma = 0,\ a = -8/7,\ b = -5/7$ and $k = 1$ such that a double-scroll Chua's attractor takes place [83], and consider the following 12-dimensional result-system

$$\begin{aligned} x_1' &= 15.6[x_2 - (2/7)x_1 + (3/14)(|x_1+1| + |x_1-1|)] \\ x_2' &= x_1 - x_2 + x_3 \\ x_3' &= -25.58x_2 \\ x_4' &= (21.32/5.75)[x_5 - 0.13396x_4 + 0.48993(|x_4+1| + |x_4-1|)] + 2x_1 \\ x_5' &= x_4 - x_5 + x_6 + 5x_2 \\ x_6' &= -7.8351x_5 - (1.38166392/12)x_6 + 2x_3 \\ x_7' &= (21.32/5.75)[x_8 - 0.13396x_7 + 0.48993(|x_7+1| + |x_7-1|)] + 2x_4 \\ x_8' &= x_7 - x_8 + x_9 + 3x_5 \\ x_9' &= -7.8351x_8 - (1.38166392/12)x_9 - 0.001x_6 \\ x_{10}' &= (21.32/5.75)[x_{11} - 0.13396x_{10} + 0.48993(|x_{10}+1| + |x_{10}-1|)] + 4x_7 \\ x_{11}' &= x_{10} - x_{11} + x_{12} - 0.1x_8 \\ x_{12}' &= -7.8351x_{11} - (1.38166392/12)x_{12} + 2x_9. \end{aligned} \tag{10.46}$$

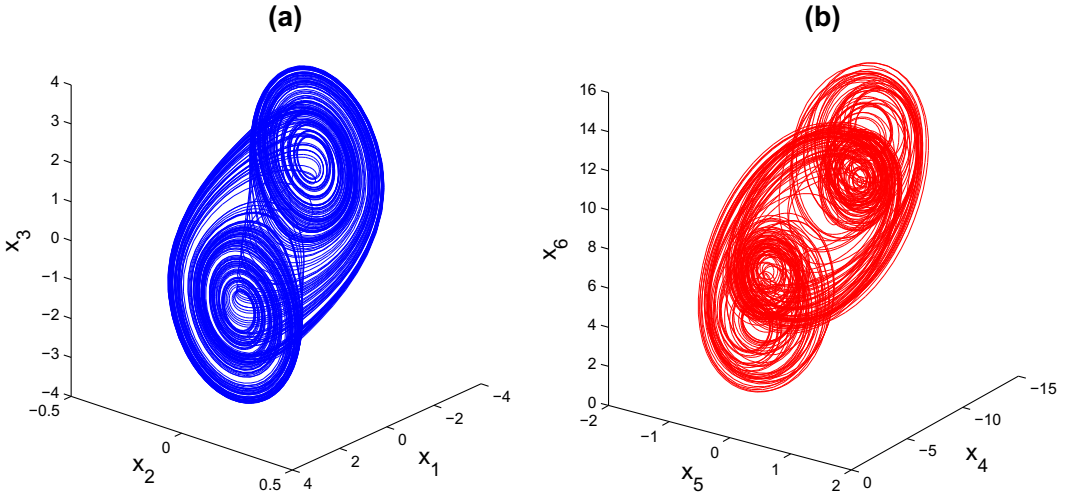

Fig. 14. 3-dimensional projections of the chaotic attractor of the result-system (10.46). (a) Projection on the x_1–x_2–x_3 space, (b) Projection on the x_4–x_5–x_6 space. The picture in (a) shows the attractor of the original prior chaos of the generator system (10.45) and (b) represents the attractor of the first replicator. The resemblance between shapes of the attractors of the generator and the replicator systems makes the extension of chaos apparent.

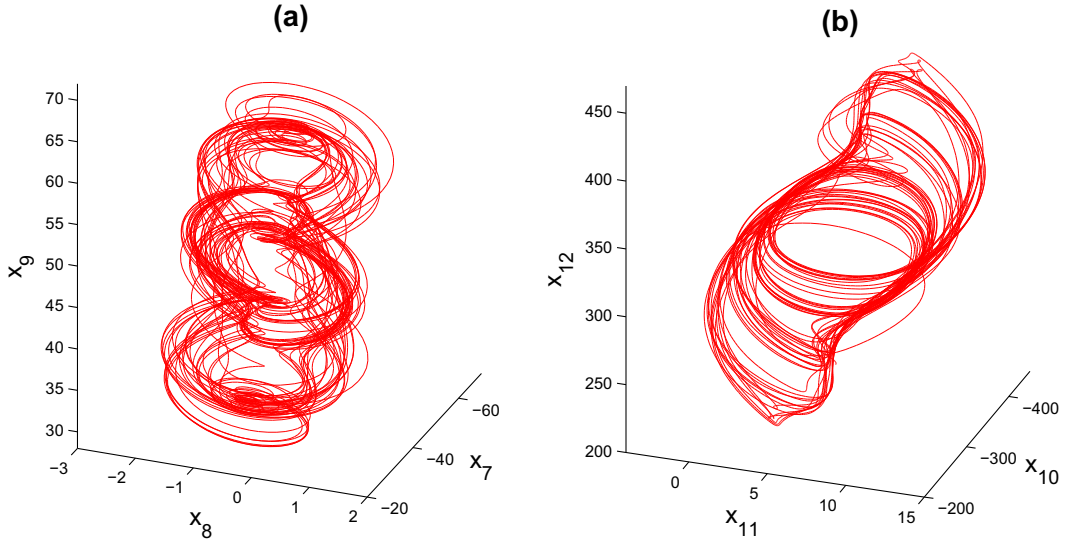

Fig. 15. 3-dimensional projections of the chaotic attractor of the result-system (10.46). (a) Projection on the x_7—x_8—x_9 space, (b) Projection on the x_{10}—x_{11}—x_{12} space. (a) and (b) demonstrates the attractors generated by the second and the third replicator systems, respectively.

System (10.46) consists of four unidirectionally coupled Chua circuits such that the subsystems with coordinates (x_1, x_2, x_3), (x_4, x_5, x_6), (x_7, x_8, x_9) and (x_{10}, x_{11}, x_{12}) correspond to the first, second, third and the fourth links of the open chain of circuits.

In Fig. 14, we simulate the 3-dimensional projections on the x_1—x_2—x_3 and x_4—x_5—x_6 spaces of the trajectory of the result-system (10.46) with the initial data $x_1(0) = 0.634$, $x_2(0) = -0.093$, $x_3(0) = -0.921$, $x_4(0) = -8.013$, $x_5(0) = 0.221$, $x_6(0) = 6.239$, $x_7(0) = -50.044$, $x_8(0) = -0.984$, $x_9(0) = 48.513$, $x_{10}(0) = -256.325$, $x_{11}(0) = 7.837$, $x_{12}(0) = 264.331$. The projection on the x_1—x_2—x_3 space shows the double-scroll Chua's attractor produced by the generator system (10.45), and projection on the x_4—x_5—x_6 space represents the chaotic attractor of the first replicator.

In a similar way, we display the projections of the same trajectory on the x_7—x_8—x_9 and x_{10}—x_{11}—x_{12} spaces, which correspond to the attractors of the second and the third replicator systems, in Fig. 15. The illustrations shown in Figs. 14 and 15 indicate the extension of chaos in system (10.46). Possibly the result-system (10.46) produces a double-scroll Chua's attractor with hyperchaos, where the number of positive Lyapunov exponents are more than one and even four.

10.4. Morphogenesis and the logistic map

Since the logistic map is very convenient to verify chaos in the sense of Devaney and Li-Yorke as well as obtained through period-doubling cascade, one can expect that it can be used as a generator. This is true in the theoretical sense, but not for simulations since only chaos through period-doubling route can be presented in this way. Chaos in the sense of Devaney [26], Li-Yorke [39] and obtained through period-doubling cascade [40,41] as well as intermittency [26] were provided in a quasilinear system of the type

$$\begin{aligned} &z'(t) = Az(t) + f(t,z) + v(t,t_0,\mu) \\ &z(t_0) = z_0, (t_0,z_0) \in [0,1] \times \mathbb{R}^n. \end{aligned} \tag{10.47}$$

In system (10.47) the relay function $v(t,t_0,\mu)$ is defined by the following equation

$$v(t,t_0,\mu) = \begin{cases} m_0, & \text{if } \zeta_{2i}(t_0,\mu) < t \leqslant \zeta_{2i+1}(t_0,\mu) \\ m_1, & \text{if } \zeta_{2i-1}(t_0,\mu) < t \leqslant \zeta_{2i}(t_0,\mu), \end{cases} \tag{10.48}$$

where i is an integer, $m_0, m_1 \in \mathbb{R}^n$, the sequence $\{\zeta_i(t_0,\mu)\}$ is defined through the equation $\zeta_i(t_0,\mu) = i + \kappa_i(t_0,\mu)$, where $\kappa_{i+1}(t_0,\mu) = h(\kappa_i(t_0,\mu),\mu)$, $\kappa_0(t_0,\mu) = t_0$, and the function $h(x,\mu) = \mu x(1-x)$ represents the logistic map.

In paper [40] it is rigorously proved that the Duffing equation perturbed with a pulse function

$$x'' + 0.18x' + 2x + 0.00004x^3 = 0.02\cos(2\pi t) + v(t,t_0,\mu_\infty), \tag{10.49}$$

with the coefficients $m_0 = 2$, $m_1 = 1$ and $\mu_\infty = 3.8$, where the function $v(t,t_0,\mu_\infty)$ is described by Eq. (10.48), admits the chaos through period-doubling cascade on the time interval $[0,\infty)$ and obeys the Feigenbaum universal behavior [85].

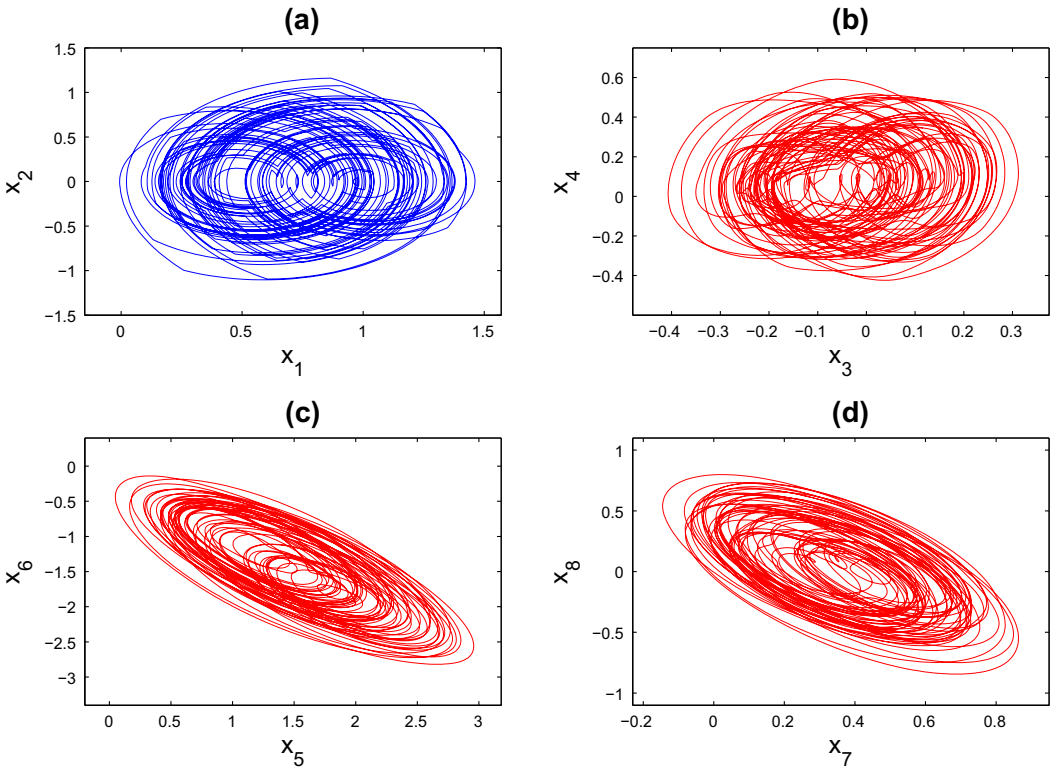

Fig. 16. 2-dimensional projections of the chaotic attractor of the result-system (10.51). (a) Projection on the x_1–x_2 plane, (b) Projection on the x_3–x_4 plane, (c) Projection on the x_5–x_6 plane, (d) Projection on the x_7–x_8 plane. The picture in (a) shows the attractor of the prior chaos produced by the generator (10.50), which is a relay-system, and in (b)–(d) the chaotic attractors of the replicator systems are observable. The illustrations in (b)–(d) repeated the structure of the attractor shown in (a), and the mimicry between these pictures is an indicator of the replication of chaos.

By favor of the new variables $x_1 = x$ and $x_2 = x'$, Eq. (10.49) can be reduced to the system

$$\begin{aligned} x_1' &= x_2 \\ x_2' &= -0.18x_2 - 2x_1 - 0.00004x_1^3 + 0.02\cos(2\pi t) + v(t, t_0, \mu_\infty). \end{aligned} \tag{10.50}$$

One can see that system (10.50) is in the form of system (10.47). For the illustration of chaos extension, we will make use of the relay-system (10.50) as the generator, in the role of a core as displayed in Fig. 4, and attach three replicator systems to obtain the 8-dimensional result-relay-system

$$\begin{aligned} x_1' &= x_2 \\ x_2' &= -0.18x_2 - 2x_1 - 0.00004x_1^3 + 0.02\cos(2\pi t) + v(t, t_0, \mu_\infty) \\ x_3' &= x_4 - 0.1x_1 \\ x_4' &= -10x_3 - 6x_4 - 0.03x_3^3 + 4x_2 \\ x_5' &= x_6 + 2x_1 \\ x_6' &= -2x_5 - 2x_6 + 0.007x_5^3 + 0.6x_2 \\ x_7' &= x_8 - 0.5x_2 \\ x_8' &= -5x_7 - 4x_8 - 0.05x_7^3 + 2.5x_1, \end{aligned} \tag{10.51}$$

where again $m_0 = 2, m_1 = 1$ and $\mu_\infty = 3.8$.

Our theoretical results reveal that system (10.51), as well as the replicators, admit the chaos through period-doubling cascade and obey the universal behavior of Feigenbaum. Fig. 16 shows the 2-dimensional projections on the x_1–x_2, x_3–x_4, x_5–x_6 and x_7–x_8 planes of the trajectory of the result-relay-system (10.51) with initial data $x_1(0) = 1.37$, $x_2(0) = -0.05$, $x_3(0) = 0.05$, $x_4(0) = -0.1$, $x_5(0) = 1.09$, $x_6(0) = -0.81$, $x_7(0) = 0.08$ and $x_8(0) = 0.21$. The

picture seen in Fig. 16(a) is the attractor of the generator (10.50) and accordingly Fig. 16(b)–(d) represent the attractors of the first, second and the third replicator systems, respectively. It can be easily verified that all replicators used inside the system (10.51) satisfy condition (A7). The resemblance of the chaotic attractors of the generator and the replicators is a consequence of morphogenesis of chaos.

Now, let us continue with the control of morphogenesis of chaos. In paper [40], it is indicated that to control chaos of system (10.50) generated through the period-doubling cascade, unstable periodic orbits of the logistic map $h(s,\mu_\infty)=\mu_\infty s(1-s)$ must be necessarily controlled, and the OGY control method [98,99] is proposed to stabilize the periodic solutions of system (10.50) by the help of the conjugate control system

$$\begin{aligned} x_1' &= x_2 \\ x_2' &= -0.18x_2 - 2x_1 - 0.00004x_1^3 + 0.02\cos(2\pi t) + v(t,t_1,\bar{\mu}_i). \end{aligned} \tag{10.52}$$

In system (10.52), the sequence $\bar{\mu}_i$ is given by the formula

$$\bar{\mu}_i = \mu_\infty\left(1+\frac{[2\kappa^{(j)}-1][\kappa_i-\kappa^{(j)}]}{\kappa^{(j)}[1-\kappa^{(j)}]}\right), \tag{10.53}$$

where $\kappa^{(j)}$, $j\geqslant 0$, with $\kappa^{(0)}=t_0\in[0,1]$ is the target periodic orbit of the logistic map $h(s,\mu_\infty)$ to be controlled, and $\kappa_{i+1}=h(\kappa_i,\mu_\infty)$, $i\geqslant 0$, with $\kappa_0=t_1\in[0,1]$.

In this method, the sequence $\bar{\mu}_i$ is supposed to vary in a small range around the value μ_∞, that is, μ can take values in the range $[\mu_\infty-\delta,\mu_\infty+\delta]$, where δ is a given small positive number. When the trajectory is outside the neighborhood of the target periodic orbit, no parameter perturbation is applied and the system evolves at its nominal parameter value μ_∞. That is, we set $\bar{\mu}_i=\mu_\infty$ when $|\bar{\mu}_i-\mu_\infty|>\delta$.

To simulate the result, let us consider the system

$$\begin{aligned} x_1' &= x_2 \\ x_2' &= -0.18x_2 - 2x_1 - 0.00004x_1^3 + 0.02\cos(2\pi t) + v(t,t_1,\bar{\mu}_i) \\ x_3' &= x_4 - 0.1x_1 \\ x_4' &= -10x_3 - 6x_4 - 0.03x_3^3 + 4x_2 \\ x_5' &= x_6 + 2x_1 \\ x_6' &= -2x_5 - 2x_6 + 0.007x_5^3 + 0.6x_2 \\ x_7' &= x_8 - 0.5x_2 \\ x_8' &= -5x_7 - 4x_8 - 0.05x_7^3 + 2.5x_1, \end{aligned} \tag{10.54}$$

which is the control system conjugate to the result-relay-system (10.51), where $m_0=2$ and $m_1=1$.

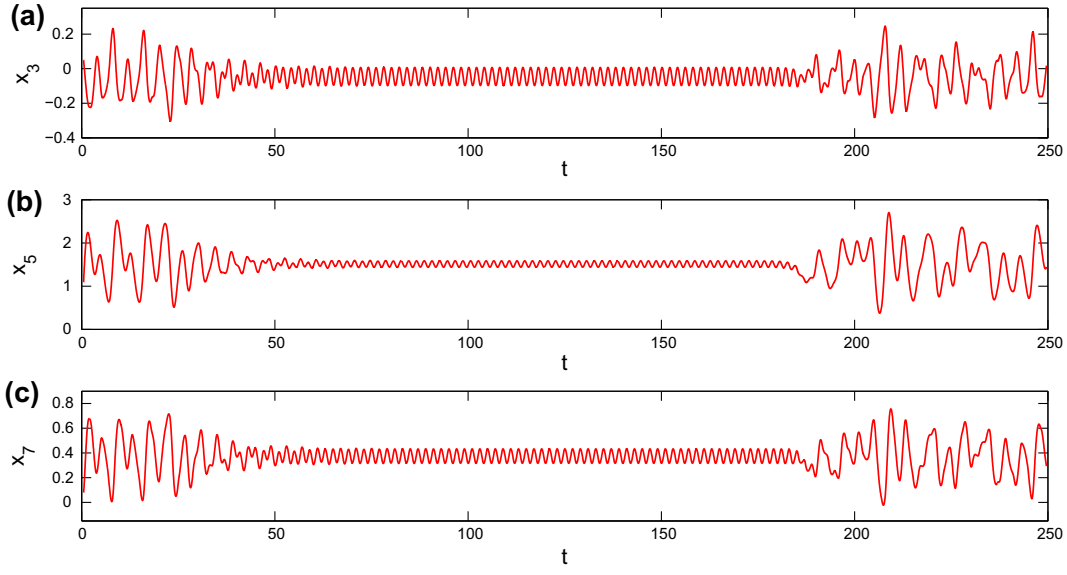

Fig. 17. OGY control method applied to the result-relay-system (10.51). (a) The graph of the x_3-coordinate, (b) The graph of the x_5-coordinate, (c) The graph of the x_7-coordinate. For stabilizing the 2-periodic solution of the result-relay-system (10.51), the OGY control method is applied to the generator system (10.50) around the fixed point 2.8/3.8 of the logistic map. The value $\delta=0.19$ is used, and the control starts at $t=\zeta_{25}$ and ends at $t=\zeta_{125}$. After approximately 60 iterations when the control is switched off, the chaos becomes dominant again and irregular motion reappears. The presented coordinates x_3, x_5 and x_7, all correspond to replicator systems and it is possible to obtain similar illustrations for the remaining ones, which are not just simulated here.

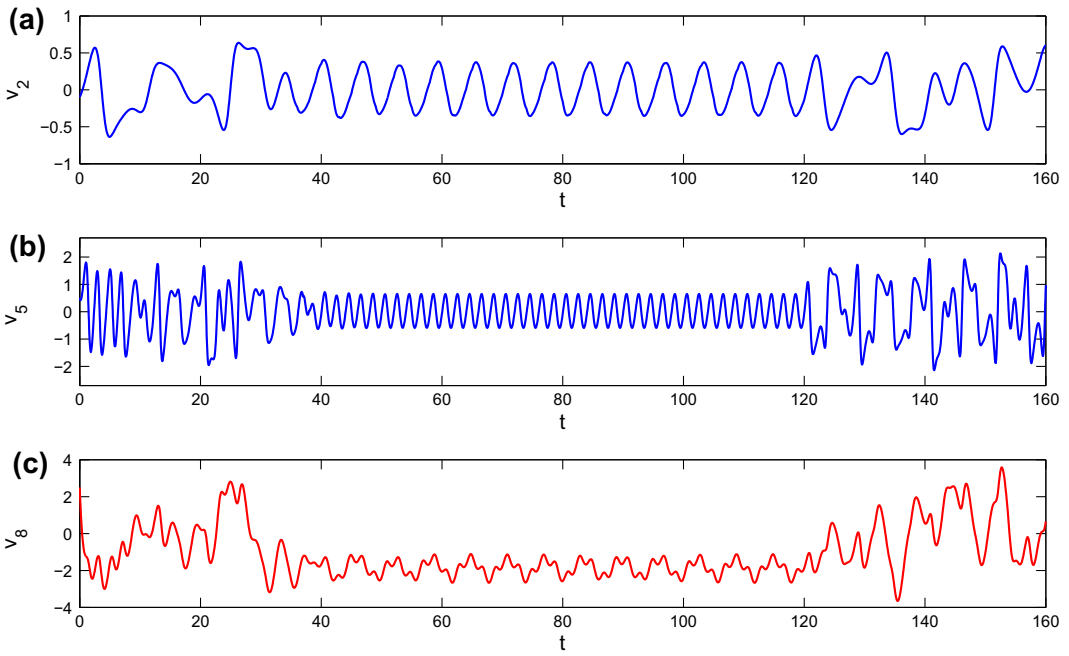

Fig. 18. Pyragas control method applied to the result-system (10.59) by means of the corresponding control system (10.60). (a) The graph of the v_2-coordinate, (b) The graph of the v_5-coordinate, (c) The graph of the v_8-coordinate. The simulation for the result-system (10.59) is provided such that in (a) and (b) periodic solutions with incommensurate periods 2 and 2π are controlled by Pyragas method and in (c) a quasiperiodic solution of the replicator system is pictured. The control starts at $t = 35$ and ends at $t = 120$. After switching off the control, chaos emerges again and irregular behavior reappears. For the coordinates v_1, v_4 and v_7 we have similar illustrations which are not indicated here.

To simulate the control results, we make use of the values $\delta = 0.19$, $t_1 = 0.5$, $t_0 = 2.8/3.8$ and the trajectory of system (10.54) with the initial data $x_1(0) = 1.37$, $x_2(0) = -0.05$, $x_3(0) = 0.05$, $x_4(0) = -0.1$, $x_5(0) = 1.09$, $x_6(0) = -0.81$, $x_7(0) = 0.08$, $x_8(0) = 0.21$. Taking the value $t_0 = 2.8/3.8$ means that the control mechanism is applied around the fixed point of the logistic map, and consequently stabilizes the 2-periodic solutions of the generator and the existing replicators. We switch on the control mechanism at the iteration number $i = 25$ for the logistic map, such that for the continuous-time system this moment corresponds to $t = \zeta_{25}$, and switch off at $i = 125$ which corresponds to the time moment $t = \zeta_{125}$.

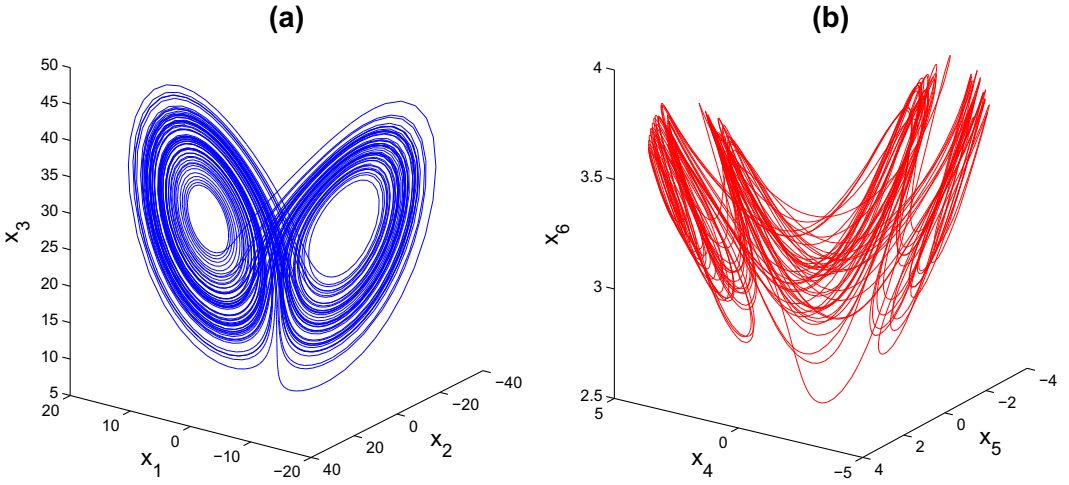

Fig. 19. 3-dimensional projections of the chaotic attractor of the result-system (10.61). (a) Projection on the x_1–x_2–x_3 space, (b) Projection on the x_4–x_5–x_6 space. In (a), the famous Lorenz attractor produced by the generator system (5.21) with coefficients $\sigma = 10$, $r = 28$ and $b = 8/3$ is shown. In (b), as in usual way, the projection of the chaotic attractor of the result-system (10.61), which can separately be considered as a chaotic attractor, is presented. Possibly one can call the attractor of the result-system as 6D Lorenz attractor.

The graphs of the coordinates $x_3,\ x_5$ and x_7 are pictured in Fig. 17. It is observable that the 2-periodic solutions of the replicators and hence of the result-relay-system (10.51) are stabilized. In other words, the extended chaos is controlled and the results of Theorem 9.1 are validated. One can see that after approximately 60 iterations when the control is switched off, the chaos becomes dominant again and irregular motion reappears.

10.5. Quasiperiodicity through chaos replication

Now, let us indicate that if there are more than one generator system then the chaos extension mechanism will lead to some new forms such as periodicity gives birth to quasiperiodicity.

In paper [100], it is mentioned that the Duffing equation

$$x'' + 0.168x' - 0.5x(1 - x^2) = \mu \sin t, \tag{10.55}$$

where μ is a parameter, admits the chaos through period-doubling cascade at the parameter value $\mu = \mu_\infty \equiv 0.21$. That is, at the parameter value $\mu = \mu_\infty$, for each natural number k Eq. (10.55) admits infinitely many periodic solutions with periods $2k\pi$. Using the change of variables $t = 2\pi s$ and $x(t) = y(s)$, and relabeling s as t, one attains the following equation

$$y'' + 0.168\pi y' - 0.5\pi^2 y(1 - y^2) = \pi^2 \mu \sin(\pi t). \tag{10.56}$$

Likewise Eq. (10.55), it is clear that Eq. (10.56), when considered with $\mu = \mu_\infty$, also admits the chaos through period-doubling cascade and has infinitely many periodic solutions with periods $2, 4, 8, \ldots$

Using the new variables $x_1 = x,\ x_2 = x'$ and $x_3 = y,\ x_4 = y'$, one can convert the Eqs. (10.55) and (10.56) to the systems

$$\begin{aligned} x_1' &= x_2 \\ x_2' &= -0.168x_2 + 0.5x_1(1 - x_1^2) + \mu \sin t \end{aligned} \tag{10.57}$$

and

$$\begin{aligned} x_3' &= x_4 \\ x_4' &= -0.168\pi x_4 + 0.5\pi^2 x_3(1 - x_3^2) + \pi^2 \mu \sin(\pi t), \end{aligned} \tag{10.58}$$

respectively. Now, we shall make use both of the systems (10.57) and (10.58), with $\mu = \mu_\infty$, as generators to obtain a chaotic system with infinitely many quasiperiodic solutions. We mean that the two systems admit incommensurate periods and consequently their influence on the replicator will be quasiperiodic. In this case, one can expect that replicator will expose infinitely many quasiperiodic solutions. For that purpose, let us consider the 6-dimensional result-system

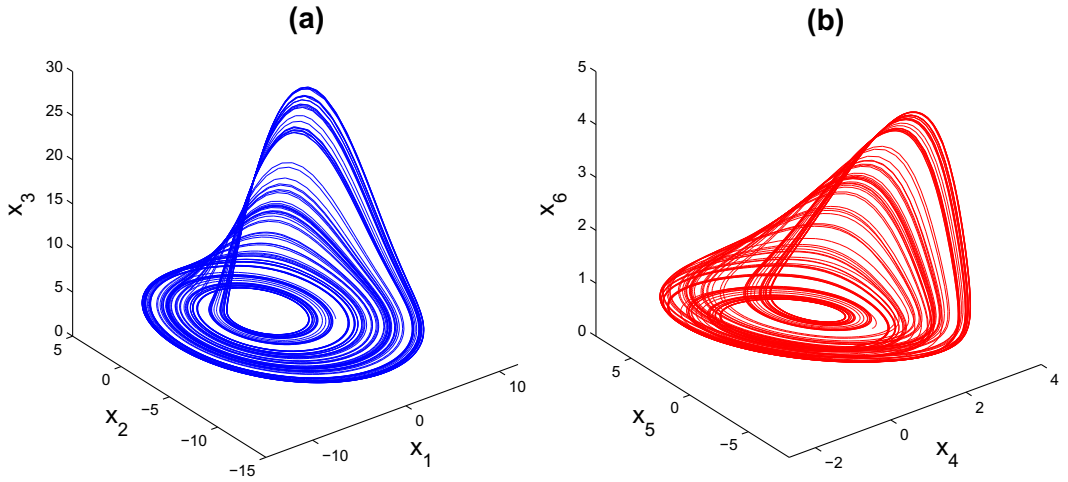

Fig. 20. 3-dimensional projections of the chaotic attractor of the result-system (10.63). (a) Projection on the x_1–x_2–x_3 space, (b) Projection on the x_4–x_5–x_6 space. The picture in (*a*) indicates the famous Rössler attractor produced by the generator system (10.62). The similarity between the illustrations presented in (a) and (b) supports the replication of chaos. The attractor of the result-system (10.63) can be possibly called as 6*D* Rössler attractor.

$$\begin{aligned}
x_1' &= x_2\\
x_2' &= -0.168x_2 + 0.5x_1(1-x_1^2) + 0.21\sin t\\
x_3' &= x_4\\
x_4' &= -0.168\pi x_4 + 0.5\pi^2 x_3(1-x_3^2) + 0.21\pi^2\sin(\pi t)\\
x_5' &= x_6 + x_1 + x_3\\
x_6' &= -3x_5 - 2x_6 - 0.008x_5^3 + x_2 + x_4,
\end{aligned} \tag{10.59}$$

where the last two equations are of a replicator.

To reveal existence of quasiperiodic solutions embedded in the chaotic attractor of system (10.59) we control the chaos of system (10.59) by the Pyragas method through the following control system

$$\begin{aligned}
v_1' &= v_2\\
v_2' &= -0.168v_2 + 0.5v_1(1-v_1^2) + 0.21\sin v_3 + C_1(v_2(t-2\pi) - v_2(t))\\
v_3' &= 1\\
v_4' &= v_5\\
v_5' &= -0.168\pi v_5 + 0.5\pi^2 v_4(1-v_4^2) + 0.21\pi^2\sin(\pi v_6) + C_2(v_5(t-2) - v_5(t))\\
v_6' &= 1\\
v_7' &= v_8 + v_1 + v_4\\
v_8' &= -3v_7 - 2v_8 - 0.008v_7^3 + v_2 + v_5.
\end{aligned} \tag{10.60}$$

We take into account the solution of the result-system (10.59) with the initial data $v_1(0) = 0.4,\ v_2(0) = -0.1,\ v_3(0) = 0,\ v_4(0) = -0.2,\ v_5(0) = 0.5,\ v_6(0) = 0,\ v_7(0) = 1.1$ and $v_8(0) = 2.5$. The simulation results are shown in Fig. 18. The control mechanism starts at $t = 35$ and ends at $t = 120$. The chaos not only in the generator systems, but also in the replicator counterpart is observable before the control is switched on. During the control, we make use of the values of $C_1 = 0.62$ and $C_2 = 2.58$ to stabilize the periodic solutions corresponding to the generator systems (10.57) and (10.58) with periods 2π and 2, respectively. Up to $t = 35$ and after $t = 120$ the values $C_1 = C_2 = 0$ are used. Between $t = 35$ and $t = 120$, the quasiperiodic solution of the replicator is stabilized and after $t = 120$ chaos in the system (10.59) develops again.

Possibly the obtained simulation result and previous theoretical discussions can give a support to the idea of *quasiperiodical cascade* for the appearance of chaos which can be considered as a development of the popular period-doubling route to chaos.

In paper [101], it has been mentioned that, in general, in the place of countable set of periodic solutions to form chaos, one can take an uncountable collection of Poisson stable motions which are dense in a quasi-minimal set. This can be also observed in Horseshoe attractor [29]. These emphasize that our simulation of quasiperiodic solutions can be considered as another evidence for the theoretical results.

10.6. Replicators with nonnegative eigenvalues

We recall that in our theoretical discussions, all eigenvalues of the real valued constant matrix A, used in system (1.2), are assumed to have negative real parts. Now, as open problems from the theoretical point of view, we shall discuss through simulations the problem of chaos replication in the case when the matrix A possesses an eigenvalue with positive or zero real part.

First, we are going to concentrate on the case of the existence of an eigenvalue with positive real part. Let us make use of the Lorenz system (5.21) together with the coefficients $\sigma = 10,\ r = 28$ and $b = 8/3$ as the generator, which is known to be chaotic [31,57], and set up the 6-dimensional result-system

$$\begin{aligned}
x_1' &= -10x_1 + 10x_2\\
x_2' &= -x_2 + 28x_1 - x_1x_3\\
x_3' &= -(8/3)x_3 + x_1x_2\\
x_4' &= -2x_4 + x_1\\
x_5' &= -3x_5 + x_2\\
x_6' &= 4x_6 - x_6^3 + x_3.
\end{aligned} \tag{10.61}$$

It is crucial to note that system (10.61) is of the form of system (1.1)+(1.2), where the matrix A admits the eigenvalues $-2,\ -3$ and 4, such that one of them is positive. We take into account the solution of system (10.61) with the initial data $x_1(0) = -12.7,\ x_2(0) = -8.5,\ x_3(0) = 36.5,\ x_4(0) = -3.4,\ x_5(0) = -3.2,\ x_6(0) = 3.7$ and visualize in Fig. 19 the projections of the corresponding trajectory on the x_1–x_2–x_3 and x_4–x_5–x_6 spaces. It is seen that the replicator system admits the chaos and the input-output mechanism works for system (10.61).

Next, we continue to our discussion with the case of the existence of an eigenvalue with a zero real part. This time we consider the chaotic Rössler system [57,102] described by

$$\begin{aligned} x_1' &= -(x_2 + x_3) \\ x_2' &= x_1 + 0.2x_2 \\ x_3' &= 0.2 + x_3(x_1 - 5.7) \end{aligned} \tag{10.62}$$

as the generator and constitute the result-system

$$\begin{aligned} x_1' &= -(x_2 + x_3) \\ x_2' &= x_1 + 0.2x_2 \\ x_3' &= 0.2 + x_3(x_1 - 5.7) \\ x_4' &= -4x_4 + x_1 \\ x_5' &= -x_5 + x_2 \\ x_6' &= -0.2x_6^3 + x_3. \end{aligned} \tag{10.63}$$

In this case, one can consider system (10.63) as in the form of (1.1)+(1.2) where the matrix A is a diagonal matrix with entries $-4, -1, 0$ on the diagonal and admits the number 0 as an eigenvalue. We simulate the solution of system (10.63) with the initial data $x_1(0) = 4.6,\ x_2(0) = -3.3,\ x_3(0) = 0,\ x_4(0) = 1,\ x_5(0) = -3.7$ and $x_6(0) = 0.8$. The projections of the trajectory on the x_1–x_2–x_3 and x_4–x_5–x_6 spaces are seen in Fig. 20. The simulation results confirm that the replicator mimics the complex behavior of the generator system.

These results of the simulations request more detailed investigation which concern not only the theoretical existence of chaos, but also its resistance and stability.

11. Conclusion

Replication of different types of chaos such as obtained by period-doubling cascade, Devaney's and Li-Yorke chaos is recognized in the paper. The definitions of chaotic sets as well as the hyperbolic sets of functions are introduced and the replication of the chaos is proved rigorously. The morphogenesis mechanism considered in our paper is based on a chaos generating element inserted in a network of systems. Replication of intermittency as well as Shil'nikov orbits are discussed. Morphogenesis of the double-scroll Chua's attractor and quasiperiodical motions as a possible skeleton of a chaotic attractor are demonstrated numerically. Moreover, control problem of the extended chaos is realized. Some of the results are illustrated through the relay system's dynamics and appropriate simulations are presented using the indicated method successively.

The concept of self-replicating machines, in the abstract sense, starts with the ideas of von Neumann [103] and these ideas are supposed to be the origins of cellular automata theory [63]. Morphogenesis was deeply involved in mathematical discussions through Turing's investigations [62] as well as in the concept of structural stability [104]. In the present paper the term "morphogenesis" is used in the meaning of "processes creating forms" where we accept the *form* not only as a type of chaos, but also accompanying concepts as the structure of the chaotic attractor, its fractal dimension, form of the bifurcation diagram, the spectra of Lyapunov exponents, inheritance of intermittency, etc. This is similar to the idea such that morphogenesis is used in fields such as urban studies [105], architecture [106], mechanics [107], computer science [108], linguistics [109] and sociology [110,111].

Replication of a known type of chaos in systems with arbitrary large dimension is a significant consequence of the paper. More precisely, by the method presented, we show that a known type of chaos, such as obtained through period-doubling cascade and in the sense of Devaney or Li-Yorke, can be extended to systems with arbitrary large dimension. To be more precise, we provide replication of chaos between unidirectionally coupled systems such that finally to obtain a result-system admitting the same type of chaos. One can construct the morphogenesis mechanism by the formation of consecutive replications of chaos or replication of chaos from a core system. It is also possible to construct a result-system using these two mechanisms in a mixed style.

Acknowledgments

The authors wish to express their sincere gratitude to the referees for the helpful criticism and valuable suggestions, which helped to improve the paper significantly.

This research was supported by the Grant (111T320) from TUBITAK, the Scientific and Technological Research Council of Turkey.

References

[1] Fink AM. Almost periodic differential equations. Lecture notes in mathematics. Berlin, Heidelberg, New York: Springer-Verlag; 1974.
[2] Corduneanu C. Almost periodic functions. New-York, London, Sydney: Interscience Publishers; 1968.

[3] Thompson JMT, Stewart HB. Nonlinear dynamics and chaos. John Wiley; 2002.
[4] Davies JA. Mechanisms of morphogenesis: the creation of biological form. United States of America: Elsevier Academic Press; 2005.
[5] Thom R. Mathematical models of morphogenesis. Chichester, England: Ellis Horwood Limited; 1983.
[6] Mandelbrot BM. The fractal geometry of nature. San Fransisco: Freeman; 1982.
[7] Mandelbrot BM. Fractals: form, chance and dimension. San Fransisco: Freeman; 1977.
[8] Milnor J. Dynamics in one complex variable. United States of America: Princeton University Press; 2006.
[9] Branner B, Keen L, Douady A, Blanchard P, Hubbard JH, Schleicher D, Devaney RL. Complex dynamical systems: the mathematics behind mandelbrot and julia sets. In: Devaney RL, editor. United States of America: American Mathematical Society; 1994.
[10] Peitgen HO, Jürgens H, Saupe D. Chaos and fractals: new frontiers of science. Verlag, New York: Springer; 2004.
[11] Gonzales-Miranda JM. Synchronization and control of chaos. London: Imperial College Press; 2004.
[12] Pecora LM, Carroll TL. Synchronization in chaotic systems. Phys Rev Lett 1990;64:821–5.
[13] Kapitaniak T. Synchronization of chaos using continuous control. Phys Rev E 1994;50:1642–4.
[14] Ding M, Ott E. Enhancing synchronism of chaotic systems. Phys Rev E 1994;49:R945–8.
[15] Pecora LM, Carroll TL. Driving systems with chaotic signals. Phys Rev A 1991;44:2374–83.
[16] Cuomo KM, Oppenheim AV. Circuit implementation of synchronized chaos with applications to communications. Phys Rev Lett 1993;71:65–8.
[17] Hadamard J. Les surfaces à courbures opposées et leurs lignes géodésiques. J Math Pures Appl 1898;4:27–74.
[18] Morse M, Hedlund GA. Symbolic dynamics. Am J Math 1938;60:815–66.
[19] Wiggins S. Global bifurcations and chaos: analytical methods. New York: Springer-Verlag; 1988.
[20] Wiggins S. Introduction to applied nonlinear dynamical systems and chaos. New York: Springer-Verlag; 2003.
[21] Devaney R. An introduction to chaotic dynamical systems. United States of America: Addison-Wesley; 1987.
[22] Kennedy J, Yorke JA. Topological horseshoes. Trans Am Math Soc 2001;353:2513–30.
[23] Grebogi C, Yorke JA. The impact of chaos on science and society. Tokyo: United Nations University Press; 1997.
[24] Hale J, Koçak H. Dynamics and bifurcations. New York: Springer-Verlag; 1991.
[25] Robinson C. Dynamical systems: stability, symbolic dynamics, and chaos. Boca Raton/Ann Arbor/London/Tokyo: CRC Press; 1995.
[26] Akhmet MU. Devaney's chaos of a relay system. Commun Nonlinear Sci Numer Simul 2009;14:1486–93.
[27] Akhmet M. Nonlinear hybrid continuous/discrete-time models. Amsterdam-Paris: Atlantis Press; 2011.
[28] Akhmet MU. Li-Yorke chaos in the impact system. J Math Anal Appl 2009;351:804–10.
[29] Smale S. Differentiable dynamical systems. Bull Am Math Soc 1967;73:747–817.
[30] Guckenheimer J, Holmes P. Nonlinear oscillations, dynamical systems, and bifurcations of vector fields. New York: Springer-Verlag; 1997.
[31] Lorenz EN. Deterministic nonperiodic flow. J Atmos Sci 1963;20:130–41.
[32] Cartwright M, Littlewood J. On nonlinear differential equations of the second order I: The equation $\ddot{y} - k(1-y^2)'y + y = bk\cos(\lambda t + a), k$ large. J London Math Soc 1945;20:180–9.
[33] Levinson N. A second order differential equation with singular solutions. Ann Math 1949;50:127–53.
[34] Guckenheimer J, Williams RF. Structural stability of lorenz attractors. Publ Math 1979;50:307–20.
[35] Levi M. Qualitative analysis of the periodically forced relaxation oscillations. United States of America: Memoirs of the American Mathematical Society; 1981.
[36] Akhmet M. Principles of discontinuous dynamical systems. New York: Springer; 2010.
[37] Akhmet MU. Shadowing and dynamical synthesis. Int J Bifurcation Chaos 2009;19:3339–46.
[38] Akhmet MU. Dynamical synthesis of quasi-minimal sets. Int J Bifurcation Chaos 2009;19:2423–7.
[39] Akhmet MU. Creating a chaos in a system with relay. Int J Qual Theory Differ Equat Appl 2009;3:3–7.
[40] Akhmet MU, Fen MO. Chaotic period-doubling and OGY control for the forced Duffing equation. Commun Nonlinear Sci Numer Simul 2012;17:1929–46.
[41] Akhmet MU, Fen MO. The period-doubling route to chaos in the relay system. Proc Dyn Syst Appl 2012;6:22–6.
[42] Kaneko K, Tsuda I. Complex systems: chaos and beyond, a constructive approach with applications in life sciences. Berlin, Heidelberg, New York: Springer-Verlag; 2000.
[43] Kaneko K, Tsuda I. Chaotic itinerancy. Chaos 2003;13:926–36.
[44] Ikeda K, Matsumoto K, Otsuka K. Maxwell–Bloch turbulence. Prog Theor Phys Suppl 1989;99:295.
[45] Tsuda I. Chaotic itinerancy as a dynamical basis of hermeneutics in brain and mind. World Futures 1991;32:167–84.
[46] Tsuda I. Dynamic link of memory–chaotic memory map in nonequilibrium neural networks. Neural Networks 1992;5:313–26.
[47] Kaneko K. Clustering, coding, switching, hierarchical ordering, and control in network of chaotic elements. Phys D 1990;41:137–72.
[48] Kaneko K. Globally coupled circle maps. Phys D 1991;54:5–19.
[49] Sauer T. Chaotic itinerancy based on attractors of one-dimensional maps. Chaos 2003;13:947–52.
[50] Freeman WJ, Barrie JM. Chaotic oscillations and the genesis of meaning in cerebral cortex. In: Buzsaki G, Christen Y, editors. Temporal coding in the brain. Berlin: Springer-Verlag; 1994. p. 13–37.
[51] Kim P, Ko T, Jeong H, Lee KJ, Han SK. Emergence of chaotic itinerancy in simple ecological systems. Phys Rev E 2007;76(065201(R)):1–4.
[52] Pomeau Y, Manneville P. Intermittent transition to turbulence in dissipative dynamical systems. Commun Math Phys 1980;74:189–97.
[53] Moon FC. Chaotic vibrations: an introduction for applied scientists and engineers. Hoboken, NJ: John Wiley & Sons; 2004.
[54] Chua LO. Chua's circuit: ten years later. IEICE Trans Fund Electron Commun Comput Sci 1994;E77-A:1811–22.
[55] Kapitaniak T, Chua LO. Hyperchaotic attractors of unidirectionally-coupled Chua's circuits. Int J Bifurcation Chaos Appl Sci Eng 1994;4:477–82.
[56] Lorenz HW. Nonlinear dynamical economics and chaotic motion. Berlin, New York: Springer-Verlag; 1989.
[57] Sprott JC. Elegant chaos: algebraically simple chaotic flows. Singapore: World Scientific Publishing; 2010.
[58] Rössler OE. An equation for hyperchaos. Phys Lett A 1979;71:155–7.
[59] Kapitaniak T, Chua LO. Hyperchaotic attractors of unidirectionally-coupled Chua's circuits. Int J Bifurcation Chaos Appl Sci Eng 1994;4:477–82.
[60] Kapitaniak T. Transition to hyperchaos in chaotically forced coupled oscillators. Phys Rev E 1993;47:R2975–8.
[61] Kapitaniak T, Chua LO, Zhong G. Experimental hyperchaos in coupled Chua's circuits. IEEE Trans Circuits Syst I Fund Theory Appl 1994;41:499–503.
[62] Turing AM. The chemical basis of morphogenesis. Philos Trans R Soc London Ser B Biol Sci 1952;237:37–72.
[63] Schiff JL. Cellular automata: a discrete view of the world. Hoboken, NJ: John Wiley & Sons, Inc.; 2008.
[64] Smale S. A mathematical model of two cells via Turing's equation. In: Some mathematical questions in biology, V, proc. seventh sympos., mathematical biology, Mexico city, 1973. Lectures on mathematics in the life sciences, vol. 6. Providence, RI: American Mathematical Society; 1974. p. 15–26.
[65] Drubi F, Ibáñez S, Rodriguez JA. Coupling leads to chaos. J Differ Equat 2007;239:371–85.
[66] Drubi F, Ibáñez S, Rodriguez JA. Singularities and chaos in coupled systems. Bull Belg Math Soc Simon Stevin 2008;15:797–808.
[67] Drubi F, Ibáñez S, Rodriguez JA. Hopf–Pitchfork singularities in coupled systems. Phys D 2011;240:825–40.
[68] Yuan W-J, Luo X-S, Jiang P-Q, Wang B-H, Fang J-Q. Transition to chaos in small-world dynamical network chaos. Chaos Solitons Fract 2008;37:799–806.
[69] Hale JK. Ordinary differential equations. Malabar, FL: Krieger Publishing Company; 1980.
[70] Corduneanu C. Principles of differential and integral equations. The Bronx, NY: Chelsea Publishing Company; 1977.
[71] Corduneanu C. Integral equations and applications. New York: Cambridge University Press; 2008.
[72] Li TY, Yorke JA. Period three implies chaos. Am Math Mon 1975;82:985–92.

[73] Čiklová M. Li-Yorke sensitive minimal maps. Nonlinearity 2006;19:517–29.
[74] Kloeden P, Li Z. Li-Yorke chaos in higher dimensions: a review. J Differ Equat Appl 2006;12:247–69.
[75] Akin E, Kolyada S. Li-Yorke sensitivity. Nonlinearity 2003;16:1421–33.
[76] Palmer K. Shadowing in dynamical systems. Dordrecht, The Netherlands: Kluwer Academic Publishers; 2000.
[77] Lerman LM, Shil'nikov LP. Homoclinical structures in nonautonomous systems: nonautonomous chaos. Chaos 1992;2:447–54.
[78] Scheurle J. Chaotic solutions of systems with almost periodic forcing. J Appl Math Phys (ZAMP) 1986;37:12–26.
[79] Meyer KR, Sell GR. Homoclinic orbits and Bernoulli bundles in almost periodic systems. Can Math Soc Conf Proc 1987;8:527.
[80] Palmer KR, Stoffer D. Chaos in almost periodic systems. J Appl Math Phys (ZAMP) 1989;40:592–602.
[81] Zadiraka KV. Investigation of irregularly perturbed differential equations. In: Questions of the theory and history of differential equations. Kiev: Nauk. Dumka; 1968. p. 81–108. in Russian.
[82] Barbashin EA. Introduction to the theory of stability. Groningen: Wolters–Noordhoff Publishing; 1970.
[83] Alligood KT, Sauer TD, Yorke JA. Chaos: an introduction to dynamical systems. New York: Springer-Verlag; 1996.
[84] Sander E, Yorke JA. Period-doubling cascades galore. Ergod Theory Dyn Syst 2011;31:1249–67.
[85] Feigenbaum MJ. Universal behavior in nonlinear systems. Los Alamos Sci/Summer 1980:4–27.
[86] Schuster HG, Just W. Deterministic chaos, an introduction. Federal Republic of Germany: Wiley-Vch; 2005.
[87] Zelinka I, Celikovsky S, Richter H, Chen G, editors. Evolutionary algorithms and chaotic systems. Berlin, Heidelberg: Springer-Verlag; 2010.
[88] Sato S, Sano M, Sawada Y. Universal scaling property in bifurcation structure of Duffing's and of generalized Duffing's equations. Phys Rev A 1983;28:1654–8.
[89] Horn RA, Johnson CR. Matrix analysis. United States of America: Cambridge University Press; 1992.
[90] Pyragas K. Continuous control of chaos by self-controlling feedback. Phys Rev A 1992;170:421–8.
[91] Fradkov AL. Cybernetical physics. Berlin, Heidelberg: Springer-Verlag; 2007.
[92] Arneodo A, Coullet P, Tresser C. Oscillators with chaotic behavior an illustration of a theorem by Shil'nikov. J Statist Phys 1982;27:171–82.
[93] Shilnikov LP. A case of the existence of a denumerable set of periodic motions. Sov Math Dokl 1965;6:163–6.
[94] Anishchenko VS, Kapitaniak T, Safonova MA, Sosnovzeva OV. Birth of double–double scroll attractor in coupled Chua circuits. Phys Lett A 1994;192:207–14.
[95] Chua LO, Komuro M, Matsumoto T. The double scroll family. Parts I and II. IEEE Trans Circuit Syst 1986;CAS-33:1072–118.
[96] Matsumoto T, Chua LO, Komuro M. The double scroll. IEEE Trans Circuit Syst 1985;CAS-32:797–818.
[97] Chua LO, Wu CW, Huang A, Zhong G. A universal circuit for studying and generating chaos. Part I: Routes to chaos. IEEE Trans Circuits Syst I Fund Theory Appl 1993;40:732–44.
[98] Ott E, Grebogi C, Yorke JA. Controlling chaos. Phys Rev Lett 1990;64:1196–9.
[99] Schuster HG. Handbook of chaos control. Weinheim: Wiley-Vch; 1999.
[100] Dowell EH, Pazeshki C. On the understanding of chaos in Duffing's equation including a comparison with experiment. J Appl Mech 1986;53:5–9.
[101] Shilnikov L. Bifurcations and strange attractors. Proceedings of the international congress of mathematicians, vol. III. Beijing: Higher Ed. Press; 2002. pp. 349–372.
[102] Rössler OE. An equation for continuous chaos. Phys Lett 1976;57A:397–8.
[103] Von Neumann J, Burks AW, editors. The theory of self-reproducing automata. Urbana and London: University of Illinois Press; 1966.
[104] Thom R. Stabilité structurelle et morphogénèse. New York: W.A. Benjamin; 1972.
[105] Courtat T, Gloaguen C, Douady S. Mathematics and morphogenesis of cities: a geometrical approach. Phys Rev E 2011;83(036106):1–12.
[106] Roudavski S. Towards morphogenesis in architecture. Int J Archit Comput 2009;7:345–74.
[107] Taber LA. Towards a unified theory for morphomechanics. Philos Trans R Soc A 2009;367:3555–83.
[108] Bourgine P, Lesne A. Morphogenesis: origins of patterns and shapes. Berlin, Heidelberg: Springer-Verlag; 2011.
[109] Hagége C. The language builder: an essay on the human signature in linguistic morphogenesis. Amsterdam, The Netherlands: John Benjamins Publishing Co.; 1993.
[110] Archer MS. Realistic social theory: the morphogenetic approach. Cambridge: Cambridge University Press; 1995.
[111] Buckley W. Sociology and modern systems theory. New Jersey: Prentice Hall; 1967.